JAERI 1227

JAERI 1227

A Method of the Gamma-ray Spectrum Analysis: FORTRAN IV Programs "BOB73" for Ge(Li) Detectors and "NAISAP" for NaI(Tl) Detectors

June, 1973

日 本 原 子 力 研 究 所
Japan Atomic Energy Research Institute

JAERI レポート

この報告書は，日本原子力研究所で行なわれた研究および技術の成果を研究成果編集委員会の審査を経て，不定期に刊行しているものです．

入手（資料交換による），複製などのお問合わせは，日本原子力研究所技術情報部（〒319-11 茨城県那珂郡東海村）あて，お申しこみください．なお，このほかに財団法人原子力弘済会情報サービス事業部（茨城県那珂郡東海村日本原子力研究所内）で複写による実費頒布をおこなっております．

JAERI Report

Inquiries about the availability of reports and their reproduction should be addressed to the Division of Technical Information, Japan Atomic Energy Research Institute, Tokai-mura, Naka-gun, Ibaraki-ken, Japan.

編集兼発行　日本原子力研究所
印　　刷　科学図書印刷株式会社

JAERI 1227 A Method of the Gamma-ray Spectrum Analysis: FORTRAN IV Programs "BOB 73" for Ge(Li) Detectors and "NAISAP" for NaI(Tl) Detectors

Errata

Page	Line(Place)	Incorrect	Correct
4	Eq. (2-4)	$ISM=(\Delta D\times\sqrt{2\times IST+5}-5)/2$	$ISM=(\Delta D\times\sqrt{IST}-5)/2$
4	Eq. (2-5)	$\Delta D=ISM0/\sqrt{2\times ICH}+5$	$\Delta D=(2\times ISM0+5)/\sqrt{ICH}$
20	Fig. 3-7	the exponential (triangles) the cubic polynomial (inverted triangles)	the exponential (inverted triangles) the cubic polynomial (triangles)

A Method of the Gamma-ray Spectrum Analysis: FORTRAN IV Programs "BOB 73" for Ge(Li) Detectors and "NAISAP" for NaI(Tl) Detectors

Hiroshi BABA, Toshiaki SEKINE, Sumiko BABA
and Hiroshi OKASHITA

Tokai Research Establishment
Japan Atomic Energy Research Institute
Tokai-mura, Naka-gun, Ibaraki-ken

Received December 21, 1972

Abstract

The problem of the γ-ray spectrum analysis was treated by combining the peak-searching and peak-fitting processes. The stage of the peak recognition was built up by the first derivative method supplemented with various peak shape tests so that sufficient information was able to be supplied for the succeeding fitting step, rather independently of the types of the spectrum. By virtue of thus constructed function of the peak search and the success of the analytical representation of the response function, the low-resolution spectrum from NaI(Tl) detectors was successfully analyzed based on the photopeak method as in the case of Ge(Li) detectors. As a result of various tests, the background shape under the peak was found no less important than the peak shape for the consistent fitting result, even in the case of the Ge(Li) spectrum.

The core of either program, BOB 73 or NAISAP, consists of the peak-searching and the peak-fitting functions and is accompanied by various subprograms such as the data pretreatment, energy calibration and efficiency correction, and plotting of the spectrum. The parameter finding for the response function is also an important function in NAISAP. The time required for the spectrum analysis depends on the complexity of the spectrum rather than the data size or the total number of peaks involved in the case of BOB 73. A single spectrum with medium complexity is analyzed within the order of ten seconds. NAISAP requires about one second for analyzing one peak. The codes are described in some details and the instruction manuals are given for user's convenience.

JAERI 1227

放射性同位体製造資料-1128

γ線スペクトルの解析法：Ge(Li) 検出器用のコード“BOB 73”と NaI(Tl) 検出器用のコード“NAISAP”

日本原子力研究所　東海研究所

馬場　宏・関根　俊明・馬場　澄子・岡下　宏

(1972 年 12 月 21 日受理)

要　　旨

ピーク探索操作とピーク・フィッティング操作を組み合わせることにより，γ線スペクトル解析という課題を処理した．ピーク認識の段階は一次微係数法に種々の附随テストを組み込むことによって構成され，これによって，スペクトルの性質の違いにほとんど無関係に後段のピーク・フィッティング操作に必要なすべての情報を供給することが可能になった．このピーク探索機能のおかげで Ge(Li) 検出器のみならず，NaI(Tl) 検出器の与えるスペクトルをも光電ピーク法を基本とする方法で解析することを得た．種々のテストピークを解析した結果，ピークの波形に劣らず，ピークの下に隠されたバック・グラウンドの形も結果に重大な影響を及ぼすことが見出された．

BOB 73, NAISAP いずれのコードにおいても，その中心は，ピーク認識とピーク・フィットの機能であり，それに附随する機能として，データの前処理，エネルギー較正と計数効率補正，スペクトル・プロット等が加えられている．NAISAP の場合には，この他にも応答関数のパラメーター値を見出す操作もまた重要な部分を占めている．スペクトル解析に要する時間は，BOB 73 の場合，データ・サイズや含まれるピークの数よりもむしろスペクトルの複雑さに依存する．あまり複雑でないスペクトルに対しては，解析に要する時間は 10 秒の程度である．これに対し，NAISAP での解析所要時間は，1 ピーク当り約 1 秒のオーダーである．終わりに，解析コードの解説と使用法を記載した．

Contents

目　　次

1. Introduction

Automation of data analyzing processes has become an inevitable tendency in any field of science. In the analysis of γ spectra obtained with solid state detectors or with scintillation crystals, however, one encounters quite a difficult problem of recognizing a pattern.

The most naive attitude for this problem would be to store the standard spectra in the computer memory as they are, as carried out by HEATH *et al.*[1] This is the most accurate way of reproducing the response function in a sense. However, it naturally requires very severe realization of the same condition, by the aid of supreme electronic devices, for the sample spectrum measurement as the measurement of the standard spectra. It is, therefore, desirable if the response function can be replaced by a relatively simple analytical function with sufficient accuracy.

A relatively complex analytical expression of the γ-ray response of NaI(Tl) detectors has first been given by CHESTER *et al.*[2] with sufficient accuracy. SALMON uses the CHESTER's function in a simplified form[3]. As a result of the simplification, his response function reveals appreciable deviations from observed spectra. SEKINE *et al.*[4] have constructed a fairly simple analytical expression which satisfactorily reproduces observed spectra from NaI(Tl) detectors.

In contrast to the above total spectrum method or response function method, the photopeak method that is mostly applied to the high-resolution spectra from Ge(Li) detectors, concerns only the functional relationship in the peak region. More concretely, the main problems in the photopeak method are the search of peaks and the determination of the peak areas. The search of peaks is generally carried out by either the first derivative[5,6] or the second derivative[7,8] method. The Fourier transformation method by INOUYE *et al.*[9] is also placed in the category of the photopeak method.

In the determination of peak areas, the choice of the shape of the background continuum becomes a very important problem for the consistency of the peak areas. The peak area is calculated either by the summation of the surplus counts in the peak above the background continuum or by the fitting of the peak shape to an appropriate function. COVELL *et al.*[10] propose quite a different method of subtracting the contribution of the background to the peak area. Finding a suitable peak-shape function becomes another important problem in the fitting process.

The two main functions, peak finding and intensity determination, involved in the photopeak method are, in fact, commonly required for all kinds of the spectrum-analyzing program. From this aspect, we would rather classify the whole subject into (i) peak recognition and (ii) intensity determination rather than into the total spectrum and the photopeak methods.

In the previous work[5], we have set forth the following three requirements concerning the function to be fulfilled by the peak-searching procedure: (1) all true peaks must be correctly discerned while minimizing the number of spurious peaks, (2) multiplicity of a given peak should be given, and (3) the boundary channel on both sides of a detected peak must be correctly determined. As a result, we have succeeded in constructing a peak-searching subprogram " PKREC " satisfying the above requirements for γ spectra with high resolution obtained with Ge(Li) detectors. The present work concerns further extension and generalization of the function of "PKREC" to make the succeeding peak-fitting process easier.

In contrast to the peak-searching process performed in a universal fashion, we must admit individuality of different types of spectra in the intensity-determining step. In the γ spectrum given by NaI(Tl) detectors, violently changing parts, such as the full-energy peak or the Comp-

ton edge, occupy an appreciable portion of the whole spectrum because of the low resolution. Therefore, a large error is generally introduced if one estimates the intensity by separating a peak from its Compton background. On the contrary, application of the response function method at least to the violently changing portion of the spectrum would produce a remarkable success in the intensity determination.

For high-resolution spectra like those from Ge(Li) detectors, the situation is absolutely different from the above-mentioned case. There, the Compton background can be regarded as a very slowly changing function except for the peak region. Therefore, the photopeak method determining peak areas above the Compton continuum expressed with a simple function assures more reasonable success in this case. As one may see later, however, one encounters rather unexpected difficulties for Ge(Li) spectra, because the response function can not be known in such a clean form as that for NaI(Tl) spectra. Solutions for these problems are discussed and given in Chapters 3 and 4.

The rest of this report is devoted to a few accompanying problems. Firstly, procedures for energy assignment and efficiency determination need to be established. Secondly, the identification of radionuclides from thus assigned full energy peaks is also an important subject. Lastly, we must solve the problem how to feed input data into a large computer. The last problem is still the most essential in many laboratories including ourselves.

2. Peak-searching Procedure : Generalization and Improvement of the Subprogram " PKREC "

The peak-searching process is summarized as a comparison of the first derivative of the spectrum with an appropriately established threshold. Details of the procedure and the effect of the data smoothing on the peak search are described elsewhere[5].

The questions of our concern are now focussed into the followings ; (1) how to set up the threshold value and (2) how to rectify unreasonable conclusions obtained by the primary peak survey. In order to enhance the sensitivity for the detection of small peaks, the threshold must be set at a very low level. This disposition inevitably increases the frequency of picking pseudo-peaks up. In reference 5a, we have shown a set of the threshold values which proved to satisfactorily work for spectra with high resolution from Ge(Li) detectors.

The threshold was taken as the square root of the number of counts at each channel multiplied by an appropriate factor, $ATEN$. This factor naturally takes a different value depending on the peak width and the number of counts. The value of $ATEN$ was empirically found for the number of counts N at the starting channel IST for the peak search as follows ;

$$ATEN=A\times F \tag{2-1}$$

where A is given by

$$A=\begin{cases} 0.6 & N<200 \\ 0.7 & 200\leqq N<1,000 \\ 0.8 & 1,000\leqq N\leqq 3,200 \\ \sqrt{N/5,000} & N>3,200 \end{cases} \tag{2-2}$$

and the factor F was related to the number of points used in the data smoothing, n_s. The n_s value was found[5] to be taken roughly equal to the full width at half maximum ($FWHM$) of the peak.

Let us introduce an index, ISM, controlling the n_s as follows ;

$$n_s=\begin{cases} 2\times ISM+5 & \text{for } 0\leqq ISM\leqq 10 \\ 3 & \text{for } ISM=11 \\ 0 & \text{for } ISM=12 \end{cases} . \tag{2-3}$$

The values of F are listed in TABLE 2-1 in relation to the ISM. Note that Eq.(2-2) and TABLE 2-1 are slightly different from the correspondings in ref. 5a.

TABLE 2-1 Relation between ISM and F-value

ISM	0	1	2	3	4	5	6	7	8	9	10	11	12
F	1	0.8	0.6	0.45	0.4	0.35	0.3	0.275	0.25	0.225	0.2	1.1	1.25

We noted that the main difference between the high-resolution spectrum given by Ge(Li) detectors and the low-resolution spectrum from NaI(Tl) scintillators in regard to the peak search by the first derivative method appeared in the energy dependence of the peak width. In the latter, the peak width can no longer be regarded as practically constant as in the former but must be taken to be proportional to the square root of the pulse height. Therefore, we let the index ISM change linearly with the square root of the channel number for the low-resolution spectrum*) ;

*) Similar consideration may be required for the spectrum from the high-resolution Ge(Li) detector for the low-energy γ rays.

$$ISM=(\Delta D\times\sqrt{2\times IST+5}-5)/2, \tag{2-4}$$

where ΔD is the proportionality constant to be specified for each spectrum. It is determined by $ISM0$, the specified value of ISM at the reference channel numer ICH as

$$\Delta D=ISM0/\sqrt{2\times ICH+5}. \tag{2-5}$$

The reference channel number ICH is fixed at the first quarter of the whole spectrum ;

$$ICH=(INIT+IFIN)/4 \tag{2-6}$$

with the initial channel $INIT$ and the final channel $IFIN$ of the spectrum. Furthermore, IST is the channel number at which the next peak-searching procedure starts.

The values of A and F have been concluded to be used as well both for the high- and low-resolution spectra.

The next problem is then how to recognize the detailed structure of each peak region which the above-mentioned procedure, simply comparing the magnitude of the first derivative with the threshold, fails to detect. For example, one must find if a detected peak end is the true end or a spuriously produced one due to the overlap of a nearby peak. How can one recognize a small shoulder or a pair of closely locating peaks of about the same size ? How can one correctly point out the end of a peak superimposed on the Compton edge of another peak ? Noises due to statistical deviations or hardware errors also need to be filtered out. There are abrupt changes in the spectrum, such as the cutoff of the low-energy portion or the discontinuity in the connecting part of the spectrum measured partially with different counting conditions. They should also be filtered out as much as possible.

A method usually adopted for those requirements is that of introducing the exact full width at half maximum of the full energy peaks as a measure of the multiplicity. This technique was, however, rejected in the present work from the reasons discussed in Chapter 6.

Instead, we noted the fact that every visible fine structure in the peak shape requires the existence of a characteristic rule in the value of the first derivative during the corresponding interval. Conversely, the effect of pseudo-peaks such as spikes or noises on the first derivative does not last for a long interval.

In Fig. 2-1, we have shown the results of a test for finding the sensitivity of the peak-detecting function. The spectrum of the ^{137}Cs standard source, measured for 400 ksec with a small geometry by using a 50 cc, coaxial-type Ge(Li) detector ($FWHM$=2.9 keV at 1,332 keV), was artificially shifted by an appropriate number of channels, divided by a factor of several

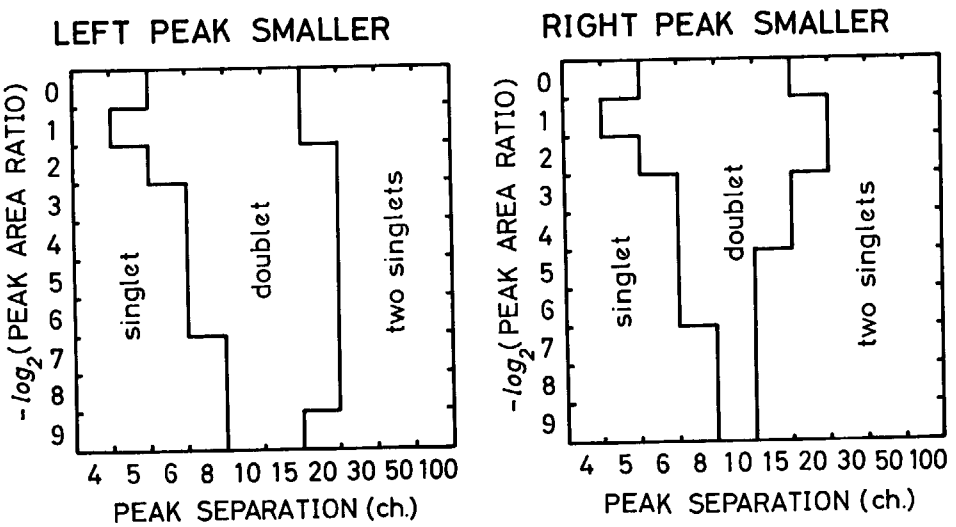

Fig. 2-1 Sensitivity of the peak-detecting function. The figure indicates how the code recognizes a doublet with a certain intensity ratio at a given peak separation. The full width at half maximum of each peak is 5.0 channels.

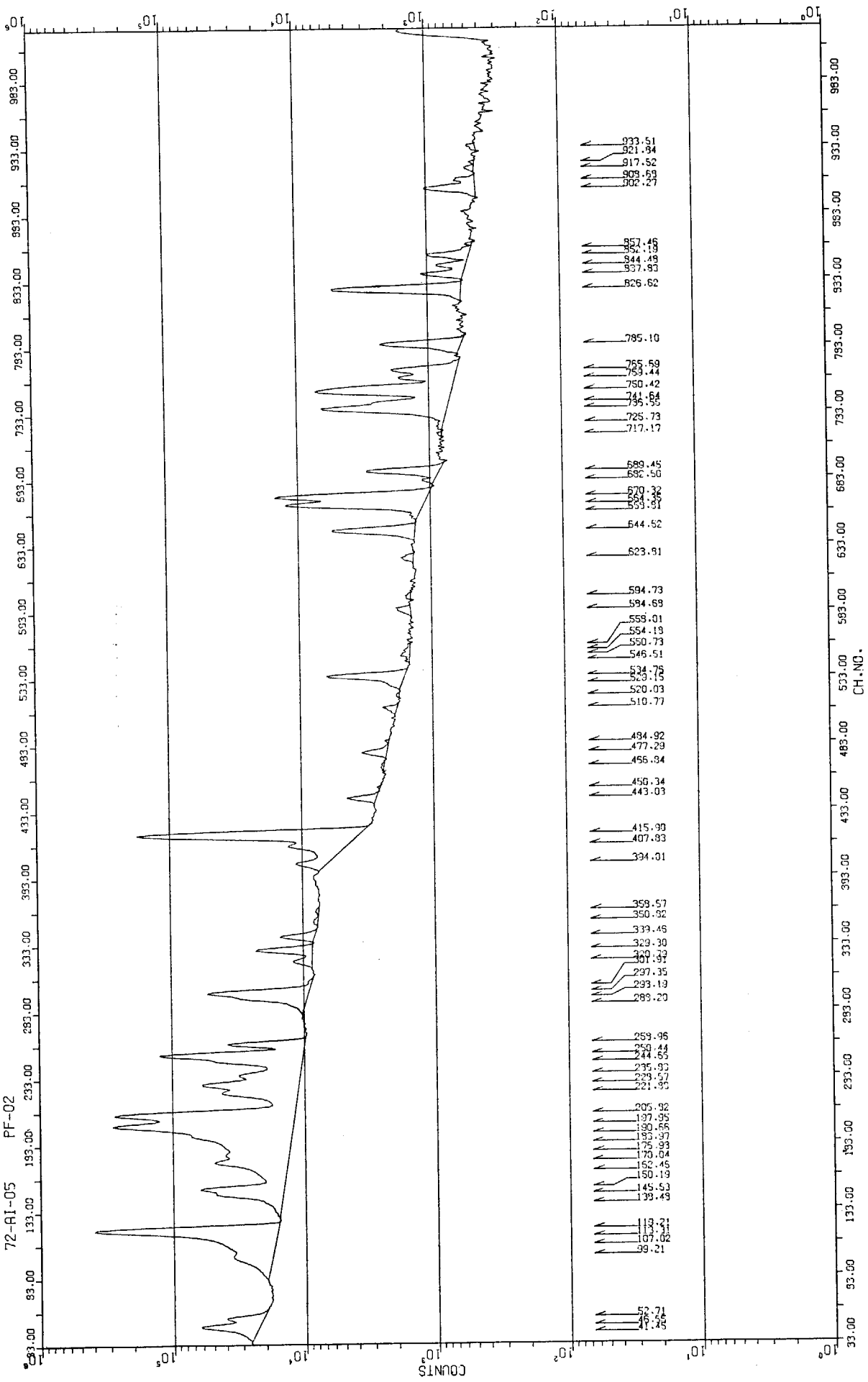

Fig. 2-2 An example of the analysis of the spectrum from the Ge(Li) detector. The predicted peak positions are indicated with vertical arrows and the determined peak regions are shown with segments of straight lines.

powers of two, and superimposed on the original spectrum. The conversion gain was set in such a way that the full width at half maximum of the 662-keV peak became 5. 0 channels. **Figure 2-1** visualizes the relationship between the detected multiplicity of the synthesized complex peak and the combined effect of the peak separation and the peak-area ratio. The left half of the figure represents the detected multiplicity when the low-energy peak is smaller while the right half gives that when the high-energy peak is smaller. Although "PKREC" worked correctly in most cases, the smaller peak was occasionally overlooked when the peak-area ratio and the separation are both small. Such mistakes are corrected in the succeeding peak-fitting process.

In order to illustrate the function of "PKREC", a result of the analysis of a spectrum of a plutonium sample containing the uranium and americium daughters, measured with the above-mentioned 50 cc Ge(Li) detector is displayed in **Fig. 2-2**. The predicted peak positions are indicated with vertical arrows and the determined peak regions are shown with segments of straight lines.

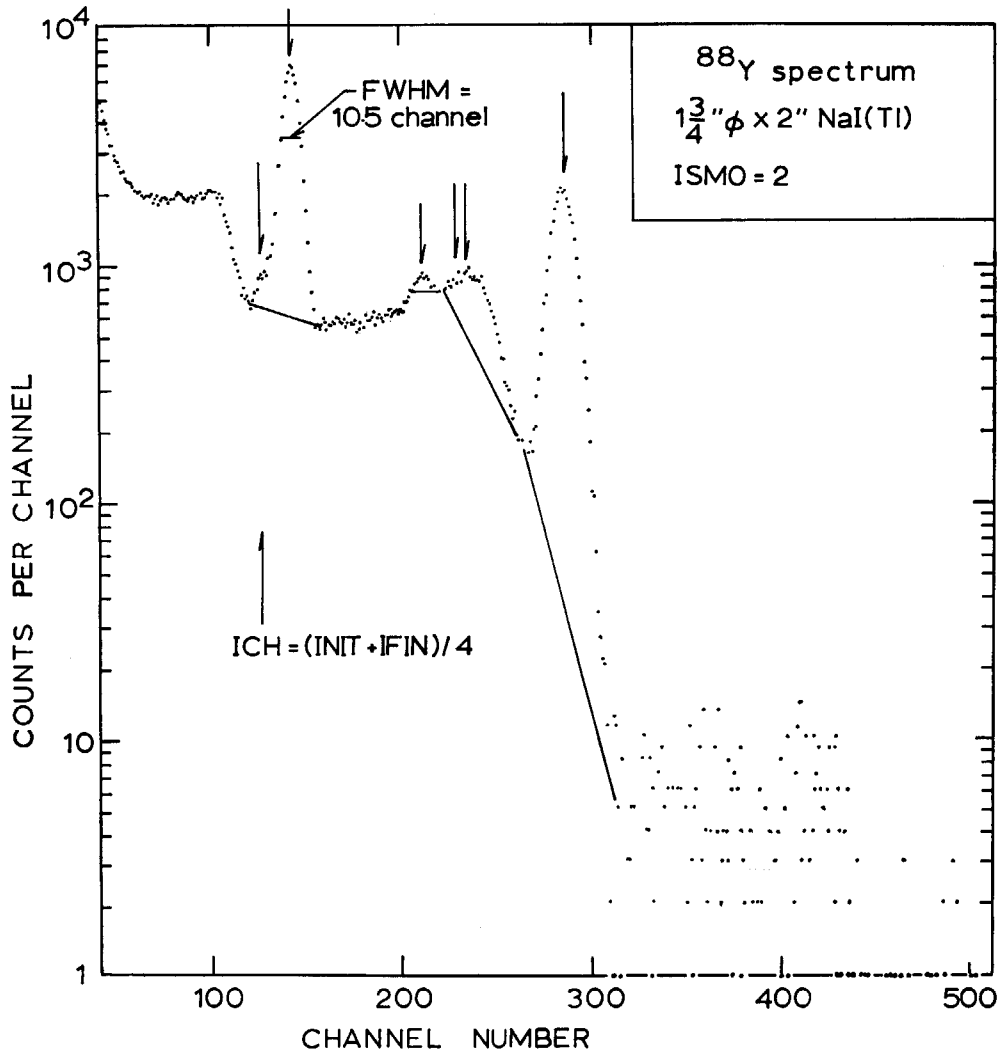

Fig. 2-3 The ^{88}Y spectrum as an example of the analysis of the low-resolution spectrum from a NaI(Tl) detector.

In **Fig. 2-3**, shown is a result of the analysis of the ^{88}Y spectrum from a $1\frac{3}{4}''\phi \times 2''$ NaI (Tl) detector. It was further found that the modified "PKREC" could be successfully applicable to rather general types of digitalized spectra, such as photometric spectra or gas chromatograms.

The peak position was found to particularly affect the fate of the succeeding fitting. The

subroutine program " PKREC " was modified in such a way that even the centroid of a half-hidden peak was assigned at the most reasonable channel as shown in **Fig. 2-2.** On the contrary, only the position where the first derivative changes its sign from positive to negative is registered in the memory core in the case of BOB 70/71[5].

The final of the major modifications of " PKREC " is the introduction of the optional choice of several functions as the Compton background level below the full-energy peaks. In BOB 70/71, only the exponential function of the channel number is used. This option was required in order to attain better consistency in the intensity determination in the photopeak method, and was subsequently introduced in the peak-fitting subprogram " PKFIT ". This option appears also in " PKREC " at the stage of judging whether a pair of closely locating peaks are well separated or overlapping each other, so as to maintain the consistency with the successive results in " PKFIT ".

The subprogram " PKREC " accompanies a subprogram " SELECT " in option, which filters small peaks out of the memory.

The general flow chart of " PKREC " is essentially the same as that given in ref. 5b.

3. Peak-fitting Process " PKFIT " in the Photopeak Method for High-resolution Spectra

3. 1 General Problems in the Peak-fitting Procedure by the Non-linear Least Squares Method

3. 1. 1 Mathematical formulation of the non-linear least squares method, " NONLIN " (Gauss's method)

Suppose $Y_i(\boldsymbol{X}_i)$ is a dependent variable of a set of m independent variables, $\boldsymbol{X}_i$;

$$\boldsymbol{X}_i=(X_{1i}, X_{2i}, \cdots\cdots\cdots\cdots, X_{mi}). \tag{3-1}$$

Let $f(\boldsymbol{X}; \boldsymbol{\alpha})$ be a function fitted to Y with a set of n adjustable parameters, $\boldsymbol{\alpha}$;

$$\boldsymbol{\alpha}=(\alpha_1, \alpha_2, \cdots\cdots\cdots\cdots, \alpha_n), \tag{3-2}$$

and one obtains the equation;

$$\begin{aligned} Y_i(\boldsymbol{X}_i)&=f(\boldsymbol{X}_i; \boldsymbol{\alpha}) \\ &=f(\boldsymbol{X}_i; \boldsymbol{\alpha}^0)+\sum_{j=1}^{n}\frac{\partial f(\boldsymbol{X}_i; \boldsymbol{\alpha}^0)}{\partial \alpha_j^0}\cdot(\alpha_j-\alpha_j^0)+O(\Delta\boldsymbol{\alpha})^2 \end{aligned} \tag{3-3}$$

where $\boldsymbol{\alpha}^0$ is a set of appropriately chosen values of $\boldsymbol{\alpha}$. The last term in Eq.(3-3) represents the residue. The condition of minimizing the sum of the squares of differences is then given by the simultaneous equations;

$$\frac{\partial \sum_{i=1}^{m} w_i\{Y_i(\boldsymbol{X}_i)-f(\boldsymbol{X}_i, \boldsymbol{\alpha}^0)\}^2}{\partial \alpha_j}=0, \quad 1\leqq j\leqq n, \tag{3-4}$$

where w_i is the weight for the i th observed value. The values of the parameters to be used after the first iteration are, therefore, given by

$$\alpha_j=\alpha_j^0+\Delta\alpha_j, \tag{3-5}$$

where $\Delta\alpha_j$ is the solution of the secular equation;

$$\boldsymbol{A}\cdot\Delta\boldsymbol{\alpha}=\boldsymbol{B} \tag{3-6}$$

with

$$\boldsymbol{A}=\begin{pmatrix} a_{11}, \cdots\cdots, & a_{1n} \\ \vdots & \vdots \\ a_{n1}, \cdots\cdots, & a_{nn} \end{pmatrix},$$

$$\boldsymbol{B}=\begin{pmatrix} b_1 \\ \vdots \\ b_n \end{pmatrix}, \quad \Delta\boldsymbol{\alpha}=\begin{pmatrix} \Delta\alpha_1 \\ \vdots \\ \Delta\alpha_n \end{pmatrix},$$

$$a_{jk}=\sum_{i=1}^{m} w_i \frac{\partial f(\boldsymbol{X}_i;\boldsymbol{\alpha}^0)}{\partial \alpha_j}\cdot\frac{\partial f(\boldsymbol{X}_i;\boldsymbol{\alpha}^0)}{\partial \alpha_k}$$

and

$$b_j=\sum_{i=1}^{m} w_i \frac{\partial f(\boldsymbol{X}_i;\boldsymbol{\alpha}^0)}{\partial \alpha_j}\cdot(Y_i-f(\boldsymbol{X}_i;\boldsymbol{\alpha}^0)).$$

The fitting process is repeated until convergence is achieved.

3. 1. 2 Initial estimates for the parameters

A non-linear least squares method does not necessarily promise the solution. Setting up an appropriate set of the initial estimates for the adjustable parameters becomes, therefore, indispensable to assure convergence of the fitting iteration and to save a long machine time and a large memory core.

By virtue of the ability of "PKREC", we have solved the problem of the initial parametrization for the non-linear least squares peak fitting. The subprogram "PKREC" points out approximate positions of all existing peaks, which are the most essential information for the fitting procedure. Consequently, the initial value for the peak height is given by the count at the channel number nearest to the appointed peak position. To complete the initial parametrization, we must estimate an approximate peak width. The peak width was taken to be constant over a given group of peaks. The preliminary peak width was calculated on the basis of the length of the peak region, n, the number of existing peaks, j, and the relative size of the main peak with respect to the height of the Compton continuum. The initial estimate for the full width at half maximum ($FWHM$) is taken as

$$FWHM=n/x\times 2\sqrt{0.69315}, \tag{3-7}$$

where the length of the peak region n is equal to $(f-i-1)$ with the boundary channel num-

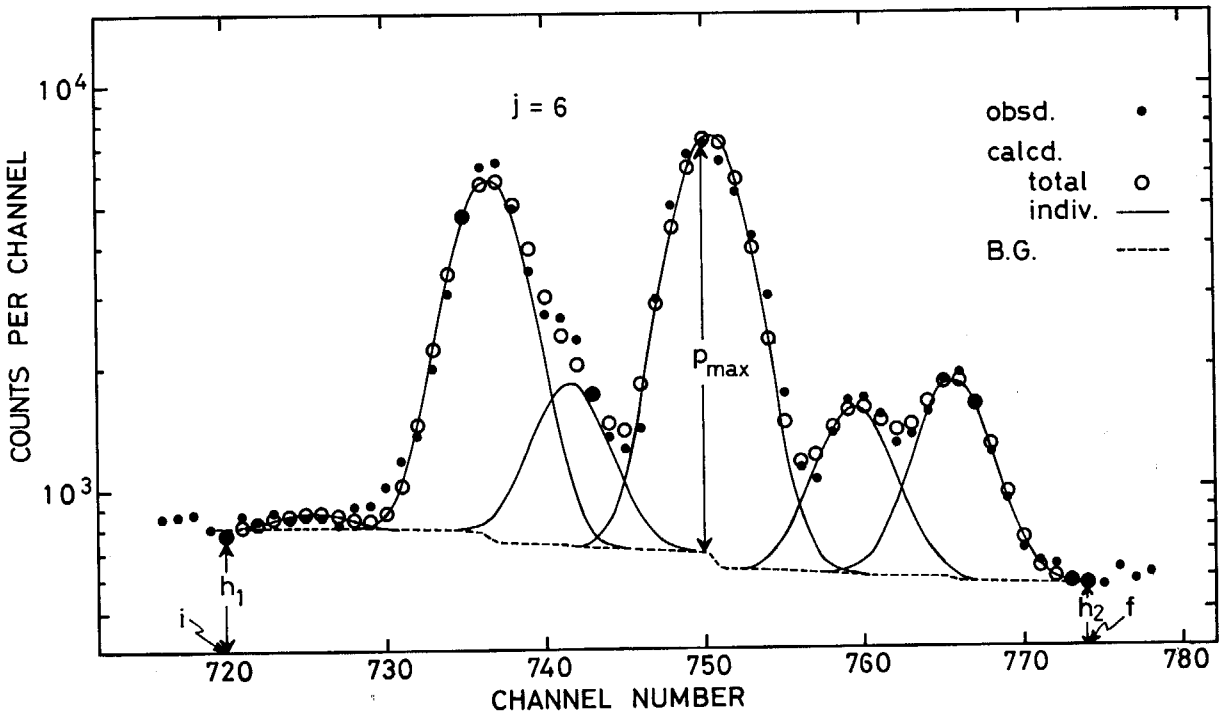

Fig. 3-1 A part of the spectrum displayed in **Fig. 2-2**, as an illustration of the initial estimation of the $FWHM$ and of the result of the least squares fit.

bers, i and f, on both sides. The x is a numerical value related to the number of peaks j and the relative size of the main peak (cf. **Fig. 3-1**);

$$x=\left\{\begin{array}{ll} 3j+3 & p_{max}/h_1>0.5 \\ 2j+3 & 0.5\geqq p_{max}/h_1\geqq 0.3 \\ j+3 & p_{max}/h_1<0.3 \end{array}\right\}. \tag{3-8}$$

3. 1. 3 Measure of the degree of agreement

The condition for judging convergence of the fitting was set as

$$|\sigma_l-\sigma_{l+1}|\leqq\sigma_0 \tag{3-9}$$

for an appropriate convergence limit σ_0, which is fixed to 10^{-6} if no specification is given by the user. The quantity σ is defined by

$$\sigma=\left[\sum_{i=1}^{m} w_i\{Y_i-f(\boldsymbol{X}_i;\boldsymbol{a})\}^2/\left(n\cdot\sum_{i=1}^{m} w_i\right)\right]^{\frac{1}{2}}\Big/\sum_{i=1}^{m} Y_i\ , \tag{3-10}$$

where the suffix l denotes the lth iteration.

There are various sources of disagreement in the peak-fitting process. Among them, the deviation due to the statistical error in counting is out of our interest at present. In the peak-fitting process, we concern the following two sources of disagreement; namely, whether the functions we have chosen for the fit to the observed data are of reasonable forms and whether we are overlooking any peaks. As for the first problem, what we should worry about is finding a function correctly reproducing the peak shapes and that giving the shape of the Compton continuum in the full-energy peak region. This problem shall be discussed in the following section together with some accompanying problems.

Let us consider the second problem first. The measure of disagreement due to the overlook of a photopeak should naturally be given by the converged value, σ_∞, of the standard deviation defined by Eq.(3-10). Because of the increase of the number of freedom, the σ_∞'s always decreases by adding extra peaks as long as the convergence is obtained. This means that we end up with either case where the fitting is failed or a better fit is obtained when an extra peak is taken in. Therefore, we can conclude that one peak has been missed in the fitting if the σ_∞'s exceeds a certain limit. In principle, one ought to be able to save any tiny half-hidden peak that "PKREC" might fail to pick up by setting the limit to a desired level.

This procedure, however, gives rise to unnecessary repetition of the fitting by failing to stop at the desirable stage, and very frequently even to misinterpretation of the spectrum by taking non-existing peaks in. That is to say, the postulate of minimizing the limit for raising the sensitivity counteracts the necessity of allowing large deviations due to the counting statistics. We have set up the above mentioned limiting condition as

$$\sigma_\infty<A_0/\{n(p_{max}\times 10^{-4})^{0.3}\} \tag{3-11}$$

with the quantities defined by Eqs.(3-7) and (3-8), where A_0 is a constant which is generally taken as unity unless otherwise given as an input data. Such a considerably large limit was chosen because "PKREC" seldom overlooks a peak with a realistic spectrum. We were, therefore, more anxious to avoid raising the multiplicity unnecessarily in the fitting stage. We have introduced an additional judging condition; namely, one disregards the second fitting trial

after the addition of one peak if the number of iterations is not smaller than the greater of 10 and twice the number of the first iterations. This condition was introduced from the experience that our non-linear least squares method generally gives very rapid convergence when it works successfully.

3. 1. 4 Fail-safe actions in the process

Since the non-linear least squares method does not always give the solution, one must build in the preventives to save the rest of the data analysis when the fitting process has ended in failure. Otherwise, the unsuccessful trial steps into a fatal error and the whole operation ceases. At the same time, one needs to extract as much information as possible even from the once failed fitting trial. We have set up a safety device at every strategic point.

First, the operation is discontinued instantly when any one of the following conditions appears; (1) the peak width becomes negative, (2) any one element of the matrix A in Eq.(3-6) protrudes over 10^{50} or under 10^{-50}, (3) an increment $\Delta\alpha_j$ of any parameter appears in Eq.(3-5) becomes more than 10^{10} and (4) the fitting procedure is iterated more than 20 times. The first three of the above conditions would be obvious to anybody. As stated in **3. 1. 3** the convergence is usually achieved very fast. We found that in most cases the operation reaches the convergence within 5 iterations or so, and the number of iterations never exceeds 20 even in the worst case if it is successful.

The above conditions concern the cases where we must give up the fitting procedure without completion. On the contrary, there are the cases in which the results are unreasonable even though the fitting has been completed. That is, solution giving the negative height to an assigned peak is a sign of the misfit and is, therefore, deleted. One may consider that we should also discard the result of the fitting if any peak position ends up outside the fitting region. However, such a result was found to give a fairly correct solution if one disregards the peaks whose positions are outside the fitting region. Therefore, the set of the final values for the parameters are not discarded but used as the initial values for another fitting run in which the peaks assigned at out-of-range positions are omitted.

When the first trial has not been succeeded, the second attempt is undertaken after adding one more peak (as in the case in which the agreement of Eq.(3-11) was not satisfactory in the first run). The new peak was assigned as the mid-point of the broader one of the intervals between either peak-boundary and the peak nearest to it, since it most likely happens at either end of a lump of peaks if "PKREC" would overlook a peak at all. The initial plan of setting up the remedy for missing a peak on the other side has been abondoned because "PKREC" does not practically miss more than one peak in a given group and the extra protection brings no useful results even if the convergence is attained.

Instead, we noted the possibility that "PKREC" might detect an extra peak besides actually existing ones in a group. This can happen especially when one treats a spectrum containing a large full-energy peak like that of the pure ^{137}Cs source (cf. **Fig. 3-2a**), measured with a detecting system of relatively poor quality*). As will be discussed in the next section, the shape of the peak given by the Ge(Li) detector is not so simple and clean as that by scintillation detectors even though the leakage current is suppressed to the least magnitude. The effect appears as the asymmetry of the peak shape and tailing at the low-energy side. It just happens

*) In order to reduce the chance of detecting such a pseudo-peak, the peak-searching procedure is repeated for a peak whose height is greater than 10^5 counts and its ratio to the foot exceeds 20, after the threshold is raised by the factor of $\sqrt{10}$.

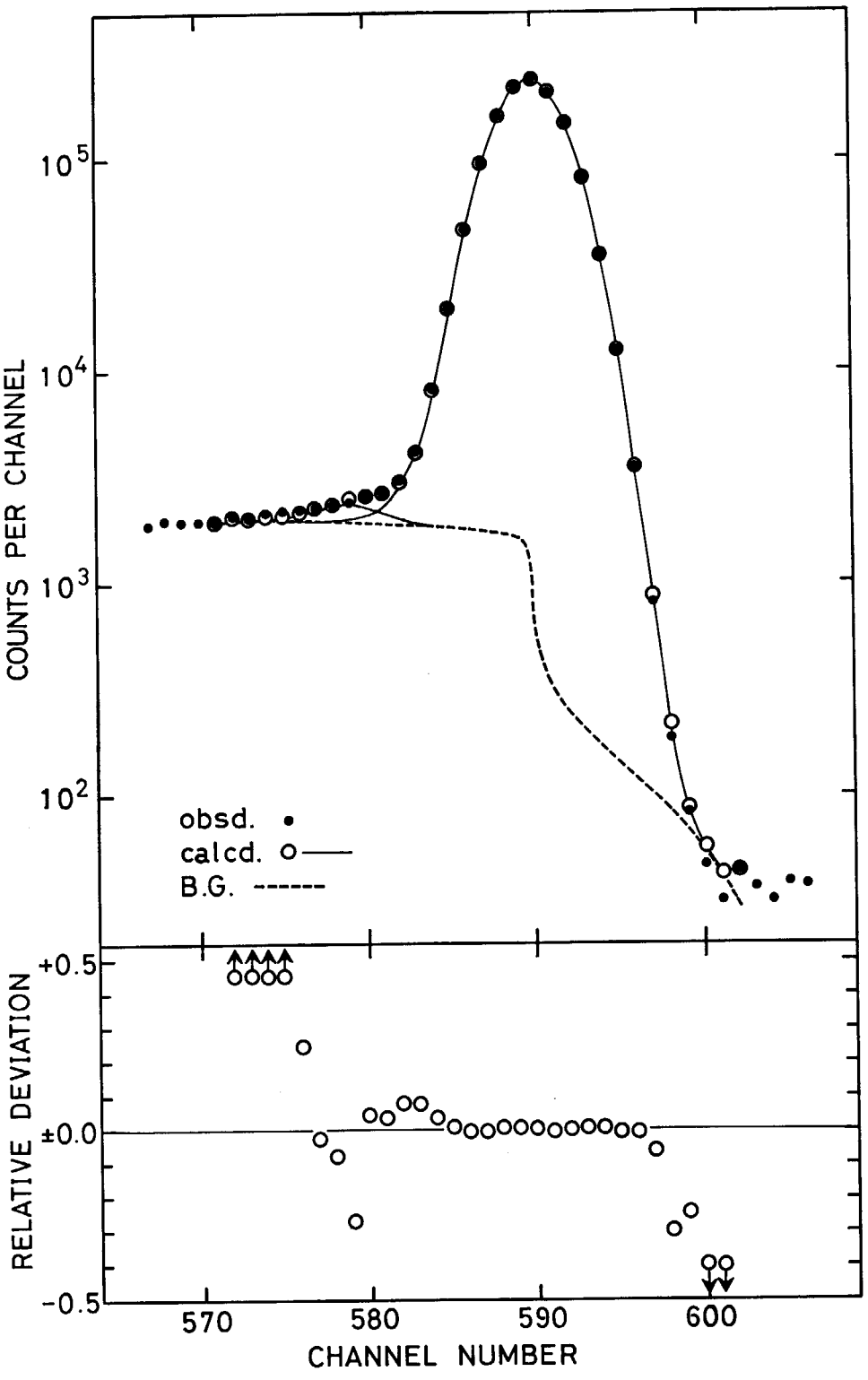

Fig. 3-2 a

Fig. 3-2 The ^{137m}Ba 662-keV peak given by a Ge(Li) detector. The tailing on the low-energy side causes an additional spurious peak (**Fig. 3-2a**). The spurious peak is removed by raising the threshold for the peak detection by a factor of $\sqrt{10}$ (**Fig. 3-2b**). The relative deviation is taken for the surplus count above the base line.

at the end of this tail, if it is large enough, that an pseudo-peak is detected by "PKREC". The countermeasure will therefore be clear. We added a third trial, which is to be performed only when the preceding two trials have both failed. The trial is such that the smallest

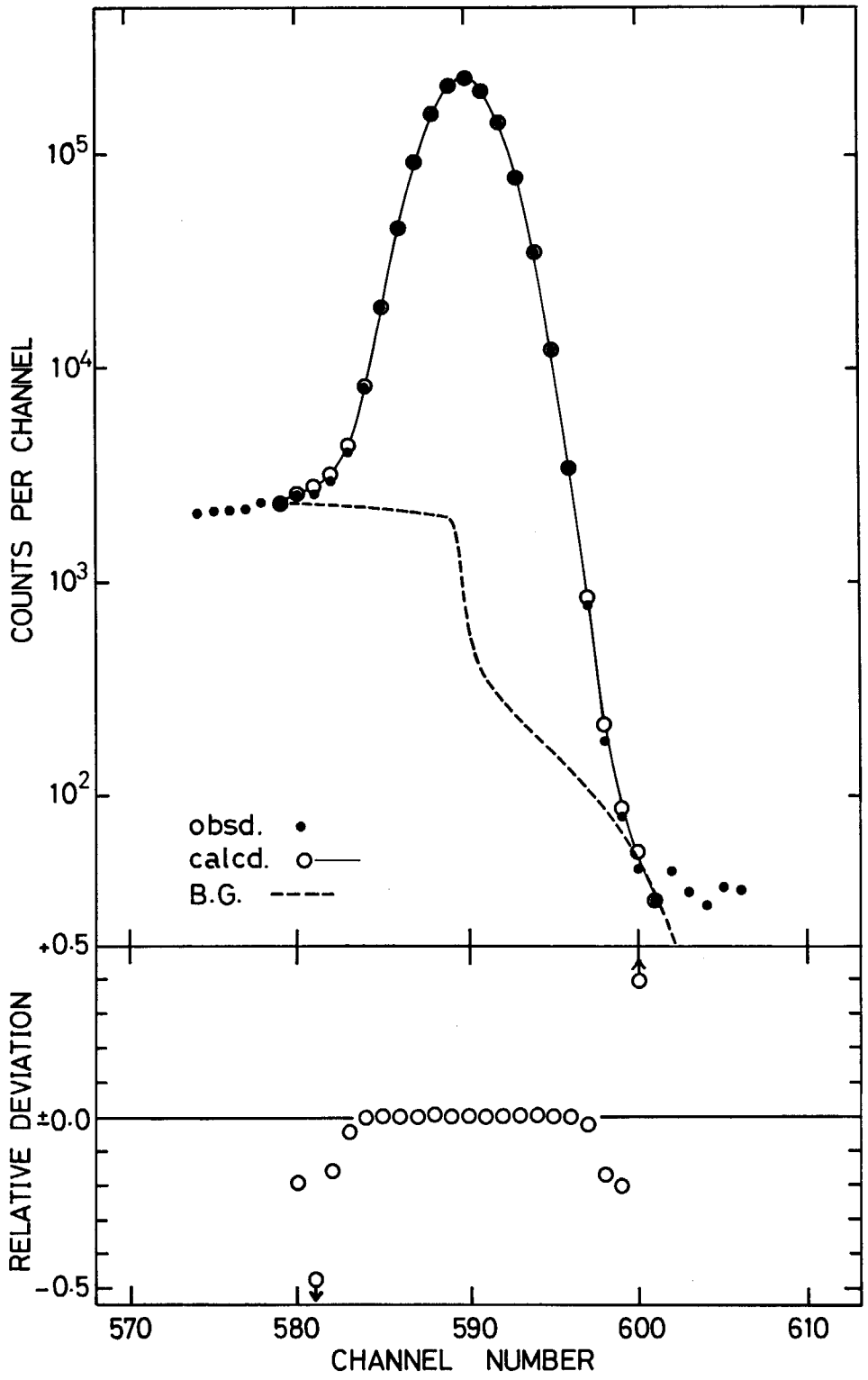

Fig. 3-2 b

among the initially appointed peaks in the group is omitted, and the fitting is started with the remaining peaks.

The flow chart of "PKFIT" is shown in **Fig. 3-3.**

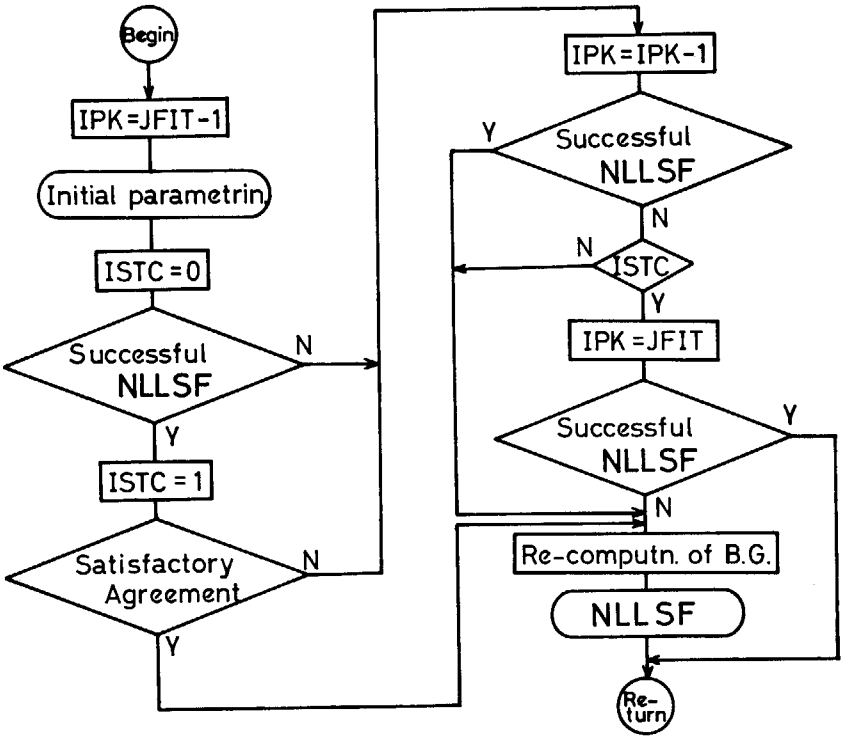

Fig. 3-3 Flow chart of "PKFIT".

3. 2 Special Problems in the Peak Fitting of the Ge(Li) Spectrum

3. 2. 1 Effects of the data smoothing and the weight in the fitting

As stated in refs. 5, the effect of the data smoothing is quite remarkable in the peak-searching step, so that we have decided to perform data smoothing as long as possible prior to the peak search. This means that there are two sets of available data, raw and smoothed, which are to be the base of the fitting. Which of them should we choose ?

On one hand, the smoothing procedure reduces statistical fluctuations. This is certainly an advantage from the viewpoint of the fitting. On the other hand, it inevitably distorts the spectrum especially in the vicinity of the full-energy peak. This effect is expected to cause a serious error when more than one peak are overlapping one another. From this reason, we have decided to perform the fitting procedure on the basis of the raw (non-smoothed) data.

The next problem is how one should weight each data point in the fitting procedure. We have chosen, as the weight of a given channel, the reciprocal of the sum of the number of counts and the background counts at the channel, or the sum of the surplus counts above the background level and twice the background counts at the channel. As a result of the comparison between the above weighting and the equal weighting, we found that the former resulted in fairly unifrom fit over the fitting range whereas the latter tended to give somewhat poorer fit in the outskirt of the peak as a consequence of laying more stress on the agreement around the top of the peak. Though this difference does not cause much deviation in the determined values of the peak center and peak area for a single peak, the situation changes in a great deal for closely overlapping peaks. In **Fig. 3-4**, we have shown the determined values of peak positions and peak areas for the artificially superimposed spectrum in which two peaks of various intensity ratios were separated by 5 channels. The peak area is normalized to that of the pure ^{137}Cs spectrum

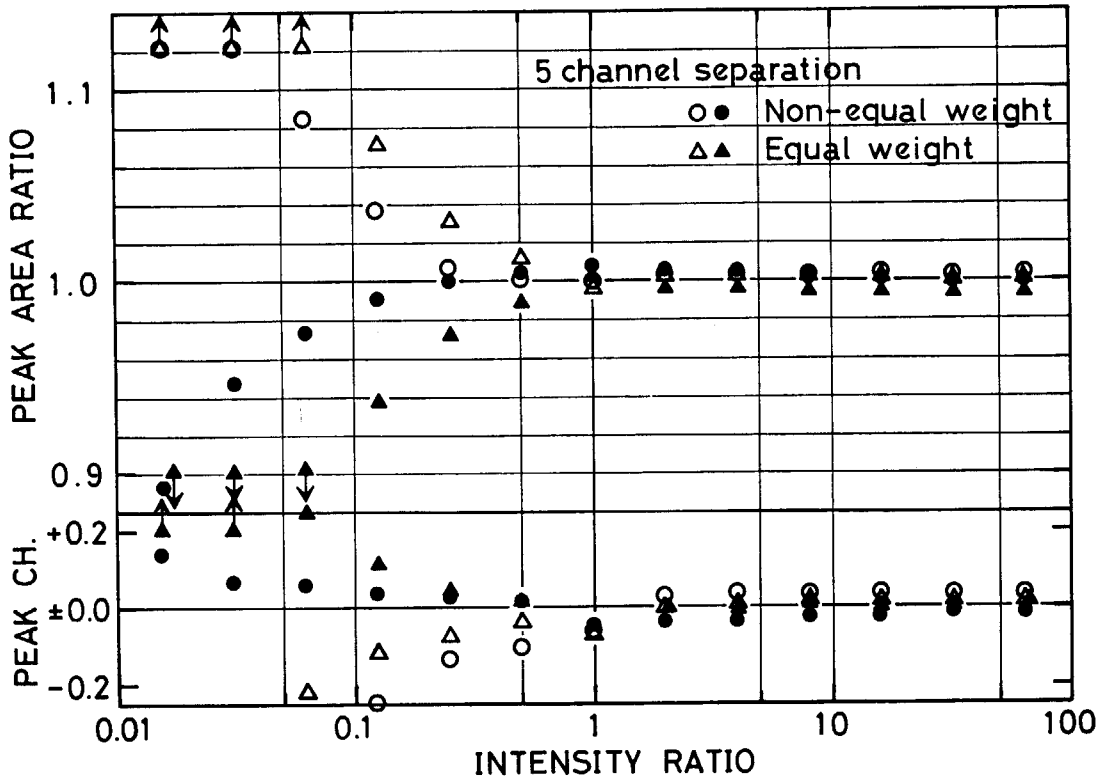

Fig. 3-4 Effect of the weight on the consistency of the peak area and the accuracy of the peak position. Results are shown for artificially composed doublets with a single peak (the ^{137m}Ba 662-keV peak) with various intensity ratios, in which the peak separation is fixed to 5.0 channels. The open marks indicate the result of the lower-energy peak, whereas the closed marks are for the higher-energy peak.

and the centroid of the ^{137m}Ba full-energy peak is taken to be the reference point of the peak position. From the result of **Fig. 3-4**, we have decided to generally use in the fitting process the former type of the weight rather than the equal weight.

3. 2. 2 Functional form of the full-energy peak

The shape of the full-energy peak may be expressed basically with the Gaussian function in the analogy of that given by the NaI(Tl) detector[4]. It is, however, well known[8] that Ge (Li) detectors give the peak shape with much greater distortion from the simple Gaussian form, because of the complex charge-collection mechanism. The distorted peak can be described as an asymmetric Gaussian curve with a tail on the low-energy side.

The asymmetric Gaussian curve can be constructed most simply by connecting two Gaussian curves with different widths at the top, the centroid of the peak. Let us define the degree of the asymmetry, the skewness factor, WDR as the ratio of the width parameter σ of the right-half Gaussian to that of the left-half. The full width at half maximum is then given by

$$\begin{aligned} FWHM &= \sqrt{1.3863}\ (\sqrt{\sigma_L} + \sqrt{\sigma_H}) \\ &= \sqrt{1.3863\ \sigma_L}\ (1 + \sqrt{WDR}). \end{aligned} \tag{3-12}$$

The skewness factor, WDR, of a given detector system can be determined beforehand by using a set of the standard spectra so as to give the best fit. **Figure 3-5** shows two cases of the results obtained for two Ge(Li) detectors. In **Fig. 3-5a**, the WDR can be regarded as independent of the energy, while it decreases with increasing energy in the case of **Fig. 3-5b**.

In SAMPO[8], ROUTTI and PRUSSIN approximate the peak shape by an analytical function that

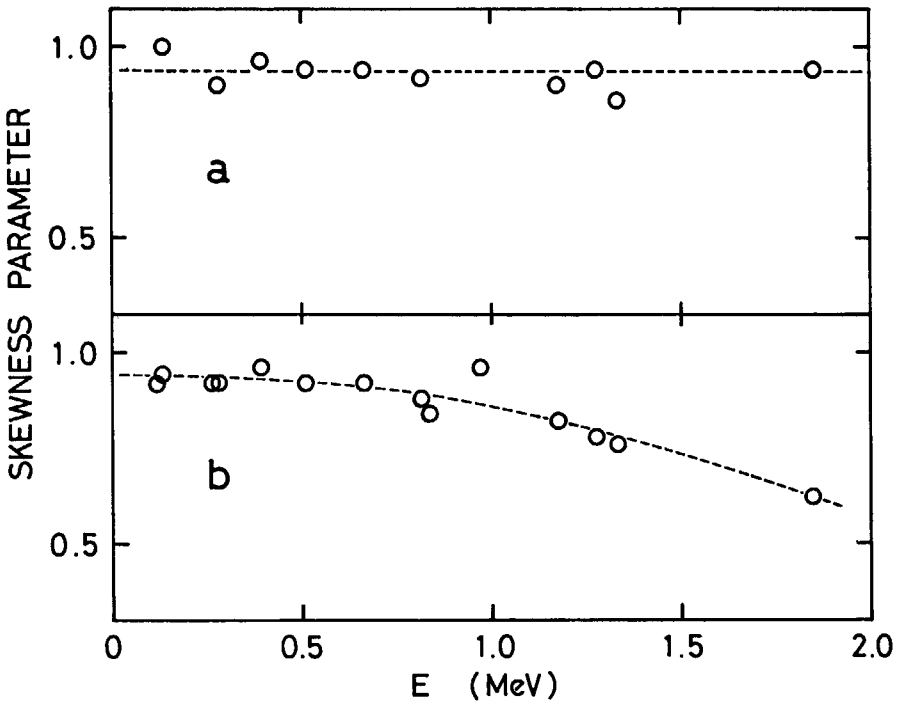

Fig. 3-5 Skewness factor as a function of the photopeak energy. Two cases are displayed ; a) the skewness factor is constant and b) it decreases with the energy.

consists of a Gaussian with provisions for tailing on both low- and high-energy sides lying on an adjustable linear background. In the present work, we use a main skew Gaussian superimposed by a similar curve with the same width parameter. Therefore, additional free parameters to describe the tail are the size ratio and the separation between the centroids of the two curves. The values of the parameters should again be determined in advance with a set of the standard spectra.

The total number of the parameters to express a single peak is five in the present work, while it is seven in SAMPO. The presently proposed shape function is believed to be more flexible in adjusting itself to the peak asymmetry and tailing since the freedom is explicitly separated for them. In **Fig. 3-6**, the situation of the fitting is depicted for various shape functions.

3. 2. 3 Background continuum and peak-area determination

The remaining problem in the determination of the peak area is how to estimate the amount of the background continuum below the peak. This problem has attracted many author's attention. One may consider that the method proposed by COVELL[10] succeeds in excluding the effect of the background shape. But it has some limitations ; first, it can be applied only to single peaks, and second, it requires a sufficient number of channels in the peak region that is rarely realized in the measurement with Ge(Li) detectors. As seen in the following chapter (cf. **Figs. 4-6** and **4-7**), the COVELL's method turned out to be considerably affected by the background shape after all as pointed out by STERLINSKI[11]. From these reasons, we have abandoned the method.

As a matter of fact, the choice among various types of the background shape does not make much difference in the resulting peak area as long as one concerns a singlet or the greater peak in a doublet. This is seen, for example, in **Fig. 3-7**. The figure indicates the consistency in the

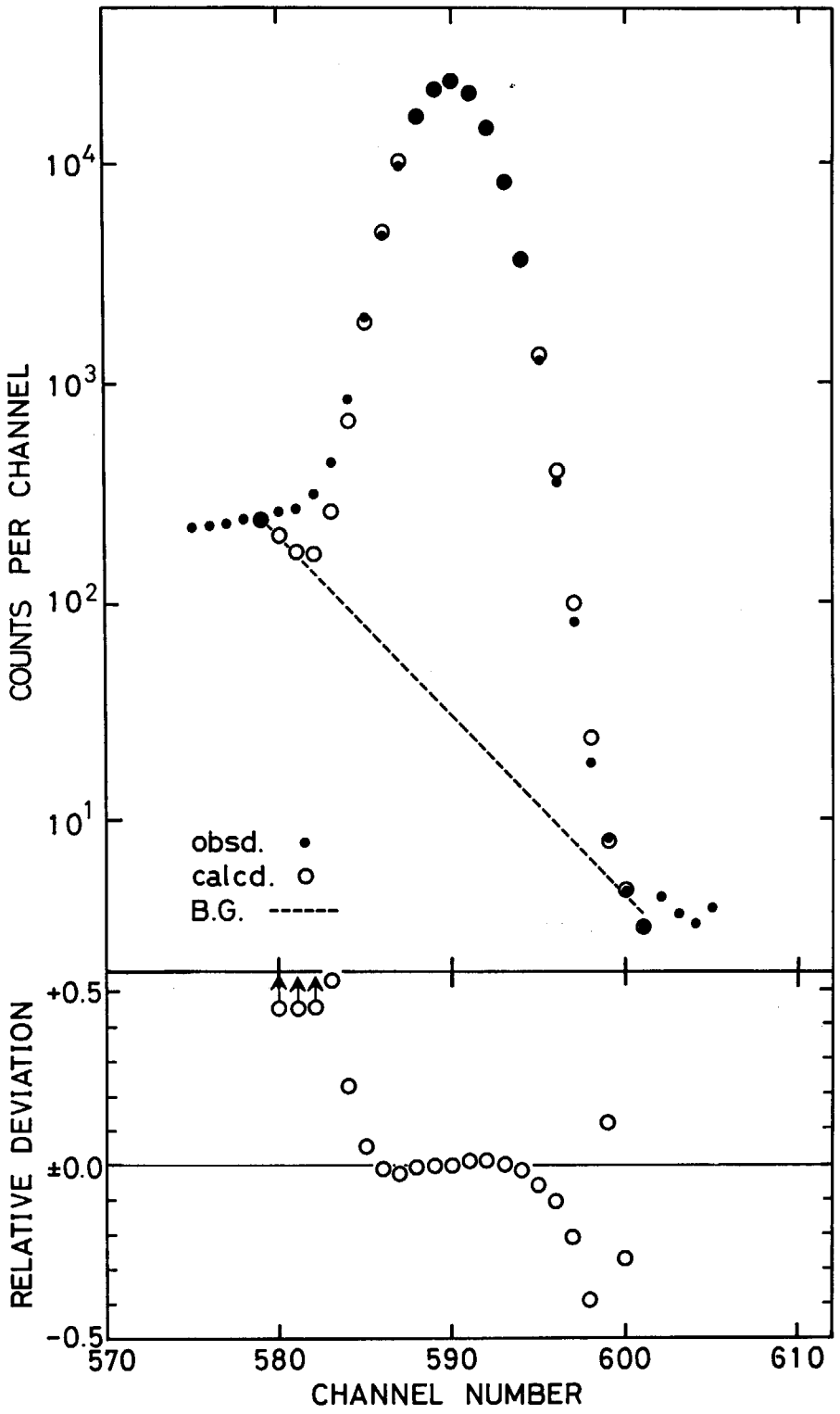

Fig. 3-6 a

Fig. 3-6 Fit of the observed full-energy peak to various shape-functions: a) a Gaussian curve on the exponential background, b) an asymmetric Gaussian curve with the skewness factor of 0.94 on the exponential background, and c) an asymmetric Gaussian curve having a tail with the skewness factor of 0.94 on the sigmoid background with $IBG=4$ (cf. Eqs.(3-13) and (3-14)). The relative deviation is taken for the surplus count above the base line.

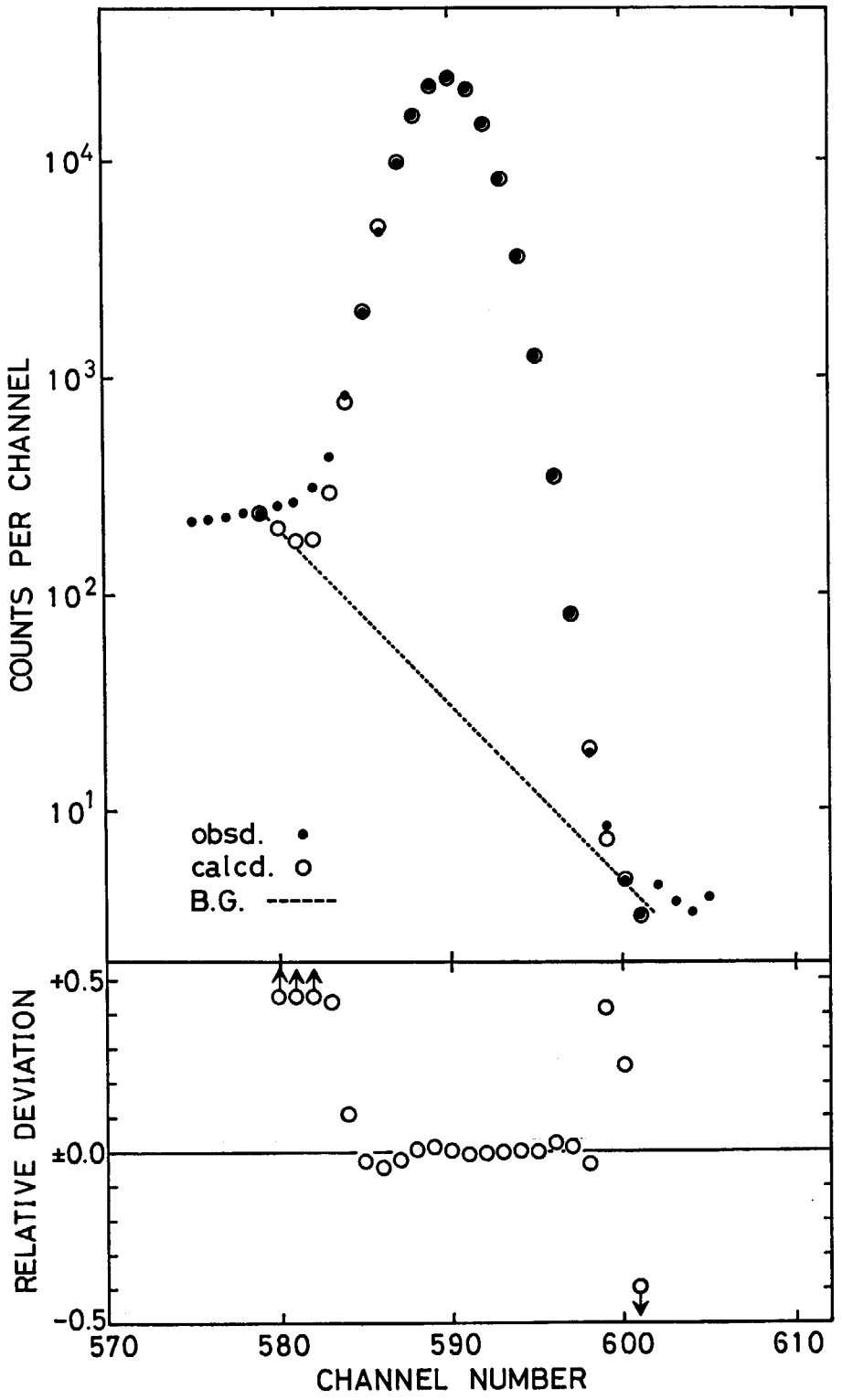

Fig. 3-6 b

evaluated peak area and the constancy of the appointed position of the centroid, found for the low-energy peak in artificially synthesized spectra with two peaks of 100 channel separation. The triangles indicate the result for the cubic background and the inverted triangles are for the exponential background, in comparison with circles for the best case of a sigmoid background, $IBG=4$. Here, the skew Gaussian curve of $WDR=0.94$ with the predetermined tail was used as the fitting function in all the cases. The peak position was found to shift by 0.02 channel

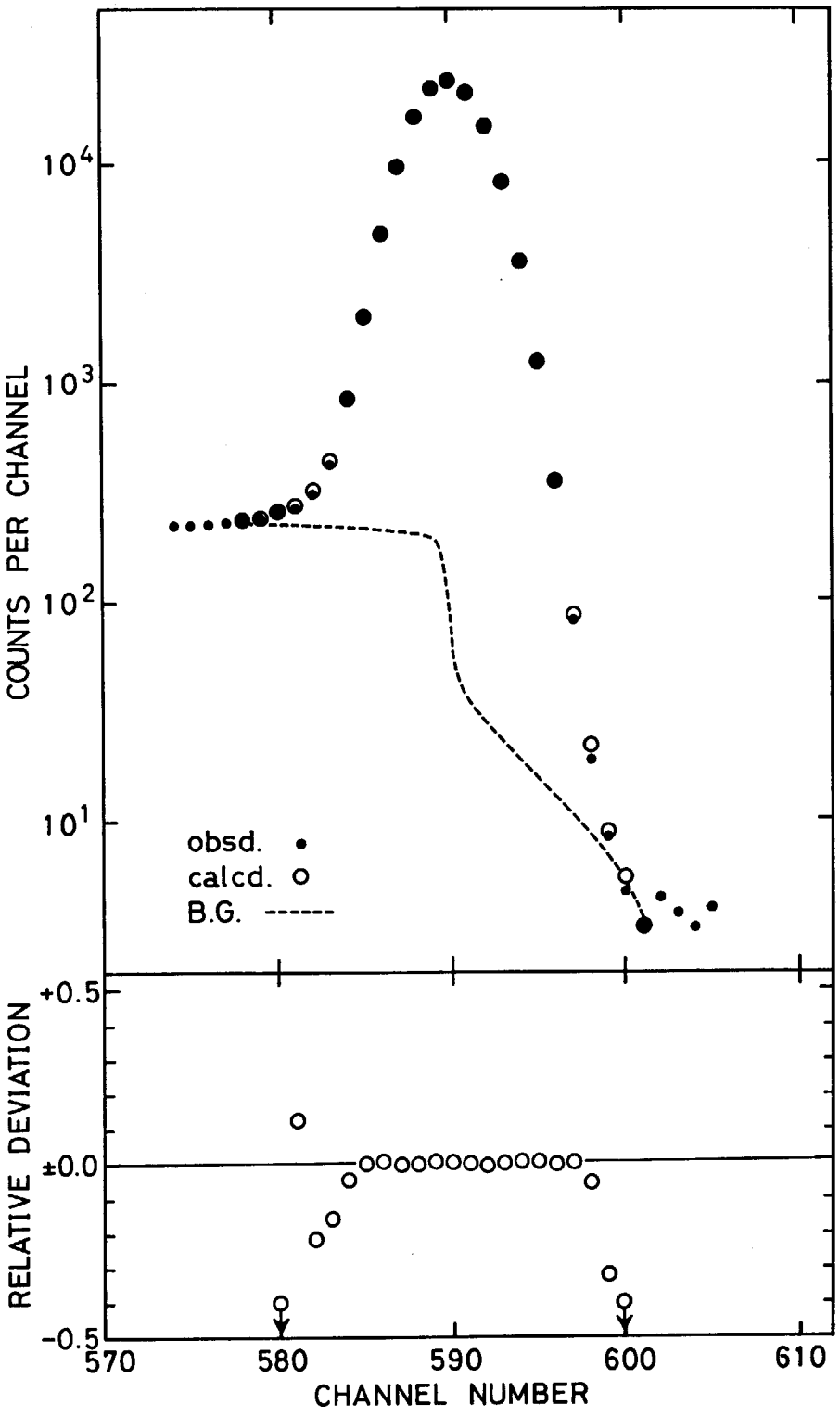

Fig. 3-6 c

when the sigmoid background was introduced. **Figure 3-8** was further added in order to show that the consistency also holds between the results of "PKREC" (no fitting) and those of "PKFIT" (fitting). The difference of 0.04 channel in the determined peak positions was brought because of the difference between the parabola fitting and the fit to the skew Gaussian curve, besides the above-mentioned 0.02-channel shift due to the introduction of the sigmoid background. These deviations of the peak position, therefore, need to be corrected in the

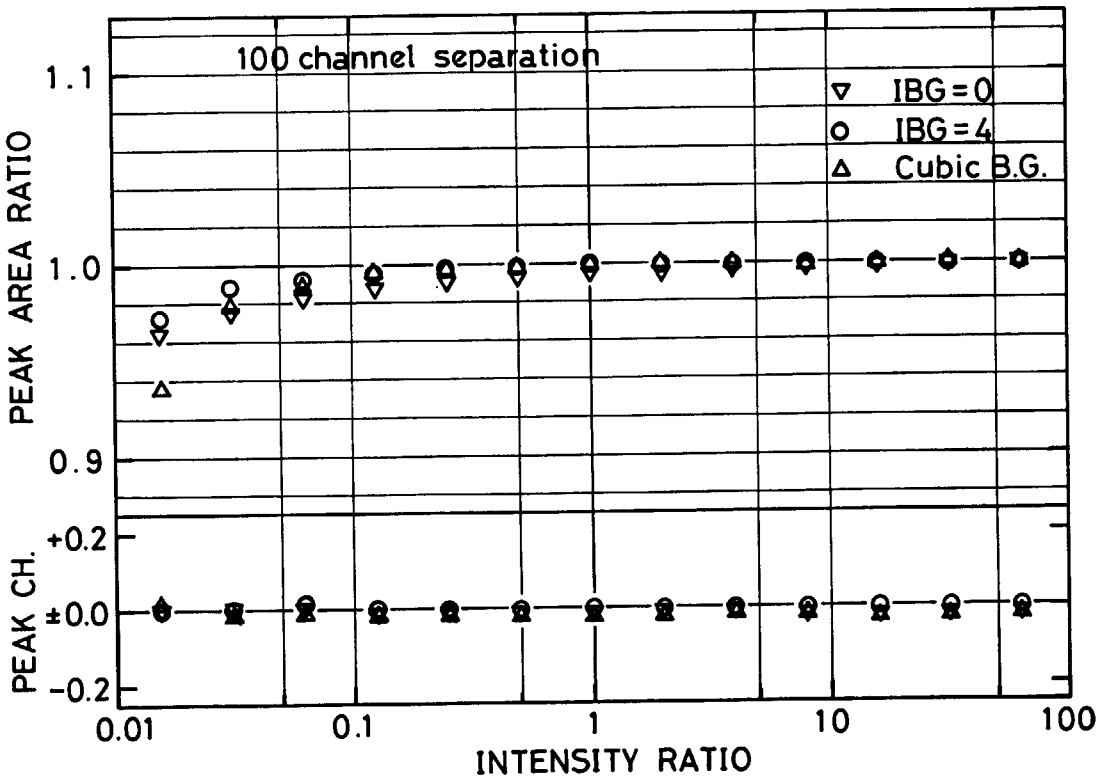

Fig. 3-7 Consistency of the evaluated peak area and the accuracy of the appointed peak position for peaks of various sizes lying on the Compton plateau. The Compton plateau underneath the peak is approximated by the exponential (triangles), the sigmoid curve with $IBG=4$ (circles), or the cubic polynomial (inverted triangles).

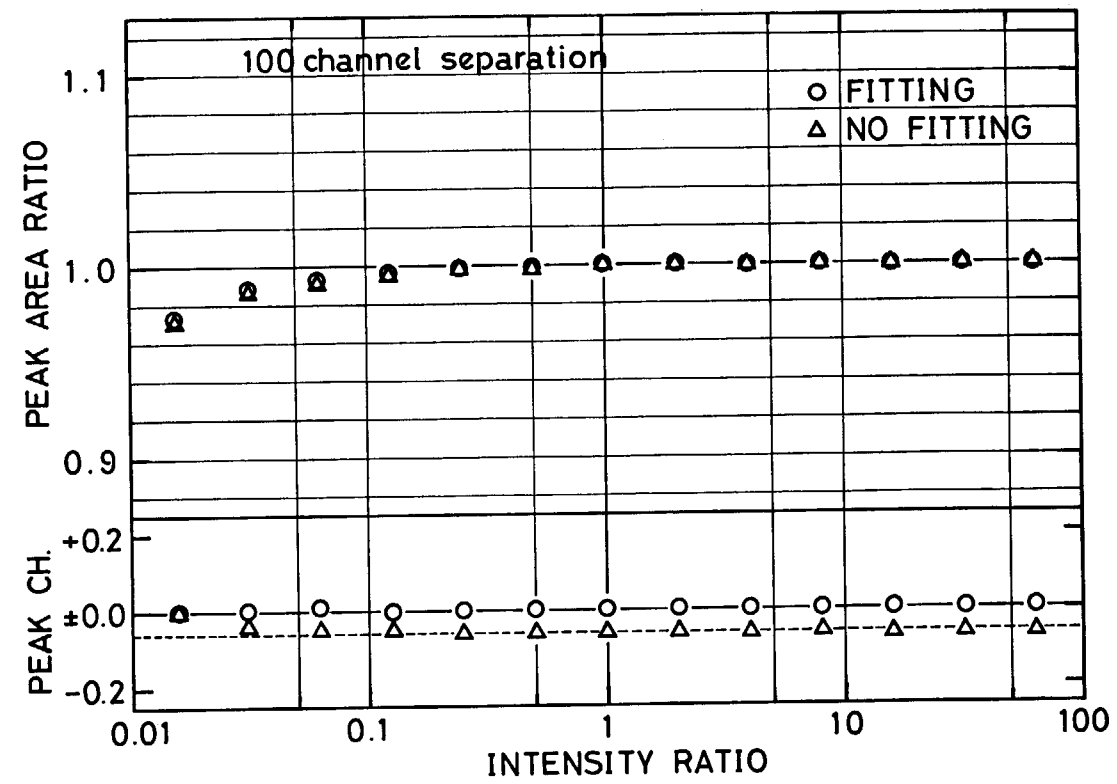

Fig. 3-8 Comparison of the results between "PKREC" (triangles) and "PKFIT" (circles) for peaks of various sizes lying on the Compton plateau. No significant discrepancy is observed between the summed and integrated peak areas, whereas there is a consistent deviation of 0.06 channel in the peak position determined in "PKREC" and in "PKFIT".

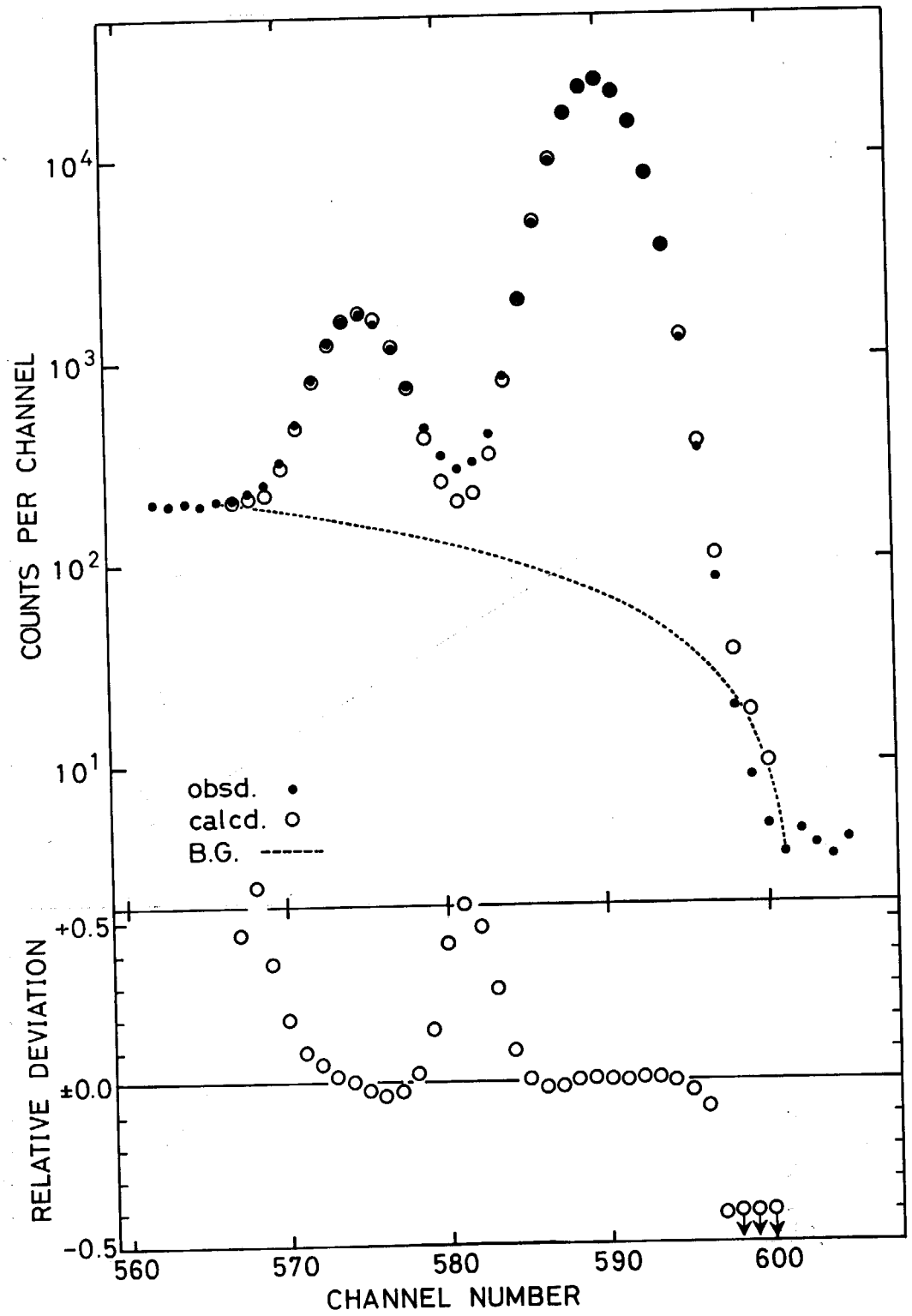

Fig. 3-9 Fit of a doublet with the intensity ratio of 1/16 and the peak separation of 15 channels (*FWHM* of each peak being 5.0 channels) to an asymmetric Gaussian curve with a tail on the linear background. The relative deviation is taken for the surplus count above the base line.

program.

For small peaks in a multiplet, different background shapes give rise to different results. The most naive function as the background continuum would be either the linear or the exponential function. Relatively speaking, the former oversubtracts the background on the high-

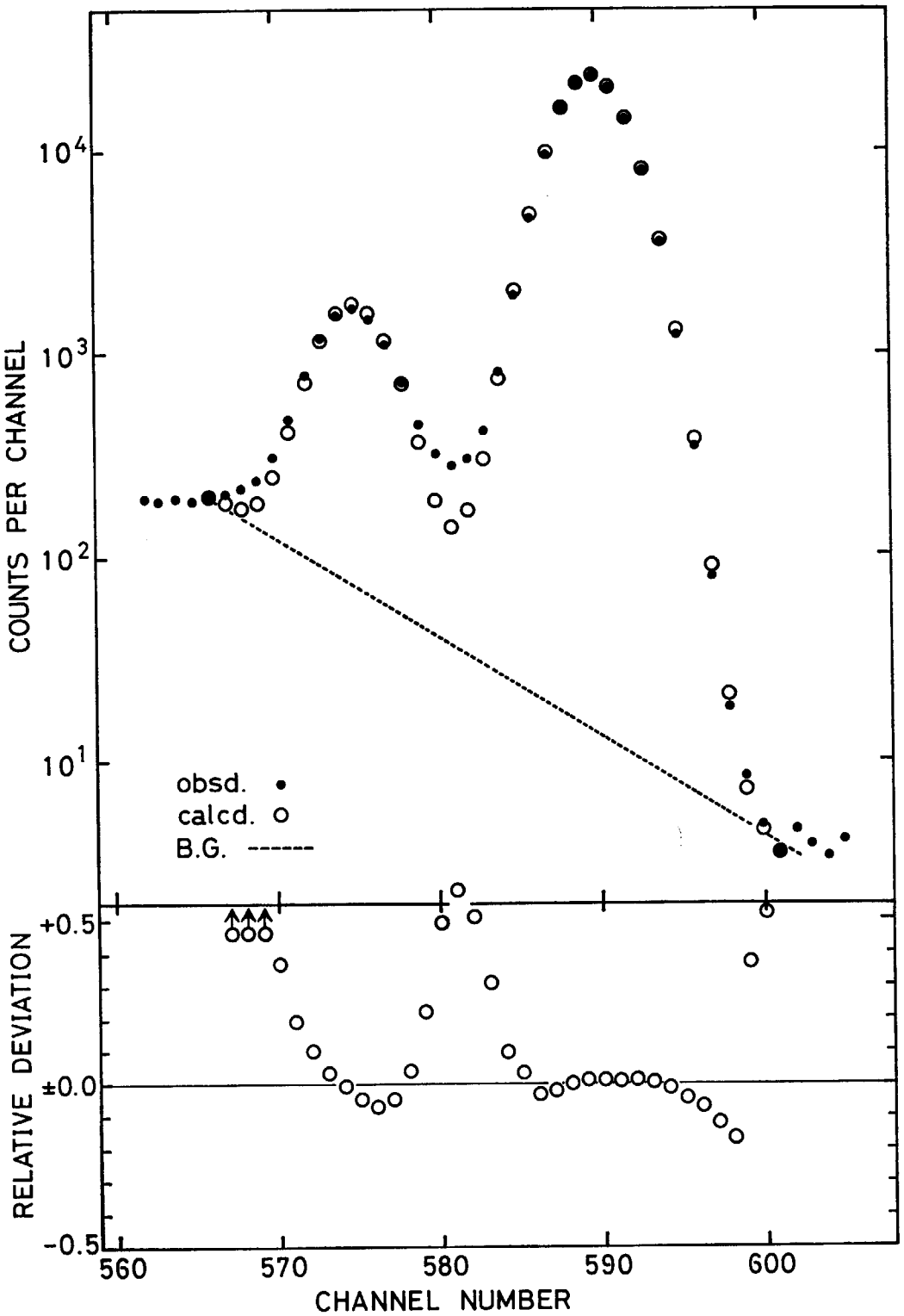

Fig. 3-10 Fit of a doublet with the intensity ratio of 1/16 and the peak separation of 15 channels (*FWHM* of each peak being 5.0 channels) to an asymmetric Gaussian curve with a tail on the exponential background. The relative deviation is taken for the surplus count above the base line.

energy side while the latter underestimates it on the low-energy side. This is seen in **Figs. 3-9** and **3-10** where the low-energy peak is separated by 15 channels the intensity of which is one-sixteenth of the high-energy peak. More prominent disagreement is, however, observed in the trough region commonly in either figure. It indicates the background being underestimated in

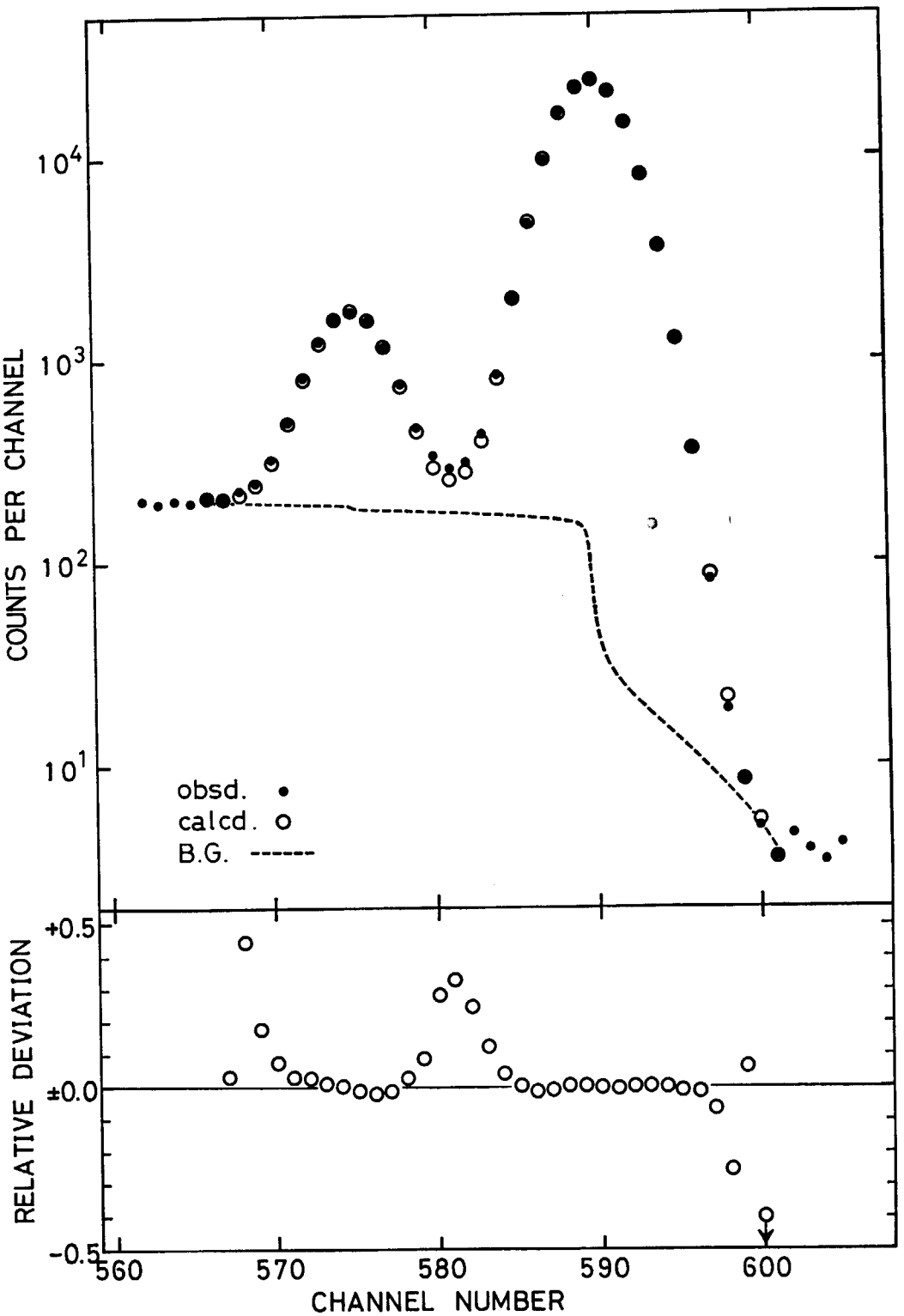

Fig. 3-11 Fit of a doublet with the intensity ratio of 1/16 and the peak separation of 15 channels (*FWHM* of each peak being 5.0 channels) to an asymmetric Gaussian curve with a tail on the sigmoid background with $IBG=4$(cf. Eqs.(3-13) and (3-14)). The relative deviation is taken for the surplus count above the base line.

the low-energy side. The situation is much improved when one assigns a stepwise function to the background of each peak, as shown in **Fig. 3-11**: The background function has been defined by

$$y(x)=\sum_{j=1}^{m} p_j a(x-x_j^0)^{1/n}+b, \tag{3-13}$$

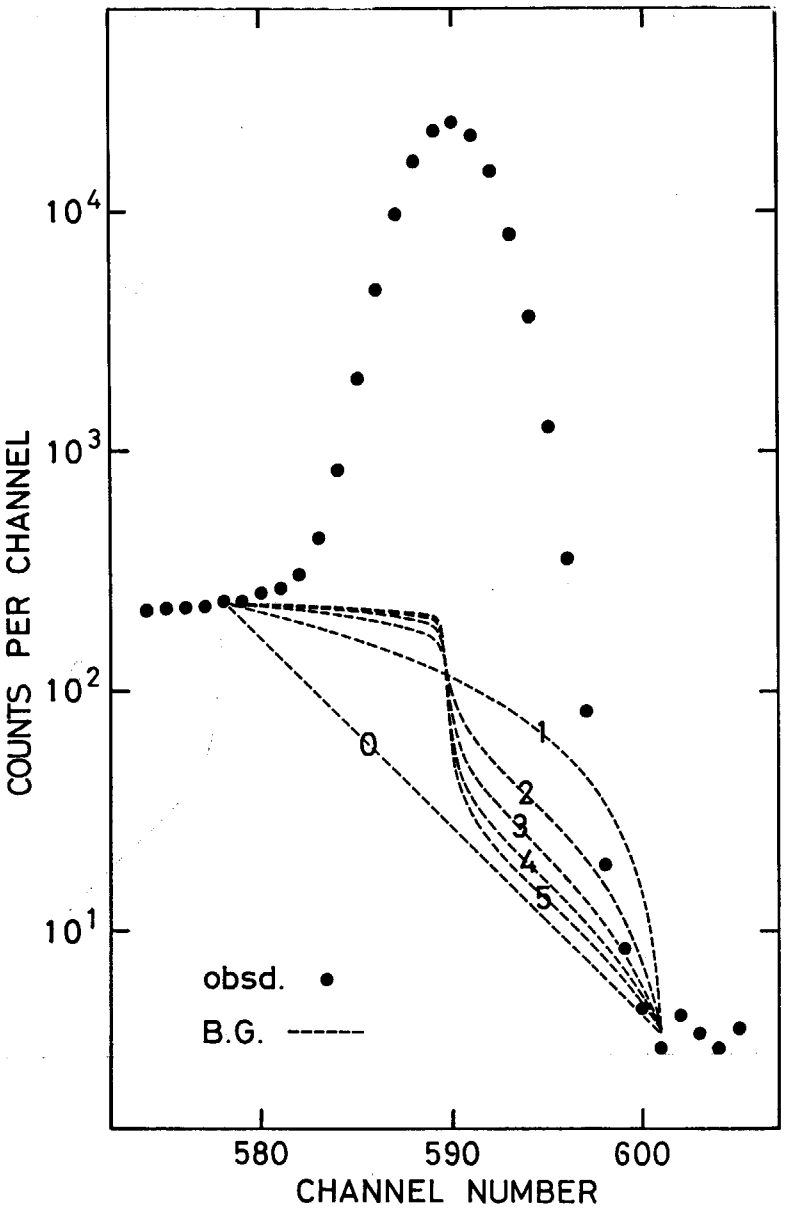

Fig. 3-12 An illustration of various background functions designated with the numbers representing the IBG : the exponential ($IBG=0$), linear ($IBG=1$), and various sigmoid ($IBG=2$ through 5) functions.

where the summation should be carried out for all the existing peaks whose relative intensity and centroid are denoted with p_j and x_j^0, respectively. The quantity n is related to the number IBG as

$$n=2\times IBG-1, \qquad \text{for } IBG\neq 1, \tag{3-14}$$

while a and b are determined from h_1 and h_2, the numbers of counts at the peak boundary channels (cf. **Fig. 3-1**), as

$$a=\frac{h_2-h_1}{\sum_{j=1}^{m} p_j\{(x_j^0-i)^{1/n}+(f-x_j^0)^{1/n}\}} \tag{3-15}$$

and

$$\begin{aligned} b&=h_1+a\sum_j p_j(x_j^0-i)^{1/n} \\ &=h_2-a\sum_j p_j(f-x_j^0)^{1/n}, \end{aligned} \tag{3-16}$$

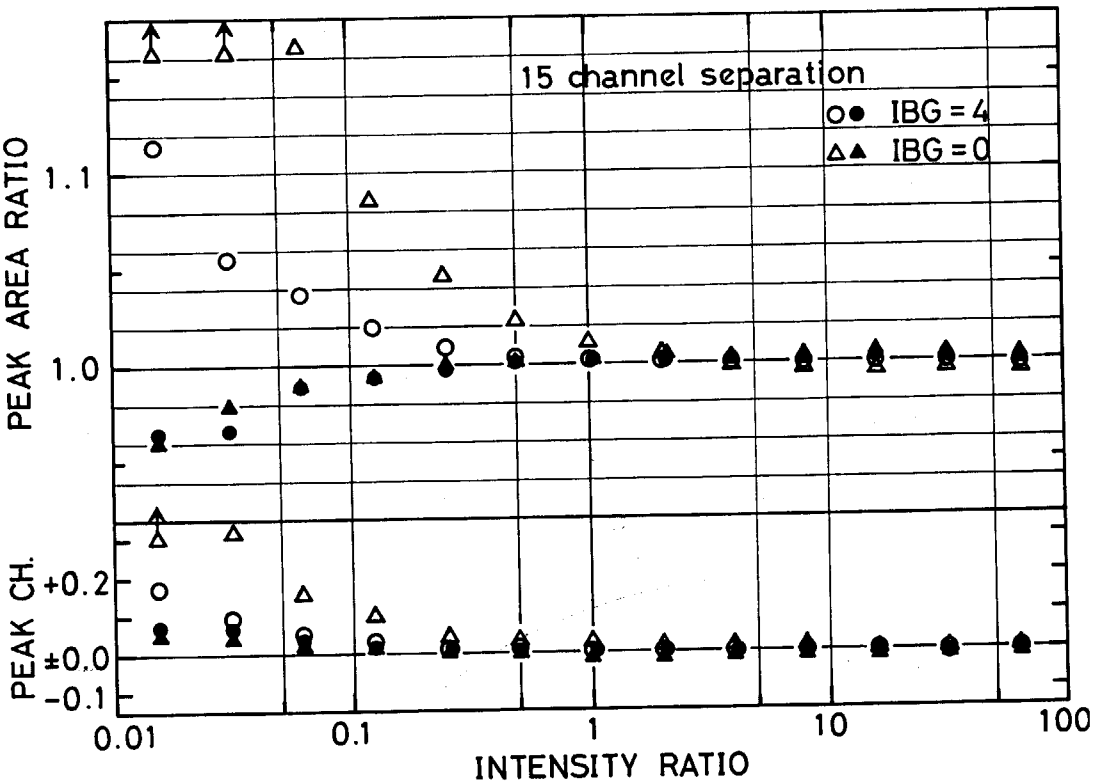

Fig. 3-13 Effect of the background shape on the estimated peak area and the determined peak position for doublets of various intensity ratios with the peak separation of 15 channels (the $FWHM$=5.0 channels). The open marks indicate the result of the lower-energy peak, whereas the closed marks are for the higher-energy peak.

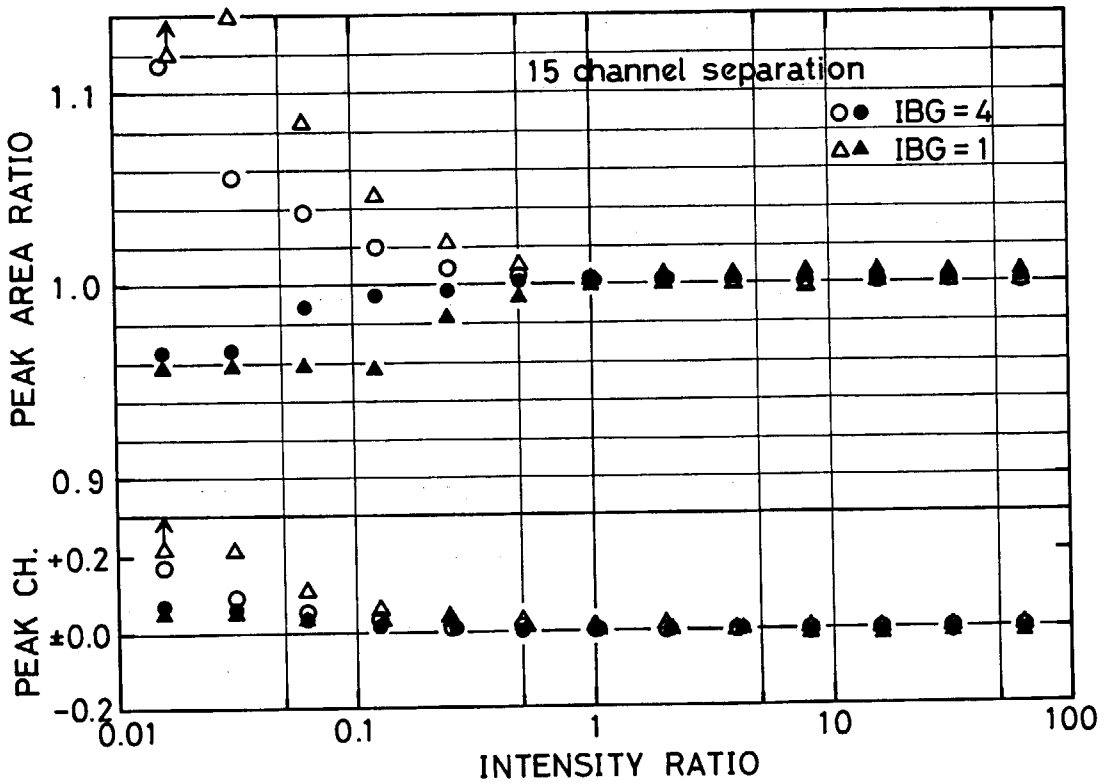

Fig. 3-14 Effect of the background shape on the estimated peak area and the determined peak position for doublets of various intensity ratios with the peak separation of 15 channels (the $FWHM$=5.0 channels). The open marks indicate the result of the lower-energy peak, whereas the closed marks are for the higher-energy peak.

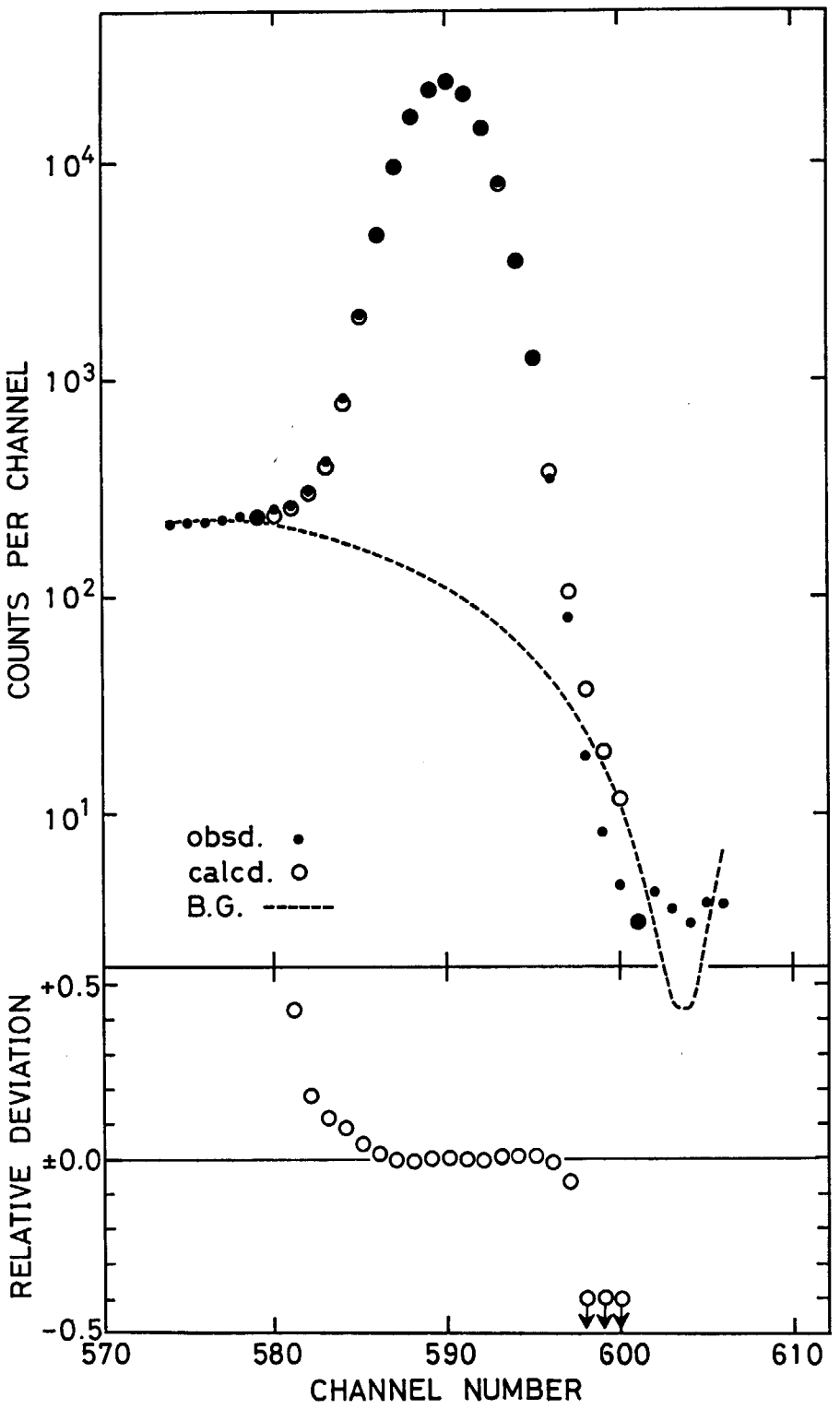

Fig. 3-15 Fit of the observed full-energy peak to the asymmetric Gaussian curve with a tail (the skewness factor being 0.94) lying on the fitted cubic polynomial background. The relative deviation is taken for the surplus count above the base line.

where i and f are the channel numbers of the peak boundary on the low- and high-energy sides, respectively. In **Fig. 3-12**, various background curves are illustrated in the case of a single peak. The number given to each background curve represents the parameter *IBG*, where the exponential curve was assigned with $IBG=0$. Consistency of the results was found to increase with increasing *IBG* from 1 to 4, whereas the situation remained more or less the same beyond *IBG*

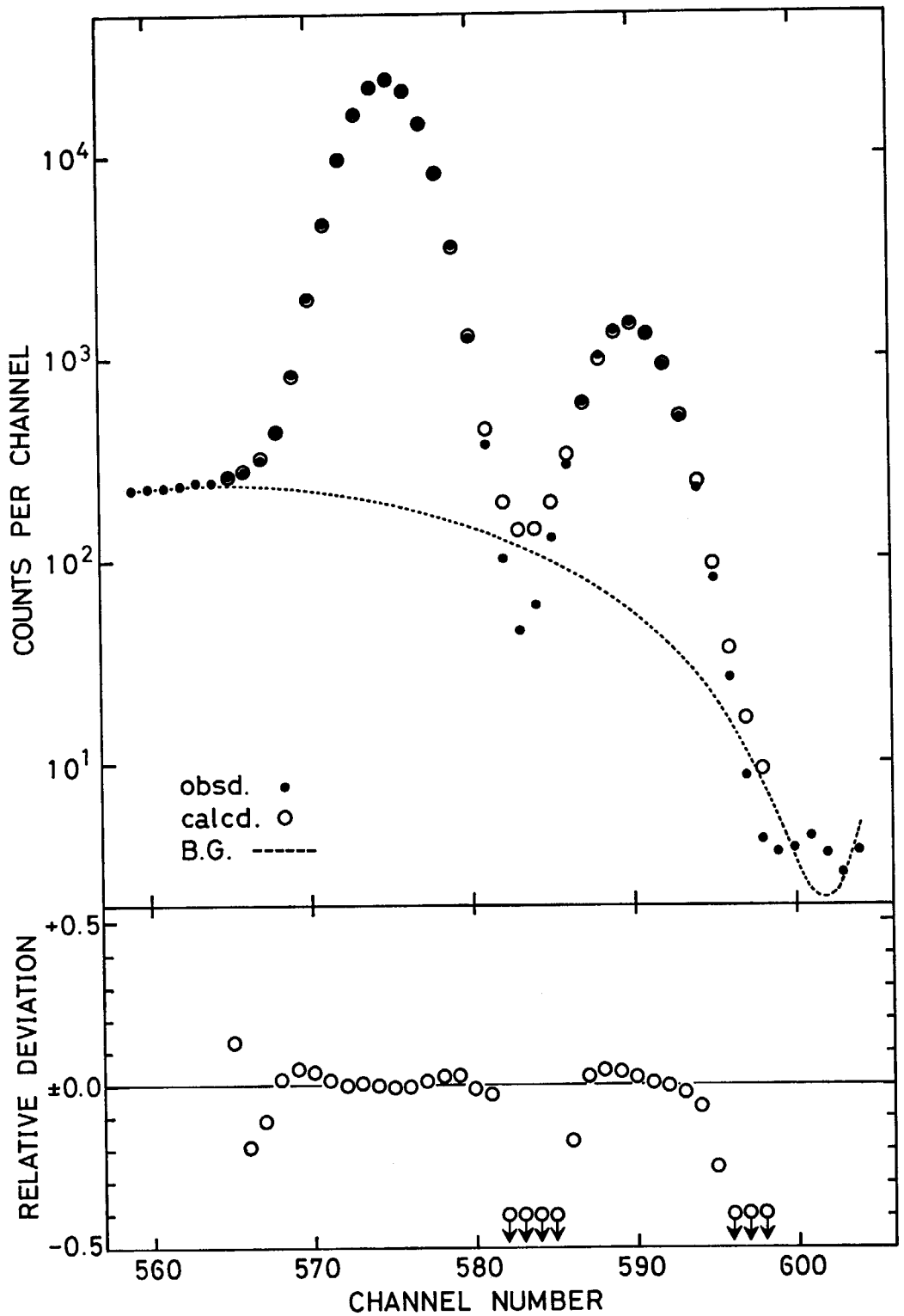

Fig. 3-16 Fit of a doublet with the intensity ratio of 1/16 and the peak separation of 15 channels (the *FWHM* being 5.0 channels) to the asymmetric Gaussian curve with a tail on the fitted cubic polynomial background. The relative deviation is taken for the surplus count above the base line.

$=4$. From **Fig. 3-12**, one may then expect that the exponential background would be the worst choice of all for a small peak on the low-energy side though it probably gives as good results as the best curve of $IBG=4$ for a small peak on the high-energy side.

On the contrary, the linear background is supposed to end up with poor agreement equally on both sides. These expectation are just shown to be correct in **Figs. 3-13** and **3-14**; the for-

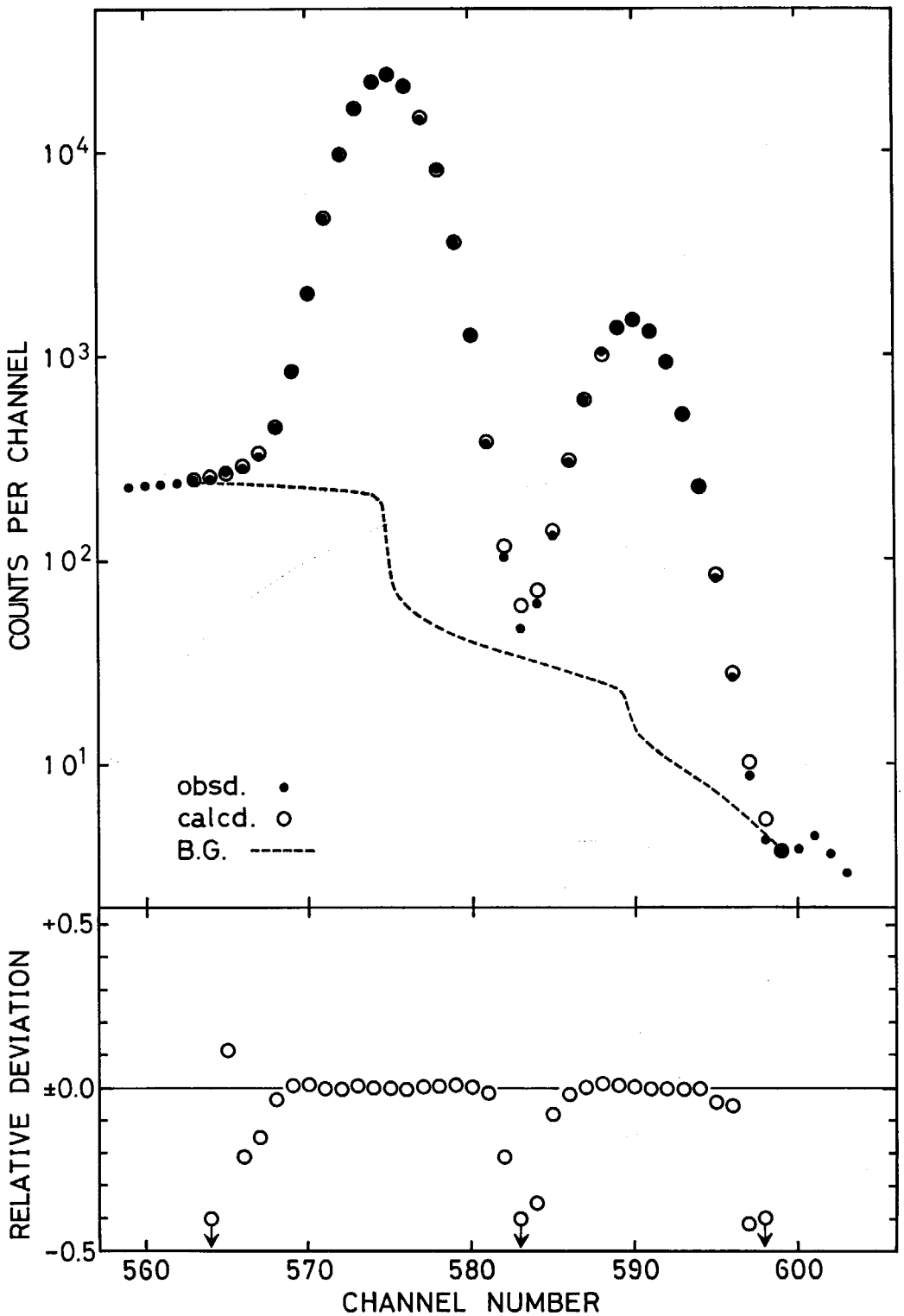

Fig. 3-17 Fit of a doublet with the intensity ratio of 1/16 and the peak separation of 15 channels (the *FWHM* being 5.0 channels) to the asymmetric Gaussian curve with a tail on the sigmoid background with $IBG=4$ (cf. Eqs.(3-13) and (3-14)). The relative deviation is taken for the surplus count above the base line.

mer displays the results obtained for the exponential background with doublets of various intensity ratios whose peak separation was 15 channels, and the latter represents the results in the case of the linear background, both in comparison with the best case of $IBG=4$.

The most widely accepted function as the background curves is a low order polynomial. For example, the quadratic background is adopted in "SAMPO" and one can find many other codes

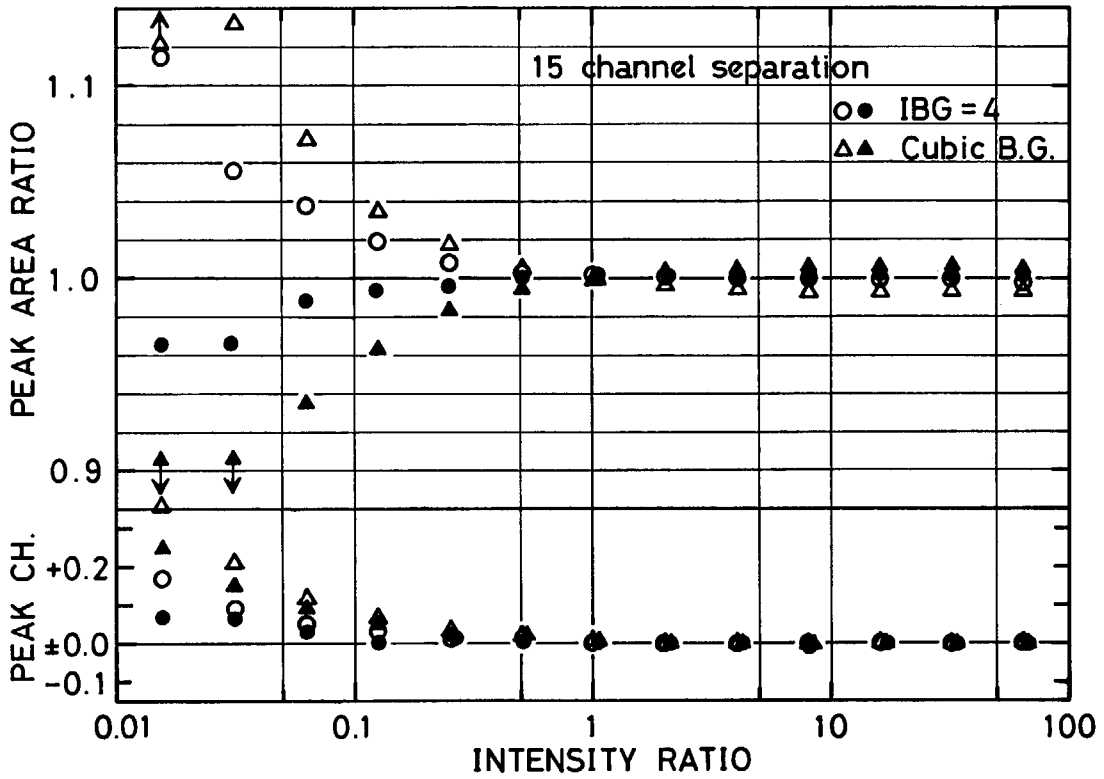

Fig. 3-18 Effect of the background shape on the estimated peak area and the determined peak position for doublets of various intensity ratios with the peak separation of 15 channels (the $FWHM$=5.0 channels). The open marks indicate the result of the lower-energy peak, whereas the closed marks are for the higher-energy peak.

also applying the quadratic or cubic background. The quadratic polynomial seems to be fitted well to the background continuum when none of the involved peaks is too large compared with the background level as seen, for example, in **Fig. 5** of ref. 8. However, the situation becomes quite discouraging when the full-energy peak is so large that the background levels are remarkably different on both sides. The cubic polynomial does not greatly improve the situation although it is expected to be more promising than the quadratic curve. **Figure 3-15**, which shows the least squares fit of a single peak to the skew Gaussian curve with a tail plus the cubic background, clearly indicates that the background is overestimated on the high-energy side as a result of more weight being laid on the higher background level of the opposite (low-energy) side. Consequently, one can expect no better results by the use of the cubic curve than those with the linear background for a small peak appearing on the higher-energy side of a large full-energy peak.

Figure 3-16 displays the least squares fit of a doublet, in which the peak separation is 15 channels and the high-energy peak is one-sixteenth of the low-energy one, to the skew Gaussian curve with a tail on the cubic background. **Figure 3-17** shows the fit of the same doublet to the same peak shape on the stepwise background of IBG=4. In **Fig. 3-16**, one finds the fitted background surmounts the observed data both in the trough and the high-energy boundary. This observation supports the statement in the preceding paragraph. As is seen in **Fig. 3-18**, the cubic background results in the poorest agreement among varions curves for a small peak on the high-energy side though it gives somewhat better result for a small peak on the opposite side.

So far we have investigated the relationship between the reliability of the result and the peak intensity ratio in a doublet of a fixed separation. Now let us consider the effect of the

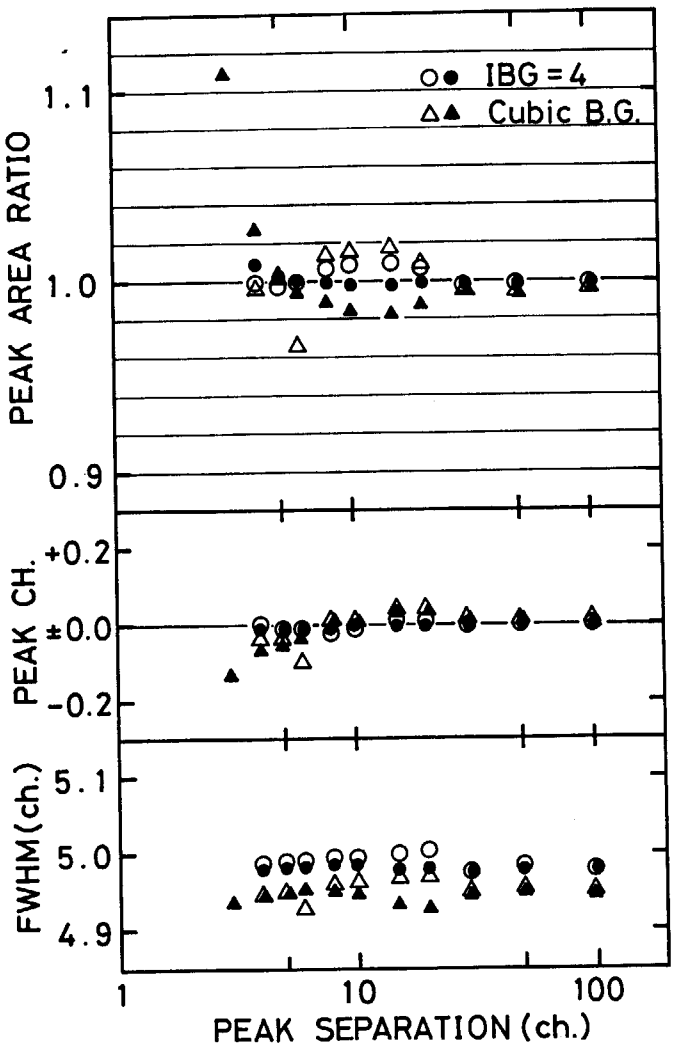

Fig. 3-19 Fluctuations of the estimated peak area, peak position, and *FWHM* in the two-peak systems with the fixed intensity ratio of 1/4 for various peak separations. The open marks indicate the results obtained for the lower-energy peak, while the closed marks are for the higher-energy peak.

peak separation on the result for a doublet with a given intensity ratio. We shall select two cases of the cubic and the sigmoid ($IBG=4$) background, and plot three quantities, the peak area ratio, peak position and full width at half maximum, versus peak separation for the fixed intensity ratios of one-fourth (**Fig. 3-19**) and one-sixteenth (**Fig. 3-20**). The agreement naturally becomes poor as the separation is reduced to the smallest possible value, to nearly half the *FWHM*, because isolation into individual peaks becomes difficult. On the other hand, the increase of the separation causes disagreement because of the increase of the deviation between the adopted and optimum background functions as the peak region is enlarged. Above the 20-channel (4 *FWHM*s) separation, the two peaks are completely isolated (cf. **Fig. 2-1**) so that the agreement becomes excellent. Concerning the observed width, it is pointed out that the least squares fitting procedure gives much different widths for peaks in the low- and high-energy sides in the cases of poor agreement. From **Fig. 3-19**, we can assure the consistency of the peak area within one per cent deviation and the reproduciblity of the peak position within an error of 0.02 channel for a smaller peak in a doublet with the intensity ratio of one-fourth by using the skew Gaussian curve and the stepwise background of $IBG=4$.

In the present code, the peak width is freely adjusted in the least squares fit. The *FWHM* values obtained for the set of IAEA standard sources are plotted versus the channel number

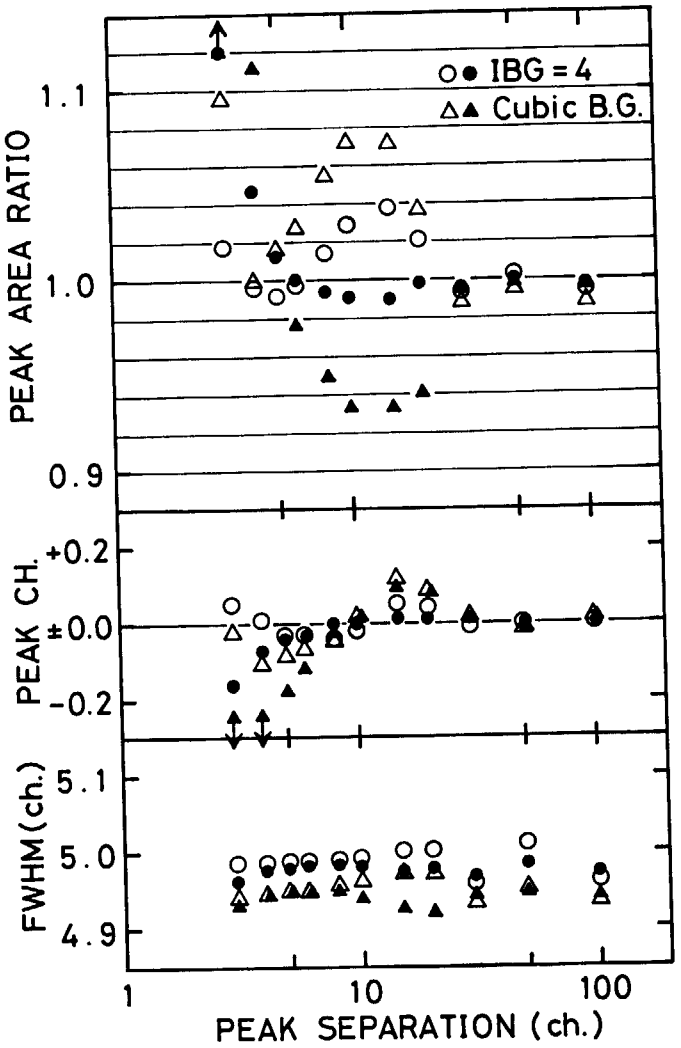

Fig. 3-20 Fluctuations of the estimated peak area, peak position, and *FWHM* in the two-peak systems with the fixed intensity ratio of 1/16 for various peak separations. The open marks indicate the results obtained for the lower-energy peak, while the closed marks are for the higher-energy peak.

or the photon energy in **Fig. 3-21**. Though the linear relationship is approximately observed among the points but one, there are some noticeable fluctuations among them. This tendency becomes much more prominent in the case of general spectra containing small and complex peaks. It is, however, concluded that such fluctuation in the peak width gives no discernible error in the resulting peak area and the agreement between the summed and the integrated peak area is remarkably good.

In **Fig. 3-21**, the exceptionally large value of *FWHM* belongs to the 511-keV annihilation peak, and this phenomenon has been known for some time[12].

The fitting procedure by previously forecasting the peak width has an advantage in finding a peak being overlooked in a multiplet by means of an extraordinarily large peak width on one hand. On the other hand, it fails to meet an abnormal situation such as the above annihilation peak. In this code, the above attitude was abandoned after all from the reasons of saving the annoyance of pre-determining the peak width and of keeping the flexibility to meet exceptional peaks. The handicap of thus losing an useful measure of detecting a dropped peak can, however, be sufficiently made up by other means (cf. section 3.1).

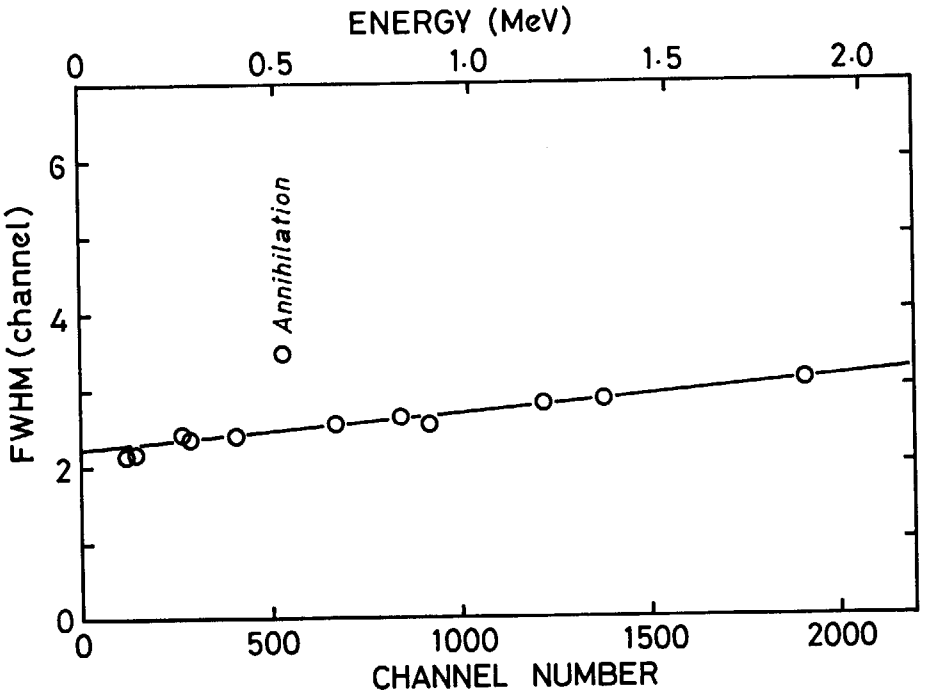

Fig. 3-21 An example of the energy dependence of the full width at half maximum resulting from the least squares peak fitting with the IAEA standard set.

4. Peak-fitting Process " RESFIT " in the Analysis of Low-resolution Spectra

4. 1 Details of the Least Squares Fit

4. 1. 1 The principle of the analysis and the structure of the subprogram " RESFIT "

For the spectrum analysis using the response function of the NaI(Tl) detector, the total-spectrum method has been adopted in which the simultaneous determination of all components is performed by means of all the peaks found in the spectrum. The total-spectrum method was thought to have superiority because statistical errors can be reduced by the use of all the data points for the fitting and it could subsequently avoid accumulation of errors which occurs seriously in the pealing-off method. It, however, requires the complete set of information on the response functions for all components such as bremsstrahlung, backscattering, escape peak due to pair production, and the sum spectrum at the high counting rate. Application of the total-spectrum method may, therefore, be rather limited. With the knowledge, we have devised a new method of the spectrum analysis using the response function[4] for the full-energy peak and the Compton edge (cf. **Fig. 4-1**), which is a sort of the photopeak method as described below.

How to assign the fitting range is an important problem in the photopeak method. First, we examined a method of the least squares fit for each peak group separated in the peak rec-

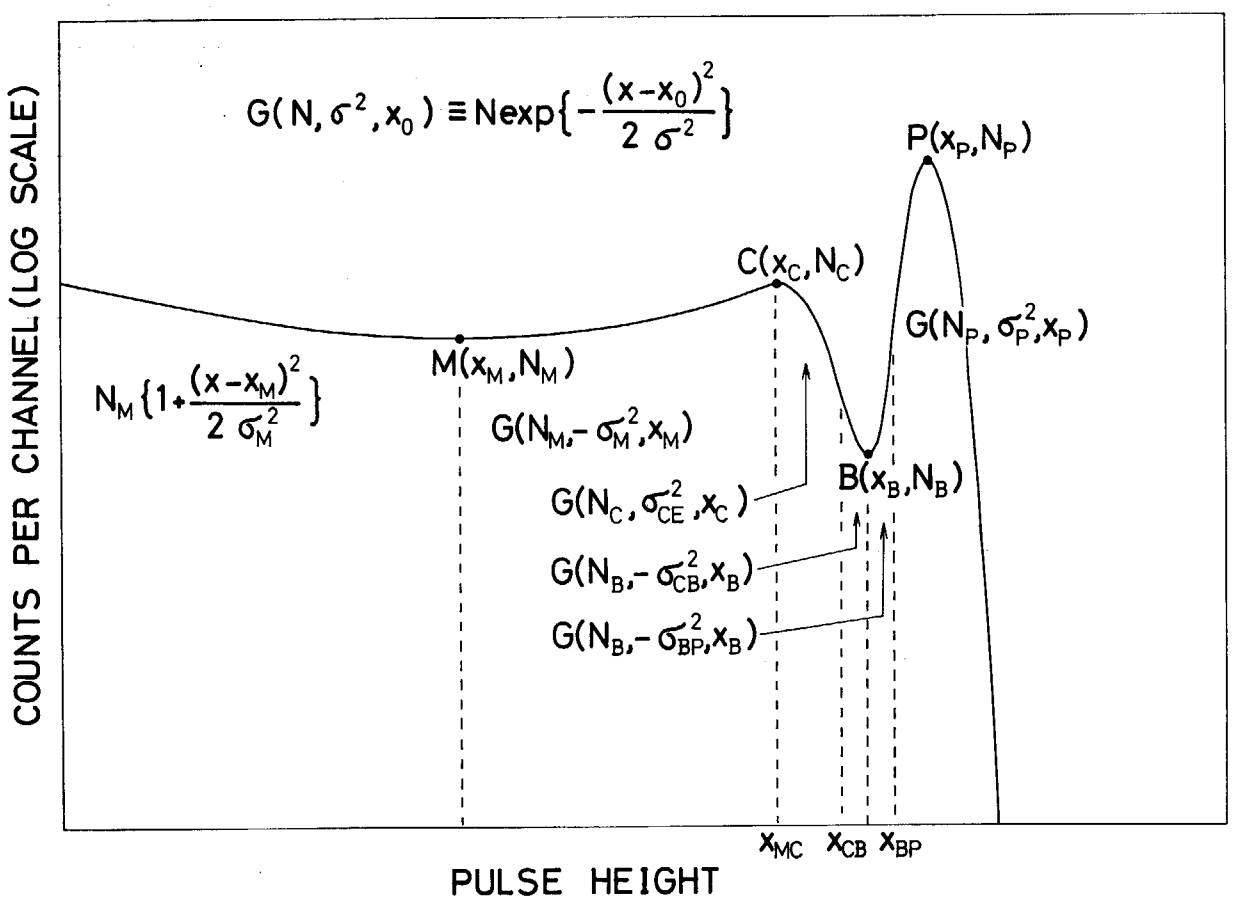

Fig. 4-1 An analytical expression of the γ response function given by NaI(Tl) detectors.

ognizing subprogram "PKREC", in which the Compton distribution of other peak groups at the higher energies were approximated with a quadratic polynomial. It was, then, concluded that (i) a sufficiently large number of data points are not supplied for the fit of the peak locating at the end of the cluster of peaks and (ii) for clusters of peaks containing many peaks and consequently requiring a broad fitting range, the quadratic polynomial is not always accurate enough to represent the Compton distribution of other peak groups throughout the region. One may remove the first disadvantage by extending the fitting range. This, however, amplifies the second disadvantage. Raising the order of the polynomial representing the Compton background for improving the reproducibility of the background distribution is undesirable because the number of the adjustable parameters increases.

An alternative solution was then found by repeating the fitting procedure for each peak instead of each peak group. The fitting range is now determined as shown in **Fig. 4-2** around the object peak. For the γ components which give violently changing distributions such as full-energy peaks or Compton edges in the fitting range, their response functions are included rigorously in the least squares fit as well as the function for the object peak. The Compton distribution of the rest of the γ rays is approximated with a quadratic polynomial whose coefficients are determined in the least squares procedure.

The flow chart of "RESFIT" is shown in **Fig. 4-3.**

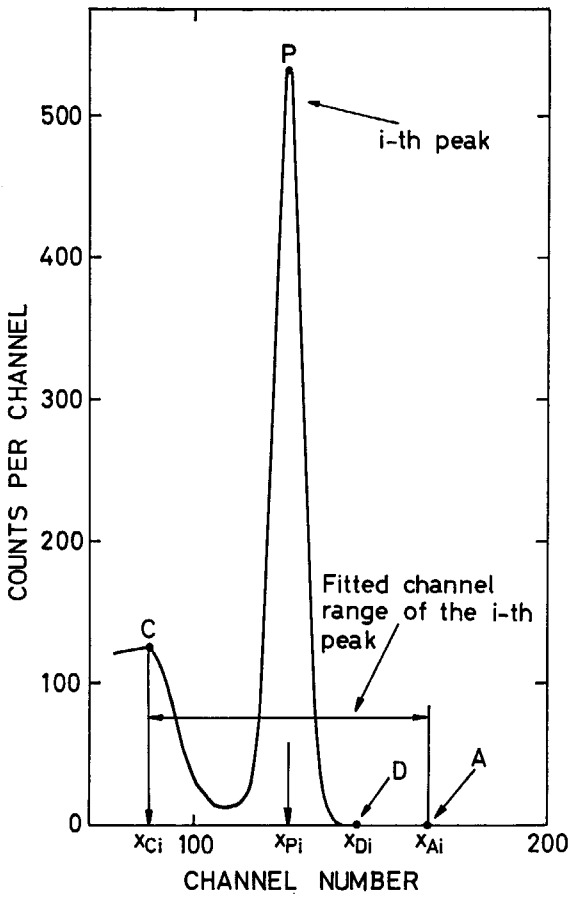

Fig. 4-2 An illustrative picture of the present photopeak method.

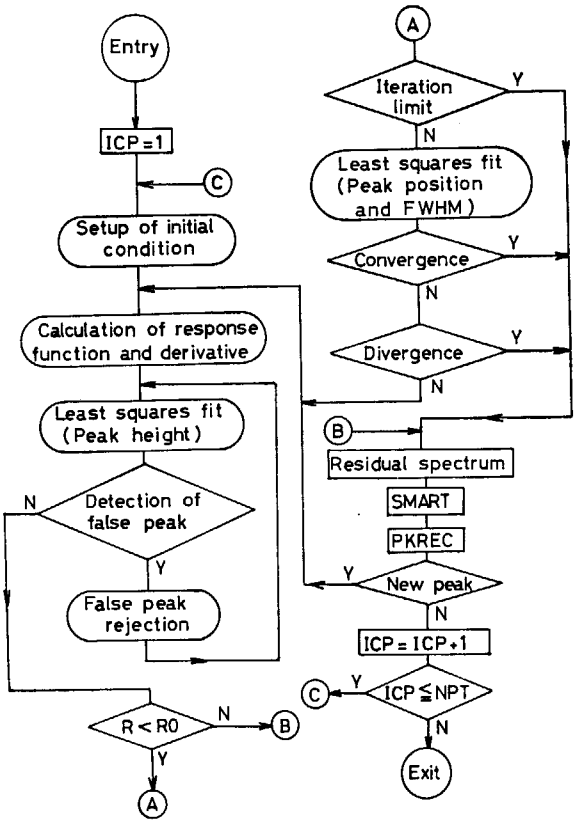

Fig. 4-3 Flow chart of "RESFIT".

4. 1. 2 Initial setup for the least squares fit

Since all the peak positions are found by the use of the peak-searching subprogram "PKREC",

the photopeak energy, E_{Pi}, of the i th γ ray is calculated with

$$E_{Pi}=A(x_{Pi}-B), \tag{4-1}$$

where x_{Pi} is the peak position of the i th photopeak and A and B are constants to be given by the user. The conversion equation (4-1) between the energy and the channel number is also used for transforming the energy-dependent response function[4] to the channel-number-dependent one $R_i(j)$. The function $R_i(j)$ is normalized so that the peak height becomes unity and consequently the contribution of the i th γ ray to the spectrum is obtained by $R_i(j)$ multiplied by the peak height, N_{Pi}.

The fitting interval for the i th peak was taken from the Compton edge C to a point A as shown in **Fig. 4-2**, where the channel number of the point A was given by

$$x_{Ai}=2x_{Pi}-x_{Ci}. \tag{4-2}$$

This fitting interval extends about $20\,\sigma_{Pi}$ which is appreciably broader than that in the ordinary photopeak method. The response function of another γ ray whose Compton edge C or a point D given by

$$x_{Di}=x_{Pi}+5\,\sigma_{Pi} \tag{4-3}$$

lies in the above region is brought into the fitting procedure (cf. **Fig. 4-2**). That is, only the smoothly changing distributions are represented by a quadratic polynomial in this method.

The function to which the observed number of counts at the j th channel, $y(j)$, in the i th peak region is to be fitted is expressed in the form of a linear combination;

$$\bar{y}(j)=N_{Pi}R_i(j)+\sum_{k\neq i}N_{Pk}R_k(j)+C_0+C_1j+C_2j^2. \tag{4-4}$$

The second through fifth terms on the right-hand side of Eq.(4-4) are regarded to give the background to the i th peak. Let us rewrite Eq.(4-4) in a simplified form;

$$\bar{y}(j)=\sum_k a_{kj}x_k, \tag{4-5}$$

where a_{kj} represent the known quantities of $R_k(j)$ etc., and x_k denote adjustable parameters of N_{Pk} and $C_r(r=0, 1 \text{ or } 2)$.

The solution of the simultaneous equations;

$$\frac{\partial v^2}{\partial x_k}=0 \qquad (k=1, 2, \cdots\cdots, m) \tag{4-6}$$

with

$$v^2=\sum_{j=1}^{n} w_j\{y(j)-\bar{y}(j)\}^2 \tag{4-7}$$

is written in a matrix representation;

$$\boldsymbol{X}=(\boldsymbol{A}^T\boldsymbol{W}\boldsymbol{A})^{-1}\boldsymbol{A}^T\boldsymbol{W}\boldsymbol{Y}, \tag{4-8}$$

where

$$\boldsymbol{X}=(x_k),$$

$$\boldsymbol{Y}=(y(j)),$$

$$\boldsymbol{A}=(a_{kj}),$$

and $\boldsymbol{W}$ is the diagonal matrix whose $j-j$ element is w_j. The matrix $\boldsymbol{A}^T$ is the transposed matrix of $\boldsymbol{A}$.

The standard deviation d_i in x_i is given by

$$d_i = \sqrt{(\boldsymbol{A}^T \boldsymbol{W} \boldsymbol{A})^{-1}_{ii} \frac{v^2}{n-m}}. \tag{4-9}$$

The peak area A_i and its standard deviation D_i of the ith peak are expressed with N_{Pi}, D_i and σ_{Pi} $(=0.4247\ FWHM)$ as

$$A_i = \sqrt{2\pi}\, N_{Pi} \sigma_{Pi} \tag{4-10}$$

and

$$D_i = \sqrt{2\pi}\, d_i \sigma_{Pi}, \tag{4-11}$$

respectively.

In the above-mentioned least squares fit, the peak positions were fixed as given in "PKREC", so that the linearization was possible. However, the subprogram "PKREC" fails to deterimine accurately the position of small peaks particularly half-hidden by a nearby large peak or appearing as shoulders on a large peak or the Compton edge. The step next to the linear least squares fit should, therefore, naturally be the non-linear least squares method in which the peak positions are freely adjusted as well, following the Gauss's method (cf. section **3.1**).

4. 1. 3 Norm for the least squares fit

Iteration of the non-linear least squares procedure is ceased whenever any of the following conditions are realized:

1) The iteration is recognized as successfully converged if

$$|\Delta x_{Pk}| < 0.1\ \text{keV} \tag{4-12}$$

for the increments Δx_{Pk} of all the involved peak positions x_{Pk}.

2) If any one of the increments Δx_{Pk} begins to exceed 30 keV or the $FWHM$ exceeds twice the initial guess value, the iteration is judged to have diverged.

3) If the χ^2 quantity;

$$\chi^2 = \sum_j \frac{\{y(j) - \bar{y}(j)\}^2}{\bar{y}(j)} \tag{4-13}$$

exceeds the value obtained in the preceding iteration, the fitting is ceased in failure.

4) When the number of iteration reaches 20, the iteration is stopped also in failure.

4. 1. 4 Rejection of false peaks

The situation that spurious peaks are detected in "PKREC" is limited in the case where the counting statistics is remarkably poor or the Compton edge forms a shoulder in the outskirt of a large peak. Inclusion of a false peak in the fitting procedure results in a poor ending, particularly concerning peak positions. On the contrary, peaks overlooked in "PKREC" if any do not cause the fatal effect to the least squares fit. What is required as the protection against the failure is, therefore, the devices of the false-peak rejection.

The following three conditions were set up empirically:

1) A peak whose peak height, N_{Pk}, is less than 2 counts/channel is ignored.

2) If the standard deviation d_k defined by Eq.(4-9) has a relation;

$$d_k > 4\sqrt{y(x_{Pk})} \times FTH, \tag{4-14}$$

the k th peak is unconditionally excluded. Here, $y(x_{Pk})$ denotes the number of counts per channel at the k th peak channel and FTH is a multiplication factor taken to be unity unless particularly specified by the user.

3) When

$$4\sqrt{y(x_{Pk})} \times FTH \geqq d_k > 2\sqrt{y(x_{Pk})} \times FTH, \tag{4-15a}$$

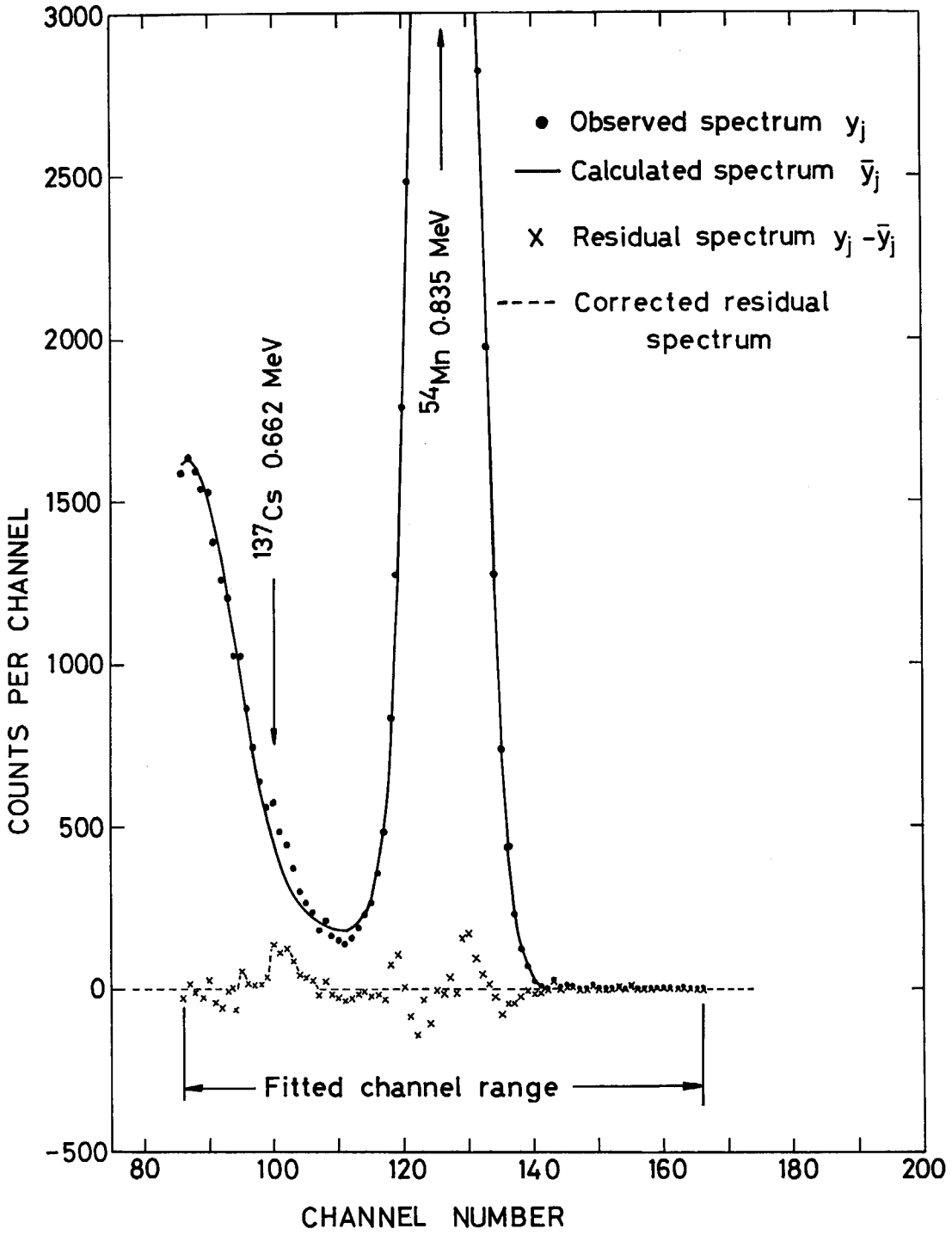

Fig. 4-4 An illustrative picture of the second peak search. The ^{137m}Ba 662-keV peak, once overlooked in the original spectrum, is successfully picked up in the smoothed residual spectrum.

the kth peak is dropped if the Compton edge of another peak k', x_{Ck}', lies within 50 keV around the peak position x_{Pk}; namely,

$$| x_{Ck}' - x_{Pk} | < 50 \text{ keV}. \tag{4-15b}$$

4. 1. 5 Search of peaks once overlooked in "PKREC"

A small peak lying on the steep Compton edge may not appear explicitly because of the low resolution of the detector (cf. **Fig. 4-4**). In the least squares fit excluding such an undetected peak, however, the observed spectrum $y(j)$ would exceed the fitted one, $\bar{y}(j)$, in the corresponding interval. Such disagreement is expected to clearly appear in the residue $r(j)$;

$$r(j) = y(j) - \bar{y}(j). \tag{4-16}$$

Since the statistical fluctuation is greatly enhanced in the residual spectrum $r(j)$, it is necessary to filter the fluctuation prior to the second peak search. The low resolution of the spectrum serves this purpose; namely, the range of the positive residue should extend over a certain length, at least an order of one $FWHM$ (actually $2\sigma_{Pi}$ is taken). We have therefore introduced the following filter for the residual spectrum; the value of the residue $r(j)$ is substituted with unity unless the positive value lasts over $2\sigma_{Pi}$. The resulting spectrum, depicted with a dashed line in **Fig. 4-4**, is then subjected to the peak search by "PKREC" once more. If a peak is found in the spectrum, the least squares fit is repeated by including the newly found peak.

4.2 Consistency Guaranteed by the Subprogram "RESFIT"

Although it is hardly expectable to obtain a universal measure for the consistency concerning the peak area determined by "RESFIT", a study on the reliability of the subprogram for a few typical cases would be valuable. As discussed before[5], the spectrum synthesized with spectra of the pure sources is generally superior to the measured spectrum with a mixed source from the viewpoint of investigation of the performance of the analyzing code. In the case of the spectrum from NaI (Tl) detectors, however, one can not apply the way of the spectrum synthesis carried out for those given by Ge(Li) detectors in the previous chapter because the response of the NaI (Tl) detector is sharply energy- (or channel-number-) dependent. What is recommended is to superimpose with a certain multiplication factor two spectra separately measured with two appropriate types of the pure nuclide.

In order to obtain a peak lying on the Compton plateau, the ^{54}Mn spectrum was superimposed on the ^{22}Na spectrum after being multiplied by a multiplication factor f. On the other hand, the spectrum from the ^{137}Cs source was combined with the ^{54}Mn spectrum for constructing a peak on the slope of the Compton edge. The reciprocal of the number of counts per channel was used as the statistical weight in the least squares fit. For comparison of the result, the COVELL's method[10] was also carried out, in which the peak range was set to about 4.5 σ_{Pi} around the relevant peak.

Figure 4-5 indicates the result of the analysis of the spectrum constructed with the responses for the pure ^{54}Mn and ^{22}Na sources. The ratio of the resulting peak area to the true value for the ^{54}Mn full-energy peak is plotted versus the ratio of the true peak area to that of the 1,275-keV peak of ^{22}Na. As the true peak area for ^{54}Mn, we adopted the value obtained with the pure ^{54}Mn spectrum multiplied by the factor f. The COVELL's method gave quite large discrepancies in the computed peak area when the pure ^{54}Mn spectrum was taken as the standard. Therefore, the normalizing value was determined by the peak area calculated for the

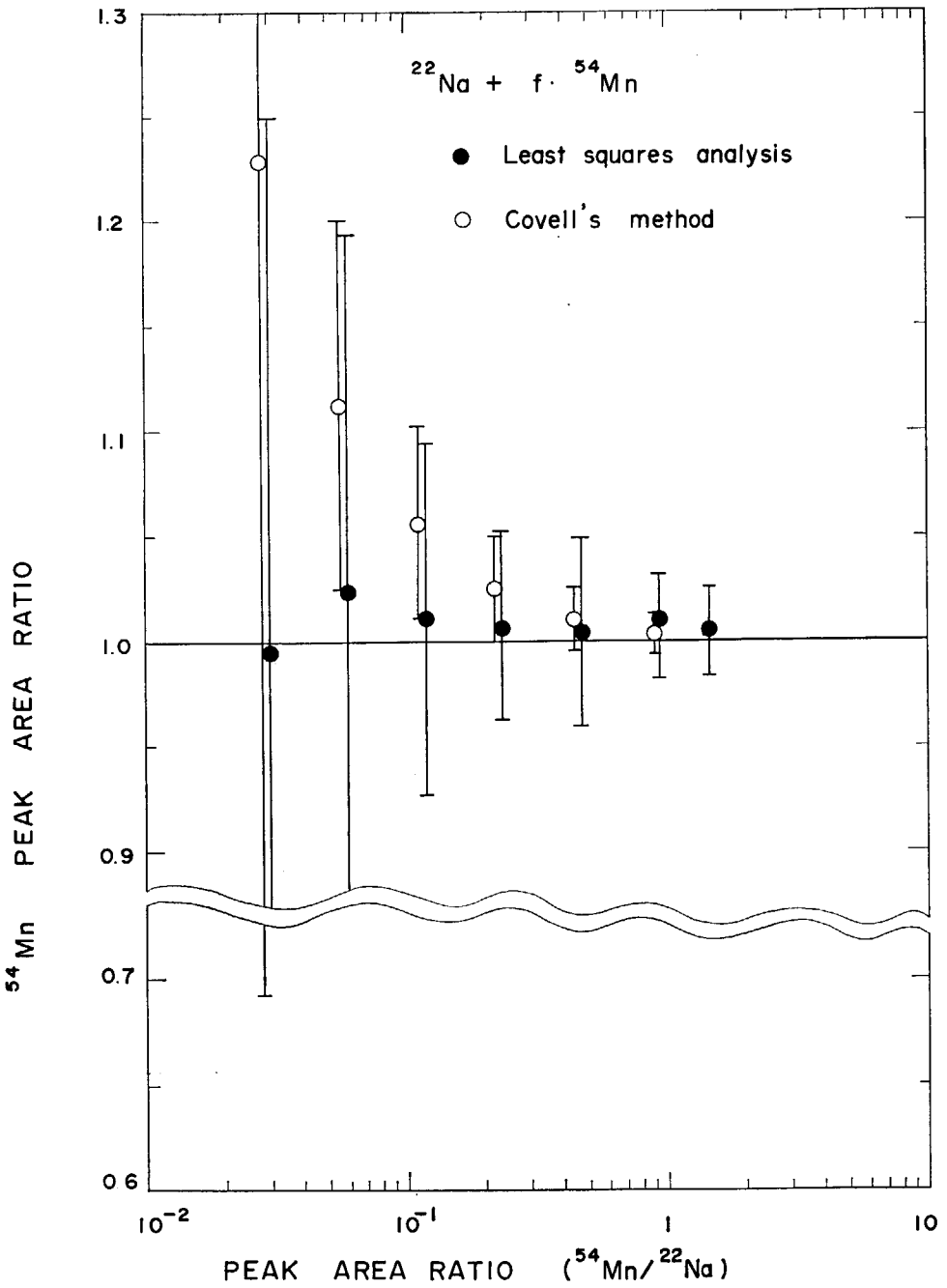

Fig. 4-5 The analyzed peak areas for the ^{54}Mn 835-keV full-energy peak in the synthesized spectrum by means of the pure ^{54}Mn and ^{22}Na spectra.

mixed spectrum with the equal photopeak intensity ($f=1$). The results of similar treatments are shown in **Fig. 4-6** for the case of the ^{137m}Ba 662-keV peak under the influence of the ^{54}Mn response.

The results displayed in **Figs. 4-5** and **4-6** indicate that the COVELL's method gives relatively good consistency for a peak on the Compton plateau or when the background level is nearly linear, while the consistency becomes very poor when the background shape considerably deviates from the linear function. On the other hand, the present response-function method is understood to give quite satisfactory results in either case, since the background shape can be reproduced quite accurately.

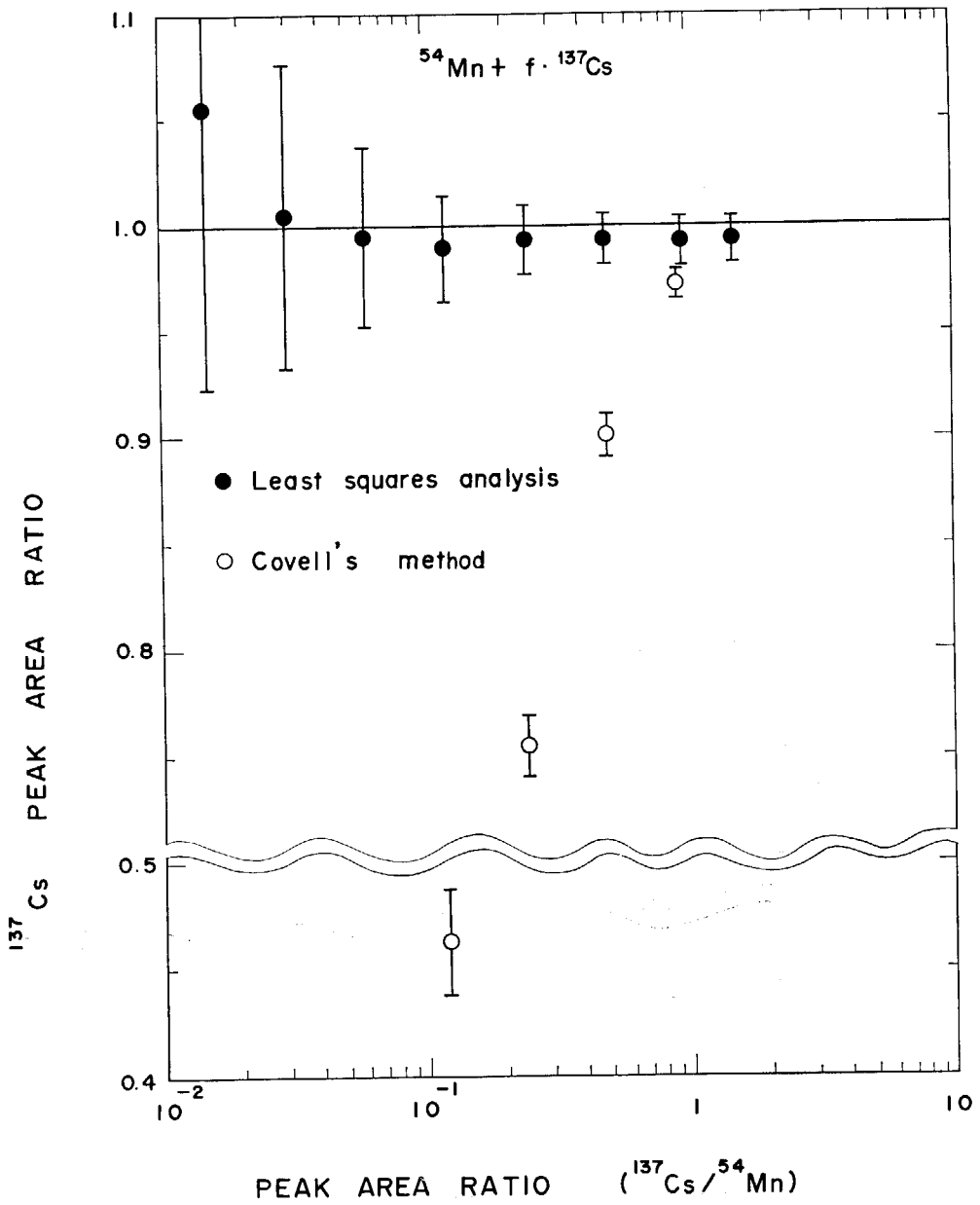

Fig. 4-6 The analyzed peak areas for the ^{137m}Ba 662-keV full-energy peak in the synthesized spectrum by means of the pure ^{137}Cs and ^{54}Mn spectra.

5. Description of the Codes

5. 1 Main Program and Subprograms

5. 1. 1 Main program and subprograms in the code "BOB 73" for the spectrum from the Ge(Li) detector

The code "BOB 73" consists of the main program and 25 subprograms as described below.

MAIN: the main program which combines all the subprograms to form the complete process. The values of the control indices are read in MAIN, which control the choices among optional conditions for the input and output formats and the way of the analysis.

CLEAR: a subroutine for the initial zero clearance of variables.

CDREAD: a subroutine for reading the input data in the form of the IBM cards, being called for $ISFG>0$.

MTREAD: a subroutine for the input data in the form of the magnetic tape, being called for $ISFG=0$.

LIVET: a subroutine for calculating the live counting time when the data are acquired in the clock-time mode. This subroutine is set for work if $ITR=0$ and all of ITC, $T0$ and TS are given in the CD-1 card in TABLE 5-3.

SMART: a subroutine for the data-smoothing following the SAVITZKY-GOLAY method[13].

PKREC: a subroutine for the peak search.

SELECT: a subroutine for filtering small or spurious peaks out.

FINDSK: a subroutine for determining the line shape function of a typical peak in the spectrum; the obtained information is used in the succeeding subprogram, PKFIT, for analyzing the rest of the peak groups in the spectrum. The procedure via FINDSK is, however, performed only when the peak shape remarkably changes with each data as in the case of the γ scanning of the nuclear fuel. Generally, the peak shape is determined beforehand with a set of the standard spectra. This subroutine is called if neither $WDR0$ nor $WDRC$ are given, and $ISEL$ is set equal to 0 or 1. This subroutine requires additional information regarding the channel number of the reference peak and the confidence interval in FORMAT(2 I 4).

PKFIT: a subroutine for the peak-fitting procedure. The peak shape is approximated by an asymmetric Gaussian curve with/without a tail in the low-energy side. The asymmetry factor and/or the shape of the tail are either fixed or floated in the least squares fit. The shape of the background level can be chosen among the linear ($IBG=1$), exponential ($IBG=0$) and various sigmoid curves ($IBG\geq 2$) (cf. Eqs.(3-13) to (3-16)).

NONLIN: a subroutine for the non-linear least squares fit.

LINEQ: a subroutine for calculating the inverse matrix.

NLIEQ and NLNIJ: subroutines giving the values of the fitting function and its first derivatives with respect to the involved free parameters at given values of the independent variable (the channel number).

GRAFIC: a subroutine visualizing the result of the least squares fit, being called when $IGFT=1$.

ENGEF: a subroutine for the energy calibration and the counting efficiency correction. The

calibration can be carried out either by constructing the calibration curve (or the efficiency curve) with the internal or the external standard peaks, or by giving the values of the coefficients of the curve. The calibration curve for the energy is fitted to a polynomial of the channel number, while the logarithm of the counting efficiency is expressed in a polynomial of the logarithm of the energy.

STDDT : a subroutine for collecting the stored data for the energy calibration and efficiency correction, being called by setting a non-zero value to *IDEC* and/or *ISTDT*.

IURU : a function calculating the number of days elapsed, being called when $IDEC \neq 0$ or $RINT = 0$.

DECAY : a function calculating the decay correction factor, being called when $IDEC \neq 0$ or $RINT = 0$.

POLIN : a subroutine for calculating the values of the coefficients of the calibration or efficiency curve and the involved errors.

POLIX : a subroutine for computing the energy and the counting efficiency of a given peak.

OUTPUT : a subroutine for listing the output data.

SPECTR : a subroutine for plotting the input data with the CALCOMP 900, being called for the positive value (1, 2 or 3) of *IPLT* (full-size version only).

SUBTRX : a subroutine for detecting a weak peak buried in the natural background spectrum. The background spectrum is smoothed and then subtracted from the smoothed data of the relevant spectrum. The residues are cleared unless positive values continue over one *FWHM*. The resulting spectrum is smoothed and subjected to the succeeding peak-searching procedure. This subroutine is set for work for a non-zero value of *ISUB*, and then the background spectrum is read in SUBTRX according to the input formats in TABLE 5-3 (full-size version only). Note that the CD-1 card is unnecessary for the background spectrum.

ECHO : a dummy subroutine which can be temporarily substituted by the user for further data treatment such as the decay correction or identification of nuclides. (cf. Appendix)

FUNX : see the next section.

The flow chart of BOB 73 is outlined in Fig. 5-1.

5. 1. 2 Main program and subprograms in the code "NAISAP" for the spectrum from the NaI(Tl) detector

The code "NAISAP" consists of the main program and 18 subprograms as described below.

MAIN : the main program which combines all subprograms to form the complete process. The input data are fed and the output formats are given in MAIN.

LIVET : explained in the preceding subsection.

SMART : explained in the preceding subsection.

FUNX : a function determining the smoothing condition for each peak group, to be used for the NaI(Tl) spectrum.

PKREC : explained in the preceding subsection.

RESNAI : a subroutine for constructing the response function and computing its first derivative with respect to the peak position, regarding all peaks found in PKREC. The response function is defined by an analytical function containing 18 parameters (17 parameters in the case of a small crystal), which are calculated in the following subprograms, PARA and PARA 2.

PARA : a subroutine for calculating nine out of the above eighteen parameters by using empirical equations with respect to the photopeak energy[4].

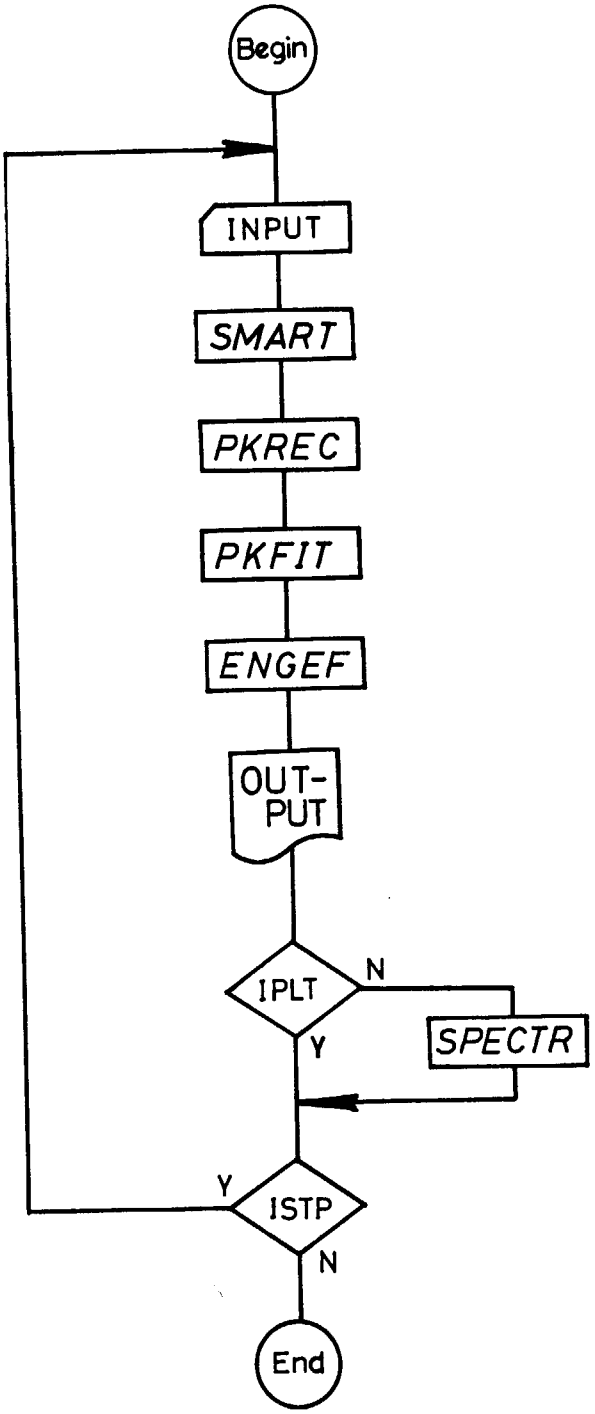

Fig. 5-1 General flow chart of BOB 73.

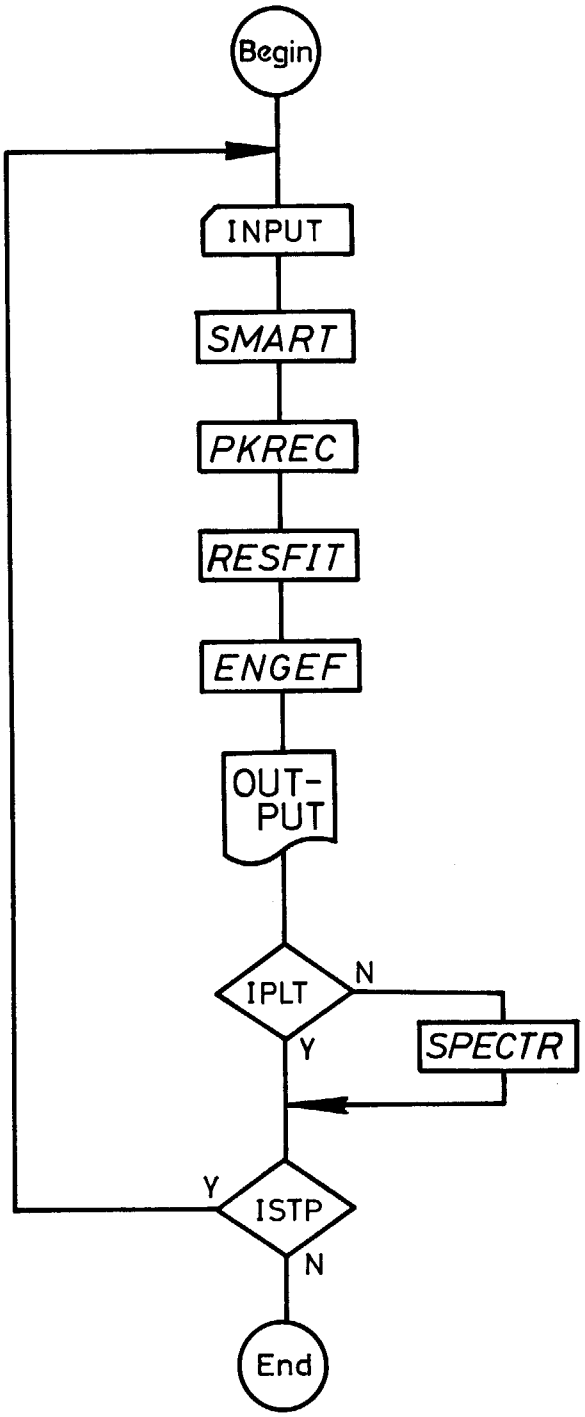

Fig. 5-2 General flow chart of NAISAP.

PARA 2 : a subroutine for determining the remaining nine parameters by the condition that any part of the response function must be smoothly joined to the neighbouring parts.

RESFIT : a subroutine for determining the peak position and area by the least squares fit in terms of thus constructed response function.

LLS : a subroutine for the linear least squares method.

MAT : a subroutine for computing the product of matrices.

LINEQ : explained in the preceding subsection.

GRAFIC : explained in the preceding subsection.

ENGEF : explained in the preceding subsection.

POLIN: explained in the preceding subsection.
POLIX: explained in the preceding subsection.
OUTPUT: explained in the preceding subsection.
SPECTR: explained in the preceding subsection.
ECHO: explained in the preceding subsection.

The flow chart of NAISAP is outlined in **Fig. 5-2**. The thorough analogy will be noticed between NAISAP and BOB 73. Only the difference appears in substituting PKFIT with RESFIT.

5. 2 Instruction Manual for "BOB 73"

5. 2. 1 Directions for use

It should first be mentioned that the present code does not assure a remarkable improvement of the results beyond the quality of the input data. For example, the pile-up effect appearing in the measurement at a high counting rate causes attenuation of the peak area[14]. The correction is not considered in the code. In order to eliminate the error, therefore, one must either use a pile-up rejector or avoid the measurement at a high counting rate. For users adopting the latter countermeasure, we recommend to set the time constant of the amplifier to 1μsec or so and to reduce the total counting rate below about 3,000 cps#). The channel shift during the measurement is not corrected by the program either. In order to reduce the amount of the channel shift, efforts should be made for keeping the room temperature and the moisture constant or maintaining a constant gain.

Since the theshold for the peak detection is devised on a delicate balance between the first derivative and the statistical variance, it is not recommended that the user raises the statistical fluctuations above the pure deviation in the disintegration rate; namely, the background spectrum should not be subtracted from the relevant spectrum. If one wants to subtract the natural background, one ought to carry out the subtraction via software with separately measured spectra of the sample and background as in the case of the search of a buried small peak by the use of "SUBTRX".

Unlike most of the prevailing codes, this program does not require the accurate *FWHM* as an input datum. A rough measure of the peak width is, however, still necessary because the conditions of the data-smooth and the threshold in the peak search loosely depend on it. An index, *ISM*, is used for denoting the measure; the correspondence between the value of *ISM* and the number of data points to be used in the smoothing is given in Chapter 2. Roughly speaking, the number of the smoothing points should be equal to the *FWHM*.

The peak-searching subprogram "PKREC" tends to pick up spurious peaks rather than overlook small real peaks, especially at the poor counting statistics. It is, therefore, recommended to filter those spurious peaks by putting $ISEL=1$ if one wants to save the computing time and does not care possible drop-out of extremely small real peaks. Furthermore, one can take out only the peaks with quite large intensities by putting $ISEL=2$.

The shape of the peaks given by the Ge(Li) detector can hardly be approximated by the pure Gaussian curve because of the complex mechanism of the charge collection. The peak asymmetry and the tailing on the low-energy side need to be taken into consideration to attain more

#) The percentage of the dead time is not suitable as the measure of the pile-up effect since it does not uniquely correspond to the magnitude of the pile-up effect, depending on the size of the AD converter or the time constant of the amplifying circuit.

reasonable fit. The values of the parameters determining the peak shape can either be sought in the fitting process or be fixed at the previously determined values. One of the advantages of this code is that the information to be given as input is restricted to the least number. There is no parameter the initial estimate of which must be given in the fitting procedure. The shape parameters are no exceptions. However, it is not recommended to freely adjust the peak shape in the fitting procedure for each peak group because the probability of the unsuccessful fitting becomes fairly high when the peak shape is not fixed. Furthermore, in order to maintain the consistency in the shape parameters when regarded as functions of energy, the skewness factor had better be determined first with a set of the standard spectra without introducing the tail. This procedure is performed by putting $WDR0=0.0$, $ISEL=2$ and $NIJ=0$. The values of the parameters describing the tail are then sought for the above standard spectra by fixing the skewness factor WDR to thus determined value; giving the $WDR0$ (and the $WDRC$ if necessary), and putting $ISEL=0$ or 1 and $NIJ=2$. The resulting values of the two parameters describing the tail will widely vary from peak to peak. However, one can obtain sufficient accuracy by selecting the most probable constant value for each of the parameters, since the tail is a minor correction in most cases.

5. 2. 2 Description of the input data for "BOB 73"

The code requires the input data either punched on the IBM cards or recorded on the magnetic tape. The input data are arranged in such a way that only two cards are read in the main program and the rest of data are parted to the corresponding subprograms.

i) Input data to be fed in "MAIN"

The first card, M-1, requested in the "MAIN" supplies the desired values for the control indices, and the second card, M-2, contains the constants to be used in the least squares fit. The details of them are illustrated in TABLE 5-1. The first control index, $ISFG$, controls the choice between the card-form ($ISFG\geqq 1$) and the form of the magnetic tape ($ISFG=0$) of the input data; that is, the subprogram "CDREAD" is called later on in the former case, while the "MTREAD" is called in the latter. The second index, $ISTD$, represents the number of the standard spectra to be used for the calibration, regardless of external or internal calibration. The rest of the indices in M-1 can be given either by the integers in the M-1 or by the appointed words in a separate card, M-1′, in an arbitrary order. The latter case is realized by giving $ISFG$ in M-1 a negative number. Definition of the words is described in TABLE 5-2. The meanings of those control indices are explained by TABLE 5-1.

The first quantity, $CONV$, in M-2 regulates the convergence limit. If the $CONV$ is not specified by the user, it is assigned to 10^{-6}. The second and third parameters, $WDR0$ and $WDRC$, define the skewness factor. The former is the extrapolated value at the zero channel and the latter determines the decrement in the skewness factor per channel; that is,

Skewness Factor$=WDR0-WDRD\times$(Channel Number).

The next two quantities are the parameters specifying the tail. The first one, $PKRTO$, represents the ratio of the top of the tail to the peak height (cf. Chapter 3. 2. 2), while the second, $POSRO$, is the channel separation between the centers of the tail and the peak. The last quantity, $ARM0$, is an attenuating factor in the measure of acceptable agreement in the least squares fit (corresponding to A_0 in Eq. (3-11)) and is put to unity unless particularly specified by the user.

This is all the input data to be fed in the "MAIN". The flow chart of the above input system is illustrated in Fig. 5-3.

TABLE 5-1 The formats of the input cards in "MAIN" of BOB 73

Card No.	Symbol	Columns	Format	Description
M-1	ISFG	1- 2	I 2	<0 Alphameric input of the control indices
				$=0$ Input via magnetic tape
				$\geqq 1$ Input in the card form (the *ISFG*=1 gives the confidence interval for the final channel, *IFIN*)
	ISTD	3- 4	I 2	Number of spectrum data in the standard set
	IRP	5- 6	I 2	$=0$ for Ge(Li) detectors
				>0 for NaI(Tl) detectors
	IE	7- 8	I 2	$=0$ External calibration
				$=1$ Internal calibration
				$=2$ Calibration with the previously constructed curve
				$=9$ No calibration
	IENG	9-10	I 2	$=0$ Energy assignment and intensity determination
				$=1$ Energy assignment only
	IDEC	11-12	I 2	$\neq 0$ Using the stored data 'Eu-14'
	IFMT	13-14	I 2	$=0$ The data format fixed (F6.0, 9F7.0)
				$=1$ An optional format
	IPLT	15-16	I 2	$=0$ Skip plotting the spectrum
				$=1$ Plot with the scale of 2.5 channels/mm
				$=2$ Plot with 5 channels/mm
				$=3$ Plot with 1 channel/mm
	IW(1)	17-18	I 2	$=0$ Print the conditions of analysis
				$=1$ No print
	IW(2)	19-20	I 2	$=0$ Blockwise printing of the original data only
				$=1$ Blockwise printing of the smoothed data only
				$=2$ Blockwise printing of both original and smoothed data
				$=3$ Channelwise printing of the results of SMART
				$=4$ No printing of the input data
	IW(3)	21-22	I 2	$=0$ Print the results of PKREC
				$=1$ No print
	IW(4)	23-24	I 2	$=0$ Print the final results
				$=1$ No print
	IBG	25-26	I 2	$=0$ Exponential background
				$=1$ Linear background
				$\geqq 2$ Sigmoid background
	IFTG	27-28	I 2	$=0$ No fitting
				$=1$ Fit multiple peaks only
				$=2$ Fit all peaks
	NIJ	29-30	I 2	$=0$ Fit to the (skew) Gaussian curve without tail
				$=1$ Fit to the Gaussian with fixed tail
				$=2$ Fit to the Gaussian with floating tail
	NONPR	31-32	I 2	$=0$ No print in NONLIN
				$=1$ Print the input to NONLIN
				$=2$ Print the output from NONLIN
				$=3$ Print both input and output of NONLIN
	IGFT	33-34	I 2	$=0$ No plotting of the peak-fitting process
				$=1$ Plot the process

TABLE 5-1 (continued)

	IPKW	35-36	I 2	=0	No printing of the results of PKFIT
				=1	Print the results
	IWT	37-38	I 2	=0	Fit with the built-in weight
				=1	Fit with equal weight
	ISEL	39-40	I 2	=0	No filtration of small peaks
				=1	Filter the small peaks
				=2	Pick up the large peaks only
	LVL	41-42	I 2	=0	Natural level
				=1	Add 100 counts to each channel
				=2	Add 1000 counts to each channel
	ISUB	43-44	I 2	≠0	Background spectrum subtraction
M-2	CONV	1-10	E10.4	Convergence limit	
	WDR0	11-20	E10.4	Constant term in the skewness factor	
	WDRC	21-30	E10.4	Channel-number dependent term in the skewness factor	
	PKRTO	31-40	E10.4	Ratio of the tail to the peak height	
	POSRO	41-50	E10.4	Separation between the peak and the tail center	
	ARM0	51-60	E10.4	Parameter determining the upper limit for allowable disagreement	

TABLE 5-2 Description of the alphameric input in the card M-1′

These symbols may be disorderly given in any sequential 4 columns starting from the (4n+1) th column. As long as the symbol is not given, the corresponding index remains to be zero.

Symbol	Description	Symbol	Description
TAPE	ISFG=0	RSUL	IW(3)=1
CARD	ISFG=1	FINL	IW(4)=1
LOWR	IRP>0	BACK	IBG=4
INTL	IE=1	PFIT	IFTG=2
COEF	IE=2	TAIL	NIJ=1
NCAL	IE=9	FOUT	NONPR=2
ENGY	IENG=1	GRAF	IGFT=1
DECY	IDEC=1	RITE	IPKW=1
FMAT	IFMT=1	WEIT	IWT=1
PLOT	IPLT=1	FILT	ISEL=1
LIST	IW(1)=1	LEVL	LVL=2
DATA	IW(2)=2		

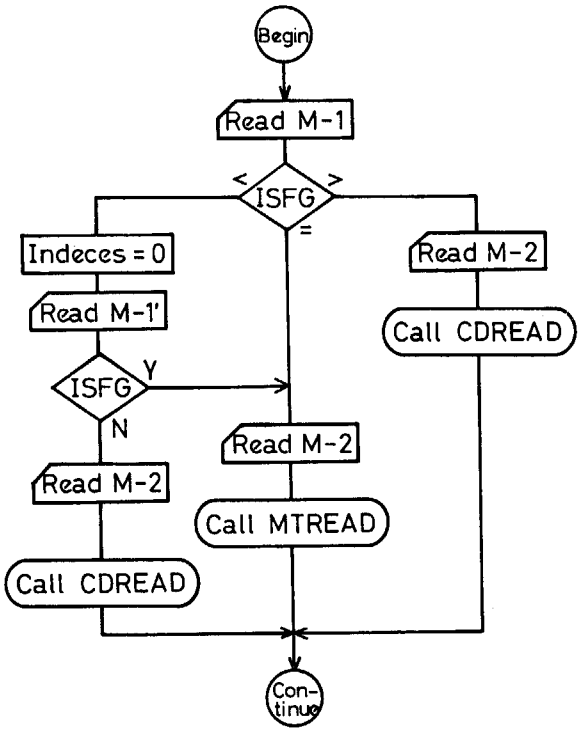

Fig. 5-3 Flow chart of the data-input part in "MAIN" of BOB 73.

ii) Input data to be fed in "MTREAD"

The subprogram "MTREAD" is called if $ISFG=0$. The format of the data stored in the magnetic tape is exemplified in **Fig. 5-4**. The four characters in the top line are the assigned name of the relevant data with which the identification between the wanted and the stored set of data is attempted. The second line contains all the necessary information, such as the identification number of the data, comments, the date of measurement, the counting duration, etc. The third line specifies the initial and the final channel of the input data, the starting channel of the analysis, the smoothing parameter *ISM*, and the parameter *ISTP* controlling the cycle of the analysis.

The fourth line and downward give the content of the measured data with the FORMAT (F 6. 0, 9 F 7. 0), together with the ID name (A4) and the sequential number (I4) starting from 30 advancing by 10. The last line is the sign of the data-ending.

The first input card in "MTREAD" gives the ID name of the data, which the user wants to pick up, and the number of the lines, *IXCN*, the contents of which are to be substituted temporarily. The *IXCN* must not exceed 10. If $IXCN\neq0$, the *IXCN* numbers specifying the lines to be substituted are fed by the cards.

iii) Input data to be fed in "CDREAD"

The subprogram "CDREAD" is called when *ISFG* is equal to or greater than 1 (cf. **TABLE 5-3**). First, the title card, CD-1, and the card specifies *INPT* etc., CD-2, are read in. The measured data start from CD-3. If $ISFG=1$, the value of *IFMT* is examined. The non-zero value of *IFMT* implies the format of the measured data is different from (F6. 0, 9F7. 0) and then the variable format must be given (C-2′).

Sometimes, the final channel, *IFIN*, of the input data may not be obvious. In this situation, one can set up a safety device against the possible misinformation on the final channel by giving *ISFG* an appropriate number greater than 1, and by adding an extra card punched with 999999 from the first to the sixth column at the end of the data deck. Here, the ($ISFG\times10$)

```
AS01                                                                          AS010000
71-A-S027109041740     40          0.7 EU-152.NO.14.    1-1024               AS010010
 11024   30 1 3                                                               AS010020
 40000      1      6      6     10     10     30     40     50     43        AS010030
    48    126    748   3067   7278  10908  11718  11740  11239  11050        AS010040
 10701  10307   9983   9801   9336   9287   8910   8665   8835   8515        AS010050
  8383   8251   7982   7973   7872   7966   7737   7512   7567   7329        AS010060
  7318   7263   7096   7035   7006   6944   6883   6829   6702   6770        AS010070
  6708   6476   6519   6403   6340   6356   6269   6232   6190   6175        AS010080
  5978   6290   6028   6083   5896   6022   5965   5999   5730   5880        AS010090
  5711   5926   5870   5540   5763   5661   5709   5729   5638   5647        AS010100
  5560   5505   5570   5739   5571   5642   5536   5607   5407   5729        AS010110
  5582   5593   5639   5507   5400   5425   5570   5341   5420   5355        AS010120
  5297   5363   5156   5172   5175   5290   5108   5231   5102   5183        AS010130
  5075   5197   5123   5225   5119   5088   5069   5131   5153   5030        AS010140
  5084   4983   5048   5146   5086   4966   5147   5021   4905   5072        AS010150
  5008   5049   5002   5065   4963   4939   5081   4968   5034   5122        AS010160
  4991   5071   5024   4994   4986   5060   4924   5061   4928   4982        AS010170
  4941   5023   5041   5101   5191   5107   5184   5137   4944   5151        AS010180
  5039   4863   5156   5198   5184   5124   5136   5088   5061   5231        AS010190
  5144   5209   5163   5159   5226   5330   5709   6368   6947   7182        AS010200
  6957   6923   7528   8248   8473   7846   6681   5667   4954   4922        AS010210
  4968   4837   4803   4785   4891   4664   4780   4875   4757   4839        AS010220
  4755   4781   4851   5034   5073   5433   5903   6360   6292   6154        AS010230
  5669   5345   5225   5375   5269   5085   5047   4808   4944   4759        AS010240
  4642   4611   4651   4753   4643   4562   4719   4704   4644   4633        AS010250
  4574   4705   4670   4689   4653   4527   4565   4623   4518   4657        AS010260
  4547   4595   4665   4623   4657   4757   4669   4664   4673   4516        AS010270
  4547   4528   4561   4737   4593   4663   4646   4561   4685   4553        AS010280
  4555   4552   4622   4646   4587   4610   4612   4715   4632   4613        AS010290
  4685   4656   4673   4652   4573   4682   4669   4653   4770   4556        AS010300
  4713   4637   4722   4763   4729   4689   4582   4635   4687   4432        AS010310
  4550   4554   4605   4549   4595   4797   4777   4733   4681   4689        AS010320
  4501   4521   4581   4554   4555   4573   4639   4546   4536   4570        AS010330
  4550   4608   4662   4551   4534   4621   4636   4584   4417   4634        AS010340
  4526   4627   4542   4564   4633   4671   4464   4581   4539   4626        AS010350
  4486   4559   4587   4599   4577   4648   4499   4680   4580   4465        AS010360
  4695   4607   4579   4554   4658   4664   4616   4584   4564   4623        AS010370
  4458   4677   4644   4724   4621   4760   4796   4713   4783   4788        AS010380
  4875   4901   4735   4682   4889   4780   4871   4839   4866   4824        AS010390
  4872   4917   4878   4858   5039   4812   4957   4801   4723   4909        AS010400
  4697   4676   4677   4801   4726   4697   4726   4778   4754   4754        AS010410
  4712   4696   4719   4622   4592   4764   4564   4674   4630   4692        AS010420
  4674   4740   4752   4785   4752   4603   4749   4823   4754   4787        AS010430
  4679   4550   4527   4711   4667   4640   4602   4610   4727   4601        AS010440
  4599   4619   4681   4718   4664   4631   4600   4643   4599   4732        AS010450
  4491   4660   4612   4614   4569   4678   4661   4674   4695   4632        AS010460
  4684   4591   4661   4638   4759   4543   4584   4800   4639   4559        AS010470
  4662   4609   4707   4582   4656   4734   4632   4552   4580   4711        AS010480
  4818   4674   4711   4754   4785   4752   4684   4606   4696   4764        AS010490
  4644   4596   4630   4617   4627   4650   4547   4554   4467   4417        AS010500
  4486   4417   4367   4441   4465   4385   4315   4290   4269   4151        AS010510
  4335   4329   4201   4253   4120   4078   4130   4206   4078   4258        AS010520
  4269   4142   4193   4161   4126   4079   4143   4002   4149   4129        AS010530
  4158   3958   3988   4025   4039   4084   3963   3992   4054   3994        AS010540
  3966   3947   4022   3981   3937   3943   3878   3884   3966   3993        AS010550
  3921   3899   4004   3944   3907   3772   3869   3782   3880   3790        AS010560
  3644   3728   3855   3755   3778   3697   3713   3603   3681   3695        AS010570
  3690   3585   3631   3586   3547   3562   3479   3529   3459   3466        AS010580
  3455   3450   3555   3485   3388   3360   3403   3390   3396   3306        AS010590
  3480   3405   3330   3383   3479   3287   3312   3316   3405   3347        AS010600
  3346   3335   3373   3256   3375   3204   3298   3284   3350   3284        AS010610
  3531   3835   5026   7916  11623  15081  16148  13557   9477   6133        AS010620
  4042   3319   3233   3101   3032   3026   3017   2959   2935   2951        AS010630
  2971   3022   3089   3046   3098   2980   3045   2947   2845   2947        AS010640
  2853   2854   2859   2850   2842   2823   2824   2842   2789   2881        AS010650
  2893   2807   2918   2835   2752   2822   2854   2739   2793   2786        AS010660
  2709   2781   2804   2836   2745   2761   2677   2855   2909   2739        AS010670
  2772   2739   2650   2765   2881   2740   2761   2724   2867   2912        AS010680
  2780   2793   2719   2752   2685   2774   2703   2704   2727   2738        AS010690
  2744   2758   2728   2722   2642   2600   2690   2738   2645   2592        AS010700
  2712   2631   2647   2606   2506   2588   2573   2580   2562   2581        AS010710
  2493   2559   2472   2438   2515   2539   2529   2554   2517   2474        AS010720
  2565   2539   2537   2490   2517   2519   2600   2443   2496   2506        AS010730
  2434   2596   2438   2531   2536   2522   2574   2739   2812   3138        AS010740
  3359   3376   3259   2941   2564   2553   2450   2472   2376   2473        AS010750
  2412   2482   2411   2383   2273   2416   2325   2468   2427   2397        AS010760
  2332   2484   2371   2313   2444   2378   2399   2427   2398   2384        AS010770
  2384   2329   2376   2419   2458   2433   2471   2386   2379   2422        AS010780
  2439   2492   2465   2347   2322   2520   2425   2544   2513   2487        AS010790
  2356   2393   2435   2398   2281   2411   2275   2393   2338   2349        AS010800
  2321   2333   2380   2384   2399   2351   2342   2398   2496   2445        AS010810
  2444   2518   2506   2511   2427   2358   2300   2490   2497   2478        AS010820
  2539   2562   2644   2570   2532   2493   2384   2355   2318   2440        AS010830
  2380   2408   2395   2342   2418   2450   2426   2541   2435   2455        AS010840
  2468   2461   2504   2543   2467   2590   2585   2576   2633   2691        AS010850
  2637   2704   2915   3827   6978  14095  28057  45264  57985  57631        AS010860
 44531  26790  13262   5943   3049   2161   1947   1923   1941   1902        AS010870
  1883   2030   2021   1939   1957   1970   2030   1975   1962   1952        AS010880
  1937   1897   1897   1873   1904   1866   1840   1932   1866   1899        AS010890
  1900   1869   1836   1900   1925   1960   1953   1856   1904   1946        AS010900
  1904   1892   1866   1921   1887   1884   1878   2011   1884   1873        AS010910
  1893   2004   2142   2530   3063   3541   3820   3410   2890   2391        AS010920
  2096   1903   1899   1829   1886   1822   1882   1844   1870   1872        AS010930
  1906   1844   1822   1764   1907   1905   1887   1845   1810   1802        AS010940
  1865   1855   1934   1825   1902   1893   1891   1935   1766   1800        AS010950
  1913   1835   1868   1791   1882   1836   1866   1953   2011   2013        AS010960
  2062   2210   2012   2004   1815   1820   1896   1926   1795   1936        AS010970
  1858   1887   1917   1862   1821   1839   1879   1878   1813   1826        AS010980
  1783   1861   1865   1823   1787   1852   1810   1812   1817   1800        AS010990
  1802   1780   1870   1767   1849   1835   1865   1783   1816   1832        AS011000
  1848   1810   1718   1856   1818   1783   1791   1881   1756   1885        AS011010
  1864   1739   1840   1774   1837   1822   1964   2052   2794   3738        AS011020
  5126   6274   6377   5357   3922   2720   2180   1808   1732   1766        AS011030
  1830   1931   1930   2004   1976   1884   1865   1815   1760   1741        AS011040
  1781   1713   1752 444444                                                 AS011050
999999999999999999999999999999999999999999999999999999999999999999999999AS011060
```

Fig. 5-4 An illustration of the input format recorded in the magnetic tape as the input data in "MTREAD"

TABLE 5-3 The formats of the input cards in "CDREAD"

Card No.	Symbol	Columns	Format	Description
CD-1	IDN	1- 8	2A4	Data-identification index
	COM	9-32	6A4	Comments on the data
	ITR	33-38	I 6	Counting duration in the live-time mode
	IUNT	39	I 1	=0 *ITR* and *ITC* (kilo sec)
				=1 *ITR* and *ITC* (hecto sec)
				=2 *ITR* and *ITC* (sec)
				=3 *ITR* and *ITC* (min)
	ITC	40-45	I 6	Counting duration in the clock-time mode
	IDATE	46-51	I 6	Date of the measurement
	ITIME	52-55	I 4	Time of the measurement
	PDT	56-60	F5.2	Ratio of the dead time (%)
	T0	61-66	F6.2	Constant term in the dead time equation (μsec)
	TS	67-72	F6.3	Channel-proportional term in the dead time equation (μsec)
CD-2	INPT	1- 4	I 4	Initial channel of the input data
	IFIN	5- 8	I 4	Final channel of the input data
	INIT	9-12	I 4	Initial channel of the analysis
	ISM	13-14	I 2	<11 $(2\times ISM+5)$-point smoothing
				=11 3-point smoothing
				=12 No smoothing
	ISTP	15-16	I 2	=0 Continuation of the executing condition
				=1 End of execution
				=2 Renewal of the executing condition
CD-2′	FORM	1-80	20A4	(Input format of the data)
CD-3	DATA(I)	1-69	F6.0, 9F7.0	The number of counts at each channel, $I=INPT, IFIN$
CD-3′	DATA	1- 6	F6.0	The end-mark of input data, 999999

works as the upper limit of the confidence interval on the *IFIN*. It should, however, be mentioned that this routine is prepared only for the fixed format of (F6.0, 9F7.0).

iv) Input data to be fed in "ENGEF"

The input data concerning the energy and the efficiency calibration are read in "ENGEF" (cf. TABLE 5-4). The input forms are different between the cases of giving the standard spectra ($IE=1$) and of supplying the calibration curve ($IE=2$).

In the former ($IE=1$), the first card, E-1, should contain the number of the peaks *NP* prepared as the standard, the order of the polynomial of the energy calibration, approximate energies (keV) corresponding to the *INIT* and *IFIN* channels of the (last) standard input data, and an index controlling whether the necessary information on the resulting calibration curve is punched out or not. A group of cards starting from E-2 carry the energies of the given *NP* standard peaks and as the end of them the allowance, *WCH*, for the error in the readings of the corresponding peaks in keV. If the finite *WCH* is not given, 10 keV is assigned to it. In case where the counting efficiency is also required, the disintegration rate of the source and the branching ratio of the relevant peaks are added in the succeeding set of cards.

In the latter ($IE=2$), the coefficients of the calibration curves and the matrix elements for computing the standard deviations are supplied. The first card, E-5, gives the numbers of the coefficients and the variances in the fit of the observed data to the calibration curves. The

TABLE 5-4 The formats of the input cards in "ENGEF" of BOB 73

Card No.	Symbol	Columns	Format	Description
	(In the case of IE=1)			
E-1	NP	1- 5	I 5	Number of peaks prepared as the standard
	M	6-10	I 5	The order of polynomial as the energy calibration curve
	EINT	11-20	E10.3	Energy corresponding to *INIT* (keV)
	EFIN	21-30	E10.3	Energy corresponding to *IFIN* (keV)
	IPCH	31-32	I 2	=0 No punchout of the results of ENGEF
				=1 Punch the results
	ISTDT	33-34	I 2	≠0 Calling the stored data for the standard spectra
	UNIT	35-44	E10.3	Unit of the activity (10^4 dps unless particularly specified)
	WCH	45-54	F10.3	Confidence interval in approximated energies of the standard peaks
E-2	EST(I)	1-80	8F10.3	Energies of the standard peaks (keV), I=1, NP
E-3	SACTY(I)	1-80	8F10.3	Activities of the standard sources, I=1, NP
E-4	GRATIO(I)	1-80	8F10.3	Branching ratios of the standard peaks, I=1, NP
	(In substitution of, or in addition to, E-2 to E-4)			
E-2′	NUC	1- 2	I 2	Number of the standard nuclides to be referred
E-3′	NAME(I)	1-40	20A4	Labeled name for the standard, I=1, NUC AM41 for Am-241 CO57 for CO-57 HG03 for Hg-203 SN13 for Sn-113 CS37 for Cs-137 MN54 for Mn-54 NA22 for Na-22 CO60 for Co-60 Y88 for Y-88 EU52 for Eu-152 (14 peaks) EU2F for Eu-152 (19 peaks)
E-4′	RINT(I)	1-80	8E10.5	Intensity of the activity, I=1, NUC
	(In the case of IE=2)			
E-5	ICEE	1- 5	I 5	Number of the coefficients in the energy-calibration polynomial
	ICEF	6-10	I 5	Number of the coefficients in the efficiency-calibration polynomial
	ES	11-21	E11.5	Variance in the fitting of the channel-energy curve to the polynomial (if *ES* is not given, the following E-7 is not required)
	FS	22-32	E11.5	Variance in the fitting of the energy-efficiency curve to the polynomial (if *FS* is not given, E-9 is not required)
	UNIT	33-42	E11.5	Unit of the activity (10^4 dps unless particularly specified)
E-6	C(I)	1-75	5E15.8	Coefficients in the energy-calibration polynomial, I=1, ICEE
E-7	XI(I, J)	1-69	3D23.16	Elements of the inverse matrix for energy assigement, I=1, M+1; J=1, M+1
E-8	CF(I)	1-75	5E15.8	Coefficients in the efficiency-calibration polynomial, I =1, ICEF
E-9	XFI(I, J)	1-69	3D23.16	Elements of the inverse matrix for efficiency assignment, I=1, M; J=1, M

second card, E-6, defines the coefficients of the energy calibration curve. The following cards, E-7, supply the matrix elements to be used in the error estimation (cf. Eq.(15) of ref. 5 a). This set of cards is omitted when $ES=0$. If the efficiency correction is required as well, the coefficients of the effiency curve and the matrix elements are added by the cards, E-8 and E-9. The set of the cards E-9 is omitted if $FS=0$. The whole set of the input of E-5 through E-9 can be prepared by the punched cards in the previous run in which $IE=1$ and $IPCH=1$. If one wants to use the calibration curves already known by other means, one can introduce only the coefficients of the calibration curves by leaving ES or FS as zero.

5. 3 Instruction Manual for "NAISAP"

5. 3. 1 Directions for use

Differences of NAISAP from BOB 73 appear in choosing the "PKREC" function for the low-resolution spectrum ($IRP=1$) and in applying the response function in the fitting procedure. The rest of the code is almost identical to that of BOB 73, or we may rather say that the both codes are attempted to be unified as much as possible.

As stated in Chapter 2, the user is required to give the ISM value appropriate at the first quarter of the entire spectrum. As an example, the suitable value of ISM is 0 for the spectrum with $INIT=1$, $IFIN=256$ and the conversion ratio being 10 keV/channel. This is because the NaI(Tl) detector usually possesses the resolving power of 7 to 8% at the 662-keV peak from ^{137}Cs, which locates at about one-fourth of the spectrum.

The values of the parameters defining the response function of the $1\frac{3}{4}''\phi\times 2''$ or $3''\phi\times 3''$ NaI(Tl) crystal are contained in the subroutine program "PARA," which can be taken out by means of the $IDET$ value; namely,

$$IDET=\begin{cases} 2 & \text{for } 1\frac{3}{4}''\phi\times 2'' \text{ NaI (Tl)} \\ 3 & \text{for } 3''\phi\times 3'' \text{ NaI (Tl).} \end{cases}$$

The effect that the response function slightly changes with the distance between the detector and the source is not taken into consideration in the present code.

The subprogram "PARA" can also be applied to general types of the NaI(Tl) detector by putting $IDET=1$ and by feeding empirical equations expressing the energy dependence of the required parameters. Though the response function is almost identical for the NaI(Tl) detectors with the same size, the full width at half maximum differs from crystal to crystal and depends on the electronic setup as a whole. Since the $FWHM$ affects the most the value of the peak area, the most appropriate peak width is searched in the least squares fitting procedure. However, it is still desirable giving the initial guess as accurate as possible. The energy dependence of the width parameter $\sigma_p(=0.4247\ FWHM)$ is given in "PARA" as

$$\sigma_p=\begin{cases} 0.0291\cdot FWID\cdot E_\gamma{}^{0.557FP} & \text{for } 1\frac{3}{4}''\phi\times 2'' \\ 0.0266\cdot FWID\cdot E_\gamma{}^{0.557FP} & \text{for } 3''\phi\times 3'' \end{cases}, \qquad (5\text{-}1)$$

where E_γ is the photon energy expressed in unit of MeV and σ_p is also given in MeV. The factors $FWID$ and FP are the correction factors for individual systems.

As mentioned in 4. 1. 1, the peak-searching subprogram "PKREC" tends to pick up spurious peaks while it hardly overlooks small true peaks. Judgement of a peak being true or false

is performed through Eqs.(4-14), (4-15a) and (4-15b). One ought to assign a small value (<1) to FTH if one wants to select large peaks only.

5. 3. 2 Description of the input data for "NAISAP"

In this code, the input data are read in the form of the IBM cards. All data but those for the energy and efficiency calibration are read in the main program. The style of the input substantially follows that of BOB 73, except for the second card M-2.

i) Input data to be fed in "MAIN"

The first card M-1 possesses the identical contents with those of the M-1 card in TABLE 5-1, though many of the contained indices (denoted as "dummy" in TABLE 5-5) are not used in NAISAP. The second card M-2 specifies the FTH, $FWID$, FP, A and B values, and an index $IWID$. Here, A and B are the constants determining the primary linear conversion relation between channel number x and energy E;

$$E=A(x-B). \tag{5-2}$$

In the case where the FTH, $FWID$ or FP is not given, the value of unity is assigned to them.

The index $IWID$ controls the choice between the fixed and non-fixed $FWHM$ in the least squares fitting. The $FWHM$ is fixed when $IWID=0$.

The cards M-3 to M-5 in TABLE 5-5 correspond to CD-1 to CD-3, respectively, in TABLE 5-3.

ii) Input data to be fed in "ENGEF"

The input data required for the energy and efficiency calibration are practically the same as those in the case of BOB 73 (cf. TABLE 5-6). Only the difference exists in the format of the second card E-2 and in the fact that $EINT$ and $EFIN$ in the first card E-1 need not be given because they are calculated by means of Eq.(5-2). Furthermore, the confidence interval WCH for energy assignment to the peak is taken to be 30 keV, instead of 10 keV in BOB 73, unless particularly given.

TABLE 5-5 The formats of the input cards in "MAIN" of NAISAP

Card No.	Symbol	Columns	Format	Descripton
M-1	ISFG	1- 2	I 2	Dummy
	ISTD	3- 4	I 2	Number of spectrum data in the standard set
	IRP	5- 6	I 2	Dummy
	IE	7- 8	I 2	=0 External calibration
				=1 Internal calibration
				=2 Calibration with the previously constructed curve
				=9 No calibration
	IENG	9-10	I 2	=0 Energy assignment and intensity determination
				=1 Energy assignment only
	IDEC	11-12	I 2	Dummy
	IFMT	13-14	I 2	Dummy
	IPLT	15-16	I 2	=0 Skip plotting the spectrum
				=1 Plot with the scale of 2.5 channels/mm
				=2 Plot with 5 channels/mm
				=3 Plot with 1 channel/mm
	IW(1)	17-18	I 2	=0 Print the conditions of analysis
				=1 No print

TABLE 5-5 (continued)

	IW(2)	19-20	I 2	=0 Blockwise printing of the original data only
				=1 Blockwise printing of the smoothed data only
				=2 Blockwise printing of both original and smoothed data
				=3 Channelwise printing of the results of SMART
				=4 No printing of the input data
	IW(3)	21-22	I 2	=0 Print the results of PKREC
				=1 No print
	IW(4)	23-24	I 2	=0 Print the final results
				=1 No print
	IBG	25-26	I 2	Dummy
	IFTG	27-28	I 2	Dummy
	NIJ	29-30	I 2	Dummy
	NONPR	31-32	I 2	Dummy
	IGFT	33-34	I 2	=0 No printing of fitting process
				=1 Print
	IPKW	35-36	I 2	=0 No printing of the results of RESFIT
				=1 Print
	IWT	37-38	I 2	=0 Fit with the built-in weight
				=1 Fit with equal weight
	ISEL	39-40	I 2	Dummy
	LVL	41-42	I 2	Dummy
M-2	IDET	1	I 1	=1 Response function parameters for user's detector
				=2 $1(3/4)''\phi\times 2''$ NaI (Tl) detector
				=3 $3''\phi\times 3''$ NaI (Tl) detector
	A	2-10	F 9.5	Channel width (keV)
	B	11-20	F10.5	Zero-shift in energy calibration equation ; $E=A(x-B)$
	FTH	21-30	F10.5	Threshold factor
	FWID	31-40	F10.5	Correction factor for *FWHM* stored in PARA
	FP	41-50	F10.5	Correction factor for *FWHM* stored in PARA
	IWID	51-52	I 2	=0 *FWHM* floated
				=1 *FWHM* fixed
M-3	IDN	1- 8	2A4	Data-identification index
	COM	9-32	6A4	Comments on the data
	ITR	33-38	I 6	Counting duration in the live-time mode
	IUNT	39	I 1	=0 *ITR* and *ITC* (kilo sec)
				=1 *ITR* and *ITC* (hecto sec)
				=2 *ITR* and *ITC* (sec)
				=3 *ITR* and *ITC* (min)
	ITC	40-45	I 6	Counting duration in the clock-time mode
	IDATE	46-51	I 6	Date of the measurement
	ITIME	52-55	I 4	Time of the measurement
	PDT	56-60	F5.2	Ratio of the dead time (%)
	T0	61-66	F6.2	Constant term in the dead time equation (μ sec)
	TS	67-72	F6.3	Channel-proportional term in the dead time equation (μ sec)
M-4	INPT	1- 4	I 4	Initial channel of the input data
	IFIN	5- 8	I 4	Final channel of the input data
	INIT	9-12	I 4	Initial channel of the analysis

TABLE 5-5 (continued)

	ISM0	13-14	I 2	<11 ($2\times ISM0+5$)-point smoothing =11 3-point smoothing =12 No smoothing
	ISTP	15-16	I 2	= 0 Continuation of the executing condition = 1 End of execution = 2 Renewal of the executing condition
M-5	DATA(I)	1-69	I 6, 917	The number of counts at each channel, $I=INPT$, $IFIN$

TABLE 5-6 The formats of the input cards in "ENGEF" of NAISAP

Card No.	Symbol	Columns	Format	Description
	(In the case of IE=1)			
E-1	NP	1- 5	I 5	Number of peaks prepared as the standard
	M	6-10	I 5	The order of polynomial as the energy calibration curve
	EINT	11-20	E10.3	Dummy
	EFIN	21-30	E10.3	Dummy
	IPCH	31-32	I 2	=0 No punchout of the results of ENGEF =1 Punch the results
	ISTDT	33-34	I 2	Dummy
	UNIT	35-44	E10.3	Dummy
	WCH	45-54	F10.3	Confidence interval in approximated energies of the standard peaks
E-2	EST(I)	1-80	8F10.3	Energies of the standard peaks (keV), I=1, NP
E-3	SACTY(I)	1-80	8F10.3	Activities of the standard sources, I=1, NP
E-4	GRATIO(I)	1-80	8F10.3	Branching ratios of the standard peaks, I=1, NP
	(In the case of IE=2)			
E-5	ICEE	1- 5	I 5	Number of the coefficients in the energy-calibration polynomial
	ICEF	6-10	I 5	Number of the coefficients in the efficiency-calibration polynomial
	ES	11-21	E11.5	Variance in the fitting of the channel-energy curve to the polynomial (if ES is not given, E-7 is not required)
	FS	22-32	E11.5	Variance in the fitting of the energy-efficiency curve to the polynomial (if FS is not given, E-9 is not required)
E-6	C(I)	1-75	5E15.8	Coefficients in the energy-calibration polynomial, I=1, ICEE
E-7	XI(I, J)	1-69	3D23.16	Elements of the inverse matrix for energy assignment, I=1, M+1; J=1, M+1
E-8	CF(I)	1-75	5E15.8	Coefficients in the efficiency-calibration polynomial, I=1, ICEF
E-9	XFI(I, J)	1-69	3D23.16	Elements of the inverse matrix for efficiency assignment, I=1, M; J=1, M

6. Discussion

The character of the resulting code is roughly controlled by the way grasping the γ-ray spectrum analysis. If one regards it as a mere curve fitting, one will put a heavy stress on the peak fitting process. However, it is not easy at all to construct a satisfactory peak detecting process faithfully reflecting fine structures in the spectrum. The function of recognizing a pattern which is the most elementary function of the human eyes is yet one of the functions that the electronic computer of the current type lacks. The graphic display system is devised just for reinforcing the computer in this respect.

Although visual inspection with the graphic display system with a light pen has solved the problem of the spectrum analysis in a sense, the situation is far from the full automation. Above all, one should realize that not many laboratories can afford such facilities.

When one intends to achieve the problem of recognizing a pattern with an electronic computer, one must content oneself with transforming any information on the given pattern into a digital quantity. A group of thus extracted quantities needs, in turn, to be recognized in a functional form. Various attempts for the γ-spectrum analysis just follow this pattern of procedure.

The guiding principle of the peak search is summarized as the comparison of the first or second derivative of the spectrum with an appropriately established threshold. There are, of course, some differences in the effectiveness between the first and the second derivative method. Which one of the two will be chosen is, however, a matter of the personal preference after all. Generally speaking, the latter is believed to be more sensitive in finding half-hidden small peaks. This also means that one tends to pick up pseudo-peaks more often by the second derivative method and, therefore, one needs to prepare appropriate preventives against the errors. On the contrary, the performance of the first derivative method is more intuitively understandable although it certainly has some disadvantages compared to the second derivative method. In other words, one can fairly easily extract from a certain fine structure in the spectrum the characteristic rule which exists among the first derivatives in the given region. This is just the reason why we have chosen the first derivative method.

The presently available codes impose more weight on the peak-fitting process rather than the peak-finding one. In these codes, the full width at half maximum *FWHM* plays an important role. The multiplicity of a given peak is determined by comparing the length of the peak region with the *FWHM*. This method was, however, rejected in the present work from the following three reasons: First, it was believed to be inferior in the ability of recognizing a narrow doublet or a small shoulder to the method described in Chapter 2. Second, it can give only the multiplicity and is ignorant of the peak positions that would be a serious handicap in the succeeding fitting process. Third, the most definite of all, we wanted to reduce any procedures retrograde against the full automation as least as possible throughout the whole process.

The present version BOB 73 possesses several advantages over the previous version BOB 70/71, which were not expected to be attained at the moment of the publication[5]. First of all, the capability of "PKREC" is much improved so that better consistency can be obtained with BOB 73. This can be seen, for example, from the results of **Fig. 3–8** with the equivalent figure, **Fig. 10** in ref. 5b. Secondly, the function of the peak recognition is extended so as to be applied not only to the spectrum from Ge(Li) detectors but also to the spectra of other types. The modified "PKREC" and an analytical representation[4] of the γ-ray response function of the

NaI(Tl) detector has been combined to form an analyzing code NAISAP for the NaI(Tl) spectrum from a unique viewpoint. Finally, particular considerations are introduced into the peak-fitting process which had not been foreseen at the moment. The stepwise background, peak-asymmetry and tailing are introduced in a unique manner.

Note that such special considerations for the peak shape and background are required to acquire better consistency in the peak position and the peak area for small nearby peaks. For a well separated peak or the greatest one in a cluster of peaks, more or less the same result can be obtained even with the combination of the simple Gaussian curve and a simple background shape.

Another advantage of the present code, either BOB 73 or NAISAP, is that practically no input data are required as the initial estimates in the peak-fitting procedure.

As the concluding remark, one ought to remember that the final result is essentially regulated by the quality of the input data after all.

7. Summary

The problem of the spectrum analysis has been solved by combining the peak-recognizing and peak-fitting processes.

The stage of the peak recognition was set up in such a way that the peak position, the multiplicity and the peak boundaries are predicted for a detected peak group. Such functions were realized by adding, to the ordinary first derivative method, various shape tests for detecting fine structures. The most prominent uniqueness of the present peak-recognizing procedure may lie in the fact that the peak width needs not be known for judging the multiplicity. Only a rough value of the *FWHM* is necessary as a measure of the condition for data smoothing and the choice of the threshold in the peak detection. The difference in the peak recognition between the Ge(Li) and the NaI(Tl) spectra was reduced only to the difference in the energy dependence of the peak width. The *FWHM* was regarded as practically constant in the former spectrum, whereas it was approximated to be proportional to the square root of the channel number in the latter.

It was pointed out that the most difficulties in the peak-fitting problem lay in the determination of the peak shape and the construction of a reasonable background shape. It should be mentioned that the photopeak method popularly applied to the Ge(Li) spectrum proved to be also quite a promising technique for the analysis of the NaI(Tl) spectrum, contrary to the general understanding. A successful attempt[4] of describing the NaI(Tl) response function with a fairly simple analytical form made this idea practical. In the Ge(Li) spectrum, the Compton continuum is regarded as background. The surplus part of the relevant peak group is subjected to the fitting procedure as a whole. On the contrary, the residual spectrum except for the response of the objective gamma ray whose intensity is to be determined is considered the background in the case of the NaI (Tl) spectrum. Therefore, the background is expressed by a compound of response functions and a smoothed curve in the latter. The establishment of the generalized peak-searching process has brought its advantage into full play, in the prosecution of the photopeak method.

Once the above course had been established, the most difficult part of the peak fitting was removed in the case of the NaI(Tl) spectrum. Difficulties were rather found in quantitatively dissolving the complex peaks in the Ge(Li) spectrum. The response given by the Ge(Li) detector turned out to be hardly expressed in an analytical form in spite of its apparent simplicity.

First, we had to solve the question how the peak shape would be best approximated. The peak shape is usually described with the Gaussian curve in the first approximation. However, asymmetry in the peak shape is rather commonly observed for Ge(Li) detectors and, therefore, it needs to be taken into account to attain better approximation. We introduced the asymmetric property by connecting two half-Gaussian curves with different widths at the peak position. It is also known[8] that the full-energy peak exhibits tailing, especially on the low-energy side. In the present code, the tail on the low-energy side was satisfactorily reproduced by superimposing a similar curve on the main asymmetric Gaussian.

Secondly, we faced a still unsolved question of estimating the background underneath the peak consistently. A popular way[8] of adopting a polynomial fitted to the outskirt of the relevant peak was found undesirable because it could cause a fatal error both in the peak position

and area of a small peak close to a huge peak. The simple linear or exponential function connecting the peak boundaries on both sides brought better results than the fitted polynomial background on the whole. A sigmoid curve (or a stepwise function) has given so far the best consistency both in the peak position and area. After all, the background shape is chosen as the superposition of the sigmoid curves each one of which is attributed to one peak in the peak compound.

Two versions of BOB 73 are prepared. The full-size version can handle a complex peak with the multiplicity of up to 18 (or up to 19 in the case of no tailing) and a spectrum containing up to 200 peaks, and the size is 103k words. The small-size version was intended so that the size was restricted below 64k words, with maintaining the same quality as the full-size version. It can handle a complex peak with the multiplicity of up to 8 (or up to 9 in the case of no tailing) and a spectrum containing up to 100 peaks, but does not accompany the plotting subroutine program "SPECTR" and also the subprogram "SUBTRX". The size is just 64k words.

The data size (the number of channels) is practically unlimited in either version. The time required for the spectrum analysis by BOB 73 depends on the number of peaks existing in the spectrum and their complexity rather than the size of the spectrum. Roughly speaking, the analysis of one compound peak with moderate complexity by FACOM 230-60 takes one second or a fraction of one second, and the energy calibration and efficiency correction need additionally an order of 10 seconds.

Two versions are prepared also for NAISAP: the 76k-word version can accept a spectrum of up to 1024 channels while the 60k-word one handles a spectrum with channels not greater than 300. Either version requires an order of one second for the analysis of each peak.

Acknowledgements

The authors wish to express their gratitude to Mr. N. SAITO of the computer center for his help and advice especially in the completion of the data conversion system via FACOM 230-35. They are also grateful to Messers. T. SUZUKI, H. YAGI, H. UMEZAWA and H. GOTOH for their valuable discussions. Their deep appreciation is also expressed to the ex-director, Mr. T. MOCHIZUKI, and Drs. H. AMANO and H. NATSUME for their interest and encouragement throughout this work.

References

1) HEATH R.L., HELMER R.G., SCHMITTROTH L.A. and CAZIER G.A.: *Nucl. Instr. and Methods* **47**, 281 (1967).
2) CHESTER R.O., PEELLE R.W. and MAIENSCHEIN F.C.: NAS-NS 3107, Proc. Symp. on applications of computers to nuclear and radiochemistry, p. 201, IAEA (Gatlinburg, 1962).
3) SALMON L.: Proc. Symp. on radiochemical methods of analysis, Vol.II, p. 125, IAEA (Vienna, 1965).
4) SEKINE T., BABA S. and BABA H.: JAERI-M 4590, unpublished (1971).
5) (a) BABA S., BABA H. and OKASHITA H.: JAERI 1216 (1971);
(b) BABA H., OKASHITA H., BABA S., SUZUKI T., UMEZAWA H. and NATSUME H.: *J. Nucl. Sci. and Tech. (Tokyo)* **8**, 703 (1971).
6) BOWMAN W.W.: *Nucl. Instr. and Methods* **96**, 135 (1971).
7) MARISCOTTI M. A.: *ibid.* **50**, 309 (1967).

8) ROUTTI J. T. and PRUSSIN S. G.: *ibid.* **72**, 125 (1969); ROUTTI J. T.: UCRL-19452, unpublished (1969).
9) INOUYE T., HARPER T. and RASMUSSEN N.C.: *Nucl. Instr. and Methods* **67**, 125 (1969).
10) COVELL D.F.: *Anal. Chem.* **31**, 1785 (1959).
11) STERLINSKI S.: *ibid.* **40**, 1995 (1968); *ibid.* **42**, 151 (1970).
12) See for example, HOTZ H.P., MATHIESEN J.M. and HURLEY J.P.: *Phys. Rev.* **170**, 351 (1968).
13) SAVITZKY A. and GOLAY M.J.E.: *Anal. Chem.* **36**, 1627 (1964).
14) NATSUME H.: *J. Atomic Energy Soc. Japan* **12**, 551 (1970).

Appendix 1

Either code, BOB 73 or NAISAP, is stored in the permanent RB file of the computer center for user's convenience. Users who wish to recall the program should prepare the following set of the control cards:

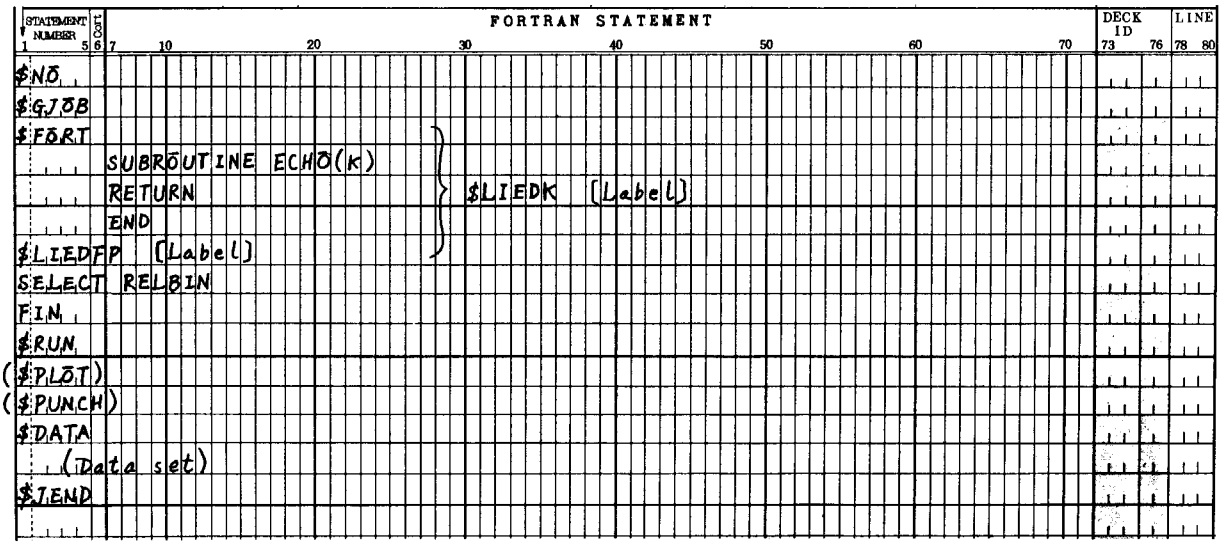

Here, the [Label] in the seventh line is to be substituted with the corresponding name among the followings.

J0458. BOB73S for the small size version of BOB 73 in the system #1,

J0458. BOB73 for the full size version of BOB 73 in the systems #1 and #2,

J2619. NAISAP for the small size version of NAISAP in the system #1 and the full size version of NAISAP in the system #2,

J2619. NAISAL for the full size version of NAISAP in the system #1.

As stated in the text, the content of the subroutine "ECHO" can be substituted temporalily with a user's program.

Appendix 2. Examples ot the output listings

Fig. A-1 Table of the counting and analyzing conditions.

```
73-04-07          ***************  GAMMA SPECTRUM ANALYSIS OF U(3)-4          1-1024
                                                  BY BOB73  ***************          MO-F-1  -  1

MO-F-1   = BOB73   IDENTIFICATION                  NO  = LIVE TIME CORRECTION
       1 = INITIAL CHANNEL OF DATA                  10 = COUNTING DURATION (LIVE TIME) (CSEC )
    1024 = FINAL CHANNEL OF DATA                  0.0 = PERCENT DEAD TIME
    1024 = NUMBER OF DATA POINTS                  NO  = PLOTTING
      54 = INITIAL CHANNEL OF ANALYSIS            YES = ENERGY ASSIGNMENT
    1020 = FINAL CHANNEL OF ANALYSIS              YES = EFFICIENCY CORRECTION
     967 = NUMBER OF ANALYZING POINTS               5 = ORDER OF ENERGY ASSIGNMENT POLYNOMIAL
       5 = POINTS USED IN SMOOTHING                 4 = ORDER OF EFFICIENCY CORRECTION POLYNOMIAL
       5 = POINTS USED IN DERIVATIVE              YES = COEFFICIENTS EVALUATED INTERNALLY
      NO = STORED STANDARD                        NO  = COEFFICIENTS GIVEN EXTERNALLY
     YES = PEAK FITTING

ALL PEAKS WERE FITTED TO THE FUNCTION WITH FOLLOWING PROPERTIES

1/ 7 POWER  = BACK-GROUND SHAPE
1.0000      = SKEWNESS OF GAUSSIAN FUNCTION
NO          = TAILING
BUILT-IN WT.= WEIGHT IN FITTING PROCESS

COEFFICIENTS OF ENERGY ASSIGNMENT POLYNOMIAL (ENERGY VS CHANNEL)

C( 1)=-2.3785471E 00+- 4.796E-01          C( 2)= 5.0565648E-01+- 2.918E-03
C( 3)=-7.0426076E-06+- 5.731E-06          C( 4)= 5.2685308E-09+- 4.738E-09
C( 5)=-1.8896696E-12+- 1.731E-12          C( 6)= 2.5027253E-16+- 2.305E-16

COEFFICIENTS OF EFFICIENCY CORRECTION (LOG(EFCY) VS LOG(ENERGY)

C( 1)= 3.4336499E 00+- 4.938E 01          C( 2)= 1.7493696E 00+- 3.346E 01
C( 3)= 3.9294700E-02+- 8.442E 00          C( 4)=-7.5262811E-02+- 9.403E-01
C( 5)= 5.5881388E-03+- 3.902E-02
```

Fig. A-2 List of the input data.

```
73-04-07          ***************  GAMMA SPECTRUM ANALYSIS OF U(3)-4          1-1024
                                                  BY BOB73  ***************          MO-F-1  -  2

                                        INPUT DATA (FROM    1 CH. TO 1024 CH.)
CH. NO.
```

CH. NO.																				
1 -	1000	0	0	1	5	0	0	0	0	0	0	2	6	10	16	20	35	45	69	75
21 -	131	172	261	685	2578	4958	5085	5097	5045	4962	4927	5066	5228	5214	5467	5698	5178	4474	3912	3788
41 -	3853	4043	4295	3956	3725	3430	3268	3105	3252	3356	3416	3314	3518	3591	3720	3968	4242	4213	3973	4050
61 -	4301	4369	3770	3151	2821	2683	2609	2659	2640	2986	3056	3077	2752	2437	2234	2297	2470	2510	2267	2140
81 -	2088	2180	2119	2123	2024	1999	2075	2121	2134	2228	2110	2126	2070	2097	2121	2119	2125	2426	2728	2844
101 -	2563	2295	2256	2166	2262	2275	2327	2236	2323	2413	2425	2493	2514	2773	3018	2871	2615	2677	2776	2792
121 -	3077	3821	4474	4261	3376	2958	2867	2847	2819	2860	2874	3019	2916	3128	3152	3163	3331	3177	3058	3171
141 -	3362	3431	3393	3591	3617	3658	3827	3924	4002	4170	4275	4152	4159	4206	4186	4126	4152	4263	4378	5145
161 -	6777	8929	8335	6055	4735	4439	4433	4626	4669	4772	4943	5035	5004	5060	5102	5278	5236	5187	5128	5336
181 -	5634	5942	6045	5755	5307	5242	5254	5239	5259	5349	5212	5084	4941	5113	5364	6163	9810	17786	25192	22340
201 -	12431	6400	4670	5108	8273	18136	33086	36685	24048	16303	26480	44080	42346	21467	6591	2465	1834	1745	1685	1597
221 -	1663	1727	1762	1788	1713	1616	1705	1733	1818	2230	3790	6321	9083	10886	9799	6269	3220	2008	2265	3467
241 -	4588	4837	3625	2631	1806	1456	1321	1244	1198	1241	1198	1198	1247	1189	1256	1203	1163	1245	1125	1153
261 -	1155	1159	1233	1199	1180	1308	1270	1299	1212	1214	1232	1170	1200	1178	1164	1208	1271	1504	2811	5326
281 -	7410	5880	3034	1429	1088	1011	996	1230	1457	2252	2537	2072	1388	1101	938	912	930	932	982	986
301 -	974	882	968	906	929	973	940	903	867	883	860	887	925	912	903	862	912	877	921	890
321 -	842	907	993	1118	1251	1201	953	937	886	884	814	833	895	854	821	866	821	870	856	829
341 -	816	885	854	852	809	875	867	843	764	804	816	815	790	783	765	786	818	808	770	875
361 -	1053	1255	1173	939	843	822	753	772	762	742	796	770	765	731	753	730	766	731	740	743
381 -	748	696	787	740	747	691	705	732	705	664	667	677	713	644	679	633	634	701	626	679
401 -	613	648	657	642	626	633	601	608	607	600	588	702	602	624	628	832	1356	2855	4300	3796
421 -	2188	983	606	586	538	515	501	515	507	519	491	539	507	523	480	533	505	490	546	512
441 -	550	539	498	553	543	507	539	581	613	680	775	1122	1958	4869	10553	15093	11967	5745	1699	577
461 -	388	423	379	391	368	395	358	346	364	360	341	358	326	356	369	412	367	403	343	365
481 -	353	351	355	383	355	331	338	349	292	305	296	312	325	305	314	307	300	305	281	253
501 -	321	283	338	317	305	289	339	428	387	389	332	320	288	303	294	281	294	284	304	300
521 -	300	307	306	319	334	337	282	279	307	293	329	304	331	309	318	292	280	272	292	340
541 -	323	302	297	351	392	378	355	369	397	487	751	2018	5258	10051	11494	7587	3001	739	268	238
561 -	213	235	211	233	216	244	323	398	651	869	762	495	304	234	210	220	181	208	175	206
581 -	192	242	237	341	540	645	541	366	240	225	189	184	211	206	192	182	192	190	179	210
601 -	197	209	197	190	193	218	244	267	288	301	254	217	203	158	188	179	186	191	178	210
621 -	187	171	214	191	211	170	216	257	485	854	1238	1052	586	298	199	168	239	208	220	204
641 -	173	164	179	183	157	149	138	144	179	161	156	188	197	261	383	673	746	616	353	211
661 -	144	141	178	240	326	580	1131	1413	1104	613	275	151	154	146	150	148	138	153	141	174
681 -	134	139	141	145	138	142	155	128	145	152	133	143	123	131	137	144	143	119	143	184
701 -	206	160	186	149	178	145	118	123	130	122	130	116	131	132	116	135	130	144	127	134
721 -	128	126	151	177	240	496	858	1260	1167	674	307	192	154	113	110	115	124	110	91	107
741 -	123	115	103	96	116	112	84	114	130	115	102	108	105	120	120	92	105	124	105	117
761 -	110	124	96	106	108	93	112	109	105	111	98	88	92	100	113	124	96	84	95	101
781 -	114	105	102	132	109	99	83	103	97	102	117	98	88	106	132	99	100	94	104	107
801 -	105	92	88	109	90	113	96	96	90	97	102	103	92	111	105	105	102	106	98	79
821 -	116	111	109	106	90	96	109	101	116	101	107	96	87	109	100	99	83	112	100	119
841 -	96	94	101	102	128	164	150	146	120	104	82	70	82	105	92	93	94	111	114	108
861 -	113	119	147	158	158	138	112	101	99	94	94	90	125	117	128	108	110	96	96	106
881 -	102	91	79	110	103	91	113	88	116	86	99	106	112	125	92	128	96	84	98	84
901 -	107	87	101	104	89	83	90	105	87	107	87	91	89	82	92	103	86	91	101	100
921 -	123	89	102	86	110	99	98	75	77	102	91	94	81	107	99	93	91	93	85	77
941 -	73	92	101	83	108	113	103	111	92	85	102	86	87	84	106	102	125	86	92	89
961 -	87	105	115	95	87	91	86	92	121	208	362	669	838	725	464	220	105	84	97	100
981 -	91	85	90	74	79	80	83	82	92	112	208	258	329	324	238	108	88	86	68	69
1001 -	67	74	80	82	81	86	67	86	88	121	156	115	90	80	77	94	73	64	76	89
1021 -	88	77	94	71																

Fig. A-3 List of the smoothed data.

73-04-07 *************** GAMMA SPECTRUM ANALYSIS OF U(3)-4 1-1024

BY BOB73 *************** MO-F-1 - 3

SMOOTHED DATA (FROM 1 CH. TO 1024 CH.)

CH. NO.																				
1 -	0	0	0	0	0	0	0	0	0	0	0	0	0	0	0	0	0	0	0	0
21 -	0	0	0	0	0	0	0	0	0	0	0	0	0	0	0	0	0	0	0	0
41 -	0	0	0	0	0	0	0	0	0	0	0	0	0	3602	3733	3988	4206	4176	4031	4068
61 -	4312	4272	3799	3186	2824	2667	2631	2605	2732	2912	3101	3021	2774	2433	2261	2304	2462	2463	2305	2131
81 -	2119	2136	2152	2093	2037	2013	2064	2111	2169	2173	2157	2095	2091	2092	2116	2097	2175	2417	2730	2791
101 -	2580	2338	2212	2209	2228	2301	2284	2279	2315	2395	2445	2460	2560	2784	2961	2859	2676	2663	2736	2806
121 -	3140	3840	4391	4180	3486	2968	2852	2834	2834	2838	2920	2938	3007	3070	3152	3219	3259	3191	3088	3175
141 -	3344	3403	3457	3540	3623	3685	3805	3919	4024	4171	4230	4190	4160	4195	4178	4137	4159	4201	4415	5193
161 -	7027	8558	8199	6276	4803	4384	4455	4578	4686	4785	4934	5013	5031	5039	5145	5230	5254	5163	5167	5328
181 -	5646	5940	6009	5729	5380	5225	5240	5241	5287	5303	5234	5054	4990	5053	5207	6233	10357	18196	24087	21677
201 -	13332	6619	4439	4816	8751	19407	32096	34455	24742	18320	27874	41770	40207	23216	7620	2096	1625	1706	1665	1626
221 -	1652	1723	1772	1773	1702	1655	1674	1720	1771	2316	3838	6360	9147	10682	9587	6403	3368	2021	2308	3447
241 -	4571	4643	3773	2601	1855	1447	1310	1237	1218	1215	1209	1212	1214	1230	1224	1205	1200	1187	1170	1136
261 -	1152	1180	1207	1198	1218	1261	1306	1266	1236	1216	1209	1197	1183	1179	1172	1192	1206	1570	2963	5458
281 -	6940	5858	3251	1517	1020	978	1034	1159	1599	2180	2471	2065	1464	1076	947	909	919	946	971	994
301 -	946	932	920	931	932	958	946	899	879	868	871	889	915	920	889	888	883	904	903	884
321 -	861	898	997	1132	1236	1163	1013	907	903	861	831	842	873	858	841	836	850	852	858	825
341 -	837	858	871	837	820	830	858	829	792	790	818	810	796	776	772	788	812	795	791	873
361 -	1075	1217	1159	969	848	800	775	760	756	762	774	783	753	747	735	750	745	745	735	749
381 -	726	737	746	766	726	707	706	723	703	672	662	690	684	678	652	642	653	660	670	639
401 -	643	637	655	642	633	621	612	604	607	589	628	644	643	593	636	786	1500	2929	4065	3739
421 -	2281	1060	599	548	544	512	507	507	516	504	514	515	527	501	508	510	508	509	518	536
441 -	538	530	523	536	538	520	536	575	617	660	774	1006	2034	5265	10776	14142	11907	6133	1934	467
461 -	353	385	398	376	385	378	365	351	359	356	353	341	342	345	383	387	397	373	368	351
481 -	357	349	363	371	358	336	342	331	312	293	302	312	317	314	309	307	305	299	275	279
501 -	287	315	316	325	298	297	351	399	411	371	346	309	300	295	293	288	285	293	297	302
521 -	302	304	309	319	337	324	293	283	293	310	310	322	315	322	308	297	277	274	300	327
541 -	327	300	307	348	384	378	361	363	392	426	739	2137	5642	9802	10922	7730	3304	809	268	197
561 -	225	219	226	219	223	249	303	432	658	830	756	511	314	229	216	203	202	187	195	187
581 -	212	218	252	356	534	623	543	371	257	209	193	190	204	207	192	186	189	186	191	197
601 -	207	202	199	189	196	217	244	268	292	291	259	223	189	177	174	185	186	184	192	196
621 -	188	186	194	209	189	191	192	277	492	893	1163	1038	624	309	186	188	209	227	213	202
641 -	176	167	178	177	163	145	139	152	166	165	163	176	203	252	425	639	741	600	379	206
661 -	152	150	184	226	327	640	1110	1350	1110	636	288	155	140	150	149	145	145	142	157	154
681 -	148	134	143	142	140	146	144	140	142	146	143	133	131	128	138	145	136	128	143	185
701 -	190	184	163	171	161	149	123	122	126	128	122	124	128	127	126	126	138	135	135	129
721 -	127	130	146	167	261	494	898	1206	1130	708	333	184	144	119	108	117	120	108	97	106
741 -	119	116	102	102	112	105	97	109	126	116	106	103	110	118	113	101	106	114	115	109
761 -	119	112	107	103	103	102	105	110	108	107	99	90	91	101	116	116	100	87	92	105
781 -	109	105	112	119	116	94	92	95	100	106	110	100	91	111	116	108	92	98	102	108
801 -	103	92	95	96	104	101	103	92	93	96	103	99	100	104	108	103	104	104	92	93
821 -	104	115	110	102	94	97	103	109	107	109	102	95	95	100	105	92	96	98	112	107
841 -	102	94	97	106	132	154	158	141	124	101	82	72	85	97	97	90	98	108	113	111
861 -	110	124	143	159	156	137	114	102	97	95	90	101	113	127	119	116	104	99	98	103
881 -	102	88	90	100	102	101	97	106	98	99	94	106	117	111	114	109	103	89	88	96
901 -	94	97	98	101	91	84	93	95	100	93	93	87	88	85	93	96	92	91	97	110
921 -	107	104	90	98	100	106	91	79	82	93	98	87	92	98	102	93	92	91	86	76
941 -	77	91	94	94	102	111	110	104	94	91	93	92	83	91	97	114	108	100	87	88
961 -	91	104	110	99	89	87	87	90	123	201	394	656	814	722	469	233	107	83	93	99
981 -	92	88	84	80	76	81	81	83	86	128	192	272	321	320	228	129	83	80	73	66
1001 -	69	73	80	81	84	78	77	77	95	125	141	123	91	78	83	85	77	66	76	87
1021 -	0	0	0	0																

***** FIRST PEAK SHOULD BE CHECKED *****

Fig. A-4 Graphic display of the peak fitting by the line-printer.

PK.GROUP	MIN.CH.	PEAK CH.	MAX.CH.	PEAK AREA	BK.GD.	STD.DEV.	PK.HEIGHT
6	178	212.27	219	321580	163063.1	804.8	41266.3

********** ID NO. 6 FROM 178 TO 219 CHANNEL

YMIN= 1584.4 LOGARITHMIC SCALE YMAX= 44142.8

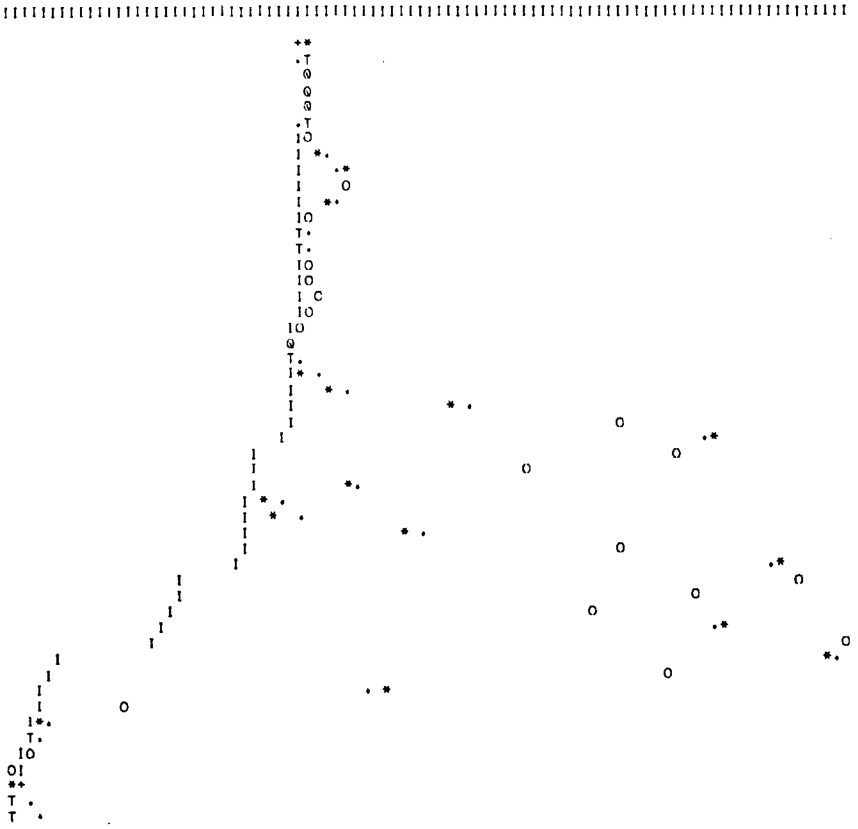

CH	BG	CAL	OBS
174	5060.0	5236.0	5060.0
175	5190.6	5236.0	5102.0
176	5181.7	5236.0	5278.0
177	5172.5	5236.0	5236.0
178	5163.0	5187.0	5187.0
179	5153.1	5165.9	5128.0
180	5142.8	5240.6	5336.0
181	5132.0	5531.3	5634.0
182	5120.1	5990.7	5942.0
183	5088.9	6101.4	6045.0
184	5075.4	5703.6	5755.0
185	5062.6	5271.0	5307.0
186	5049.7	5091.9	5242.0
187	5036.3	5080.1	5254.0
188	5022.3	5180.6	5239.0
189	5007.5	5338.0	5259.0
190	4984.2	5352.9	5349.0
191	4967.1	5186.5	5212.0
192	4949.6	5019.3	5084.0
193	4931.0	4942.9	4941.0
194	4910.9	4915.7	5113.0
195	4888.8	4962.8	5364.0
196	4863.8	5642.8	6163.0
197	4834.6	9211.5	9810.0
198	4797.4	17918.9	17786.0
199	4735.0	25721.3	25192.0
200	4244.8	22152.3	22340.0
201	4189.7	12342.0	12431.0
202	4148.5	6129.9	6400.0
203	4110.2	4402.7	4670.0
204	4071.1	4583.6	5108.0
205	4028.0	7662.6	8273.0
206	3975.7	18214.6	18136.0
207	3896.5	33666.3	33086.0
208	3150.7	36442.1	36685.0
209	3056.4	23917.9	24048.0
210	2989.9	16197.4	16303.0
211	2921.2	27137.9	26480.0
212	2813.7	44142.8	44080.0
213	1924.0	41102.5	42346.0
214	1841.3	21697.4	21467.0
215	1790.0	7159.4	6591.0
216	1750.5	2525.2	2465.0
217	1717.8	1777.5	1834.0
218	1689.6	1692.0	1745.0
219	1664.5	1685.0	1685.0
220	1641.9	1597.0	1597.0
221	1621.2	1597.0	1663.0
222	1602.2	1597.0	1727.0
223	1584.4	1597.0	1762.0

SYMBOL .=OBS, *=CAL, I=BG, O=.AND*, +=.ANDI, T=*ANDI, Q=.AND*ANDI

5 PEAKS WITH FWHM = 2.97088E 00
DEGREE OF THE OVERALL FIT = 1.58124E-04 AND BACKGROUND = 163063.1 COUNTS
CONVERGENCE LIMIT = 1.61496E-02 IBG = 4 SKEWNESS FACTOR = 1.00

PEAK NO.	PK POSITION	PK HEIGHT	PEAK AREA	STANDARD DEVIATION
9	182.74	1034.12	3270.	56.84
10	189.67	381.21	1206.	34.50
11	199.25	21394.00	67657.	258.57
12	207.67	34326.21	108553.	327.78
13	212.42	43564.72	137769.	369.50

Fig. A-5 Table of the results with "PKREC".

73-04-07 ********** GAMMA SPECTRUM ANALYSIS OF U(3)-4 1-1024
BY BOB73 ********** MO-F-1 - 4

*** RESULTS OF PEAK RECOGNITION ***

PEAK NO.	MIN	PEAK CH.	MAX	PEAK AREA	BK.GD.	STD.DEV.	PK.FT.1	PK.FT.2	JFIT	JFFT	FWHM
1	54	57.98	67	7940	37321	3.6	3.602F 03	2.631E 03	1	1	3.169
2	67	71.13	81	2708	30817	9.4	2.631E 03	2.119E 03	1	1	2.715
3	95	99.79	104	2057	17298	9.3	2.116E 03	2.209E 03	0	0	2.797
4	108	115.37	128	8160	48364	4.0	2.279E 03	2.834E 03	1	1	3.100
5	157	162.33	167	14310	38746	2.1	4.159E 03	4.455E 03	0	0	2.823
6	178	182.61	219	321580	163063	0.3	5.163E 03	1.665E 03	4	4	2.971
7	227	234.03	249	54849	29547	0.6	1.674E 03	1.218E 03	1	1	3.930
8	275	281.08	297	25483	21372	1.0	1.172E 03	9.194E 02	1	1	3.014
9	321	325.08	330	1360	6886	9.0	8.610E 02	8.605E 02	0	0	3.184
10	358	362.28	368	1502	6980	8.3	7.945F 02	7.603E 02	0	0	2.931
11	413	419.30	426	12370	6922	1.3	6.428E 02	5.120F 02	0	0	3.068
12	446	456.10	462	50102	7057	0.5	5.200E 02	3.855F 02	0	0	3.231
13	505	508.85	513	392	2091	17.3	2.979F 02	2.998E 02	0	0	3.208
14	538	540.86	561	39995	5693	0.6	2.741F 02	2.246E 02	2	2	3.166
15	564	570.20	576	2425	2281	3.4	2.185F 02	1.947E 02	0	0	3.479
16	580	586.05	592	1658	2099	4.6	1.873E 02	1.945E 02	0	0	3.378
17	604	609.30	615	418	1925	15.6	1.989F 02	1.862E 02	0	0	3.935
18	625	631.19	647	3866	3533	2.7	1.933F 02	1.554E 02	2	2	3.213
19	650	656.88	662	2190	1738	3.4	1.646F 02	1.499E 02	0	0	3.368
20	662	668.00	674	4527	1638	2.0	1.499F 02	1.480E 02	0	0	3.378
21	697	701.41	708	287	1301	18.7	1.354F 02	1.249E 02	0	0	5.294
22	721	728.29	735	4331	1583	2.0	1.329F 02	1.094E 02	0	0	3.523
23	773	775.44	778	32	400	90.2	9.897F 01	1.015E 02	0	0	FAIL
24	842	846.77	852	225	871	19.7	1.030F 02	8.996E 01	0	0	3.593
25	860	864.33	869	254	792	16.9	1.039F 02	9.410F 01	0	0	3.818
26	953	956.45	959	58	444	53.1	9.057F 01	8.737E 01	0	0	FAIL
27	960	962.79	979	2957	1597	2.7	8.823F 01	8.923F 01	1	1	3.645
28	987	993.24	999	1075	849	4.9	8.039F 01	7.370E 01	0	0	3.779
29	1007	1010.93	1015	51	685	73.9	8.009F 01	1.184E 02	0	0	1.525

Fig. A-6 Table of the final results.

73-04-07 ********** GAMMA SPECTRUM ANALYSIS OF U(3)-4 1-1024
BY BOB73 ********** MO-F-1 - 5

. FINAL RESULTS .

UNIT OF THE ACTIVITY = 1.000E 04 DPS

PEAK NO.	PEAK CH.	ENERGY(KEV)	PT. ERROR	PEAK AREA	PT. ERROR	ACTIVITY	PT. ERROR
1	57.76	26.804	1.242	288.21	1.76	1.4592E-01	484.37
2	62.00	28.944	1.118	498.83	1.32	2.4615E-01	372.57
3	71.71	33.849	0.894	204.36	2.03	9.6891E-02	224.68
4	77.99	37.016	0.783	78.32	3.14	3.6568E-02	170.45
5	99.71	47.977	0.517	206.91	9.25	9.5965E-02	78.70
6	115.06	55.719	0.397	167.91	18.68	7.8268E-02	52.93
7	123.18	59.812	0.347	595.99	5.38	2.8087E-01	99.95
8	162.30	79.523	0.191	1418.26	2.13	7.2147E-01	14.53
9	182.74	89.820	0.142	326.99	1.74	1.7452E-01	8.55
10	189.67	93.311	0.129	120.60	2.86	6.5464E-02	7.46
11	199.25	98.131	0.113	6765.67	0.38	3.7601F 00	5.21
12	207.67	102.373	0.101	10855.35	0.30	6.1607E 00	4.00
13	212.42	104.761	0.095	13776.92	0.27	7.9121E 00	3.41
14	234.02	115.633	0.073	3992.38	0.50	2.4205E 00	1.61
15	241.73	119.511	0.067	1458.56	0.82	9.0153E-01	1.45
16	281.10	139.311	0.046	1993.10	0.70	1.3580E 00	1.75
17	290.93	144.254	0.044	523.24	1.38	3.6513E-01	2.25
18	325.09	161.422	0.038	131.05	2.76	9.9183E-02	3.50
19	362.34	180.137	0.035	147.42	2.57	1.2149E-01	3.38
20	419.33	208.755	0.032	1227.99	0.90	1.1444E 00	2.09
21	456.07	227.196	0.029	4908.16	0.45	4.9296E 00	1.69
22	508.82	253.663	0.025	39.38	17.18	4.3782E-02	17.23
23	541.00	269.807	0.023	19.78	7.10	2.3320E-02	7.19
24	550.68	274.659	0.022	87.06	3.39	1.0445E-01	3.57
25	554.73	276.688	0.022	3852.93	0.51	4.6557E 00	1.22
26	570.23	284.465	0.021	236.82	2.04	2.9402E-01	2.31
27	586.03	292.387	0.020	160.63	4.74	2.0492E-01	4.86
28	609.43	304.122	0.018	44.31	4.68	5.8797E-02	4.80
29	631.21	315.043	0.017	355.02	1.67	4.8813E-01	1.98
30	638.23	318.563	0.016	24.48	6.36	3.4037E-02	6.45
31	643.21	321.058	0.016	7.04	11.83	9.8633E-03	11.88
32	656.91	327.927	0.016	216.54	2.14	3.1017E-01	2.41
33	667.98	333.475	0.015	445.14	1.50	6.4872E-01	1.87
34	702.36	350.707	0.014	29.49	5.72	4.5282E-02	5.84
35	728.29	363.705	0.014	423.77	1.53	6.7612E-01	1.97
36	775.46	387.346	0.014	3.21	89.98	5.4746E-03	89.99
37	847.05	423.221	0.014	23.88	6.29	4.4820E-02	6.45
38	864.54	431.986	0.014	25.30	6.16	4.8574E-02	6.33
39	956.47	478.053	0.015	5.81	52.95	1.2480E-02	52.97
40	962.75	481.199	0.015	5.80	98.36	1.2537E-02	98.37
41	973.12	486.397	0.015	291.38	2.68	6.3761E-01	3.07
42	993.21	496.464	0.016	106.26	3.06	2.3789E-01	3.41
43	1010.81	505.283	0.016	9.98	38.43	2.2776E-02	38.46

********** END OF BOB73

***** CALCULATION TIME 28 SEC **

Appendix 3. An example of the application of " ECHO "

In the case where one needs to treat the results from BOB 73 as a whole for a series of the spectrum data, the subroutine " ECHO " can be utilized as follows: the final results of the analysis of each spectrum are written one by one on a given file (disk) of the computer with the necessary information of the spectrum, such as ID name, counting duration and counting data. Thereafter the file is called by the objective program.

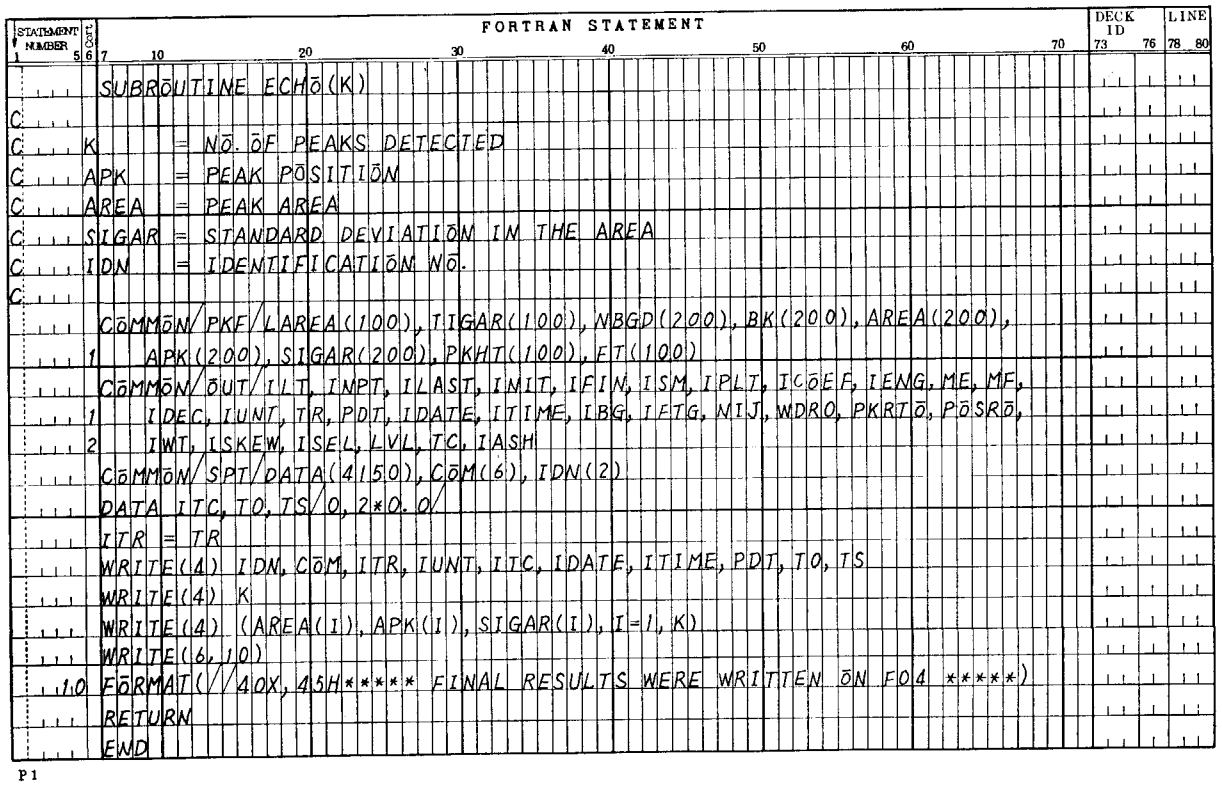

```
      SUBROUTINE ECHO(K)
C
C     K      = NO. OF PEAKS DETECTED
C     APK    = PEAK POSITION
C     AREA   = PEAK AREA
C     SIGAR  = STANDARD DEVIATION IN THE AREA
C     IDN    = IDENTIFICATION NO.
C
      COMMON/PKF/LAREA(100),TIGAR(100),NBGD(200),BK(200),AREA(200),
     1    APK(200),SIGAR(200),PKHT(100),FT(100)
      COMMON/OUT/ILT,INPT,ILAST,INIT,IFIN,ISM,IPLT,ICOEF,IENG,ME,MF,
     1    IDEC,IUNT,TR,PDT,IDATE,ITIME,IBG,IFTG,NIJ,WDRO,PKRTO,POSRO,
     2    IWT,LSKEW,ISEL,LVL,TC,IASH
      COMMON/SPT/DATA(4150),COM(6),IDN(2)
      DATA ITC,TO,TS/0,2*0.0/
      ITR = TR
      WRITE(4) IDN,COM,ITR,IUNT,ITC,IDATE,ITIME,PDT,TO,TS
      WRITE(4) K
      WRITE(4) (AREA(I),APK(I),SIGAR(I),I=1,K)
      WRITE(6,10)
   10 FORMAT(//40X,45H***** FINAL RESULTS WERE WRITTEN ON FO4 *****)
      RETURN
      END
```

P1